DEVELOPMENT OF AN ASPEN MODEL FOR THE TREATMENT OF ACID MINE DRAINAGE

By

Rinaldi Eduardo Damons

A thesis submitted in the fulfillment of the requirements for the degree of

Master of Technology in Chemical Engineering

The Cape Technikon

December 2001

Supervisor: Prof. FW Petersen

DECLARATION

I hereby certify that this thesis is my own original work, except where specifically acknowledged in the text. Neither the present thesis nor any part thereof has previously been submitted at any other Technikon or University for any degree/diploma.

RINALDI EDUARDO DAMONS
DECEMBER 2001

ABSTRACT

Although numerous methods exist to treat mine water that is rich in $CaSO_4$ they all have inherent disadvantages. A means of treating acid mine drainage is by forming a precipitate known as ettringite. Ettringite is a low solubility calcium hydrosulphoaluminate that is stable between pH values of 11.4 and 12.4. Ettringite is made up of calcium, sulphate, aluminium and a large amount of water. The formation of this precipitate is a result of calcium sulphate which is brought into contact with an aluminium-containing agent. Decomposition of ettringite takes place by reducing the pH to a near neutral value.

A 5 stage process is proposed to treat acid mine drainage of which the formation of ettringite forms the cornerstone of this process. The process incorporates the formation of more than one precipitate, namely; metal hydroxides, gypsum, $CaSO_4$ and $CaCO_3$. To facilitate the formation of ettringite, gibbsite is recycled as a result of ettringite being decomposed.

The results obtained in this paper are as a result of modeling this process on an Aspen Plus simulator. The simulation package is useful for investigating how this process behaves under non-ideal conditions and under various sensitivities. The process and its behavioral patterns are also analyzed in order to ascertain its economic viability.

ACKNOWLEDGEMENTS

First and foremost, The Lord Jesus Christ deserves all the Glory, all the honour and all of the Praise, " For the Lord is good and His love endures forever... " Psalm 100 : 5.

The work contained in this thesis was performed at the Cape Technikon's School of Mechanical and Process Engineering in the Department of Chemical Engineering, and commenced February 2000.

I am extremely thankful to the following persons and/or institutions for their assistance and contributions in completing this thesis:

- Prof. Francis Petersen for his diligent and patient supervision. His enthusiasm and positive attitude to life has been a driving force in the completion of this project.
- Dr Jaap Smit and his staff of the Hydrometallurgy Department at MINTEK for their help and assistance on the Aspen Simulator.
- MINTEK for their financial support and continuous interest in the progress of my work.
- The National Research Fund (NRF) for their financial contributions.
- My loving wife, Judy, for her continuous encouragement and support of my career.

TABLE OF CONTENTS

CHAPTER 2 Literature Review

CHAPTER 3 Experimental

CHAPTER 4 Theory

CHAPTER 5 Effects of non-ideal conditions on ettringite formation

CHAPTER 6 Sensitivity Analysis

CHAPTER 7 Conclusions and Recommendations

LIST OF FIGURES

LIST OF TABLES

Tables in Appendix A.

Tables in Appendix C.

CHAPTER 1

INTRODUCTION

1.1 Introduction

South Africa is a semi-arid country and its available freshwater supplies are already almost fully-utilized. Only 8.6% of the rainfall available is present as surface water (http://www.ngo.grida.no/soesa/nsoer/issues/water/), which is one of the lowest conversion ratios in the world. The mean annual runoff (MAR) for South Africa, which is not distributed evenly throughout the country, is estimated at some 50 million m^3/area (http://www.ngo.grida.no/soesa/nsoer/issues/water/). Groundwater shows similar trends to surface waters, in that its resources are relatively limited compared to world averages. It is unlikely that the projected demand on water resources in South Africa will be sustainable due to its projected population growth and economic development rates. The supply of water could become a major restriction to the future socio-economic development of the country, in terms of both the amount of water available and the quality of what is available.

The increased water demand and its degradation is as a result of population growth, increased economic activity and the intensification of land use practices. The economy of South Africa is largely dependent on the mining and minerals industry. This industry is the source of employment for a vast amount of people. A real and ongoing side effect of the industrial sector is the large quantities of polluted water (generally referred to as mine drainage) being produced. Presently, this mine drainage flows into local river systems and, even if neutralized, is able to increase the concentration of dissolved salts to levels, which are unacceptable for human consumption. The high level of dissolved salts also renders the water useless for industrial and agricultural purposes, as well as inhospitable to aquatic life. It is estimated that the Witwatersrand area is responsible for 240 million litres per day of polluted water. The Witbank area has similar estimates, while the

Secunda area produces 120 million litres per day (Dry, 1998). Treatment of this water could meet the basic need of a vast amount of people, as well as irrigate large areas of under-utilised farmland. The purification of this water could have a positive effect on the economy.

This project is aimed at investigating a technique of treating polluted water in South Africa. The water in question is known as acid mine drainage (AMD), and occurs at operating and abandoned mine sites as a result of oxidation of sulphide minerals. AMD is characterized by a low pH and heavy metal contamination. The water to be treated also contains large quantities of calcium and sulphate.

1.2 Formation of AMD

This contaminated water is often an orange or yellowish-orange colour, and has the smell of rotten eggs (sulphate smell). The formation of AMD is as a result of a series of complex geo-chemical and microbial reactions that occur when water comes in contact with pyrite (iron disulphide minerals) in coal mining operations. This water is usually high in acidity and dissolved metals. By disturbing pyrite, as is in done during coal mining, it reacts with water and oxygen to form iron, aluminium and sulphate in runoff water. The weathering of pyrite is described by a number of stoichiometric reactions (http://www.osmre.gov/amdform.htm).:

$$\begin{array}{l} 4FeS_2 + 15O_2 + 14H_2O \rightarrow 4Fe(OH)_3 \downarrow + 8H_2SO_4 \\ 2FeS_2 + 7O_2 + 2H_2O \rightarrow 2Fe^{2+} + 4SO_4^{2-} + 4H^+ \end{array} \quad \textbf{Step 1}$$

The first reactions (step 1) involve the oxidation of pyrite (FeS_2). Here, the sulphur is oxidised to sulphate and the ferrous iron is given off.

$$4Fe^{2+} + O_2 + 4H^+ \rightarrow 4Fe^{3+} + 2H_2O \qquad \textbf{Step 2}$$

The ferrous iron is converted to ferric iron in the second reaction. The second reaction (step 2) has been termed the "rate determining" step for the overall sequence. The rate of formation of the ferric iron is facilitated by the intervention of certain bacteria, *Thiobacillus ferroxidans*. This bacteria and several other species thought to be involved in pyrite weathering are widespread in the environment. *Thiobacillus ferroxidans* has been shown to increase the iron conversion reaction rate by a factor of hundreds to as much as one million times.

$$4Fe^{3+} + 12H_2O \rightarrow 4Fe(OH)_3 \downarrow + 12H^+ \qquad \textbf{Step 3}$$

The next reaction (step 3), which takes place, is the hydrolysis of ferric iron, resulting in a split of the water molecule. A large number of metals are able to react with water in this way. Ferric hydroxide (ferrihydrite) is precipitated and its formation is pH dependent. Under very acidic conditions of less than about pH 3.5, the solid mineral does not form and ferric iron remains in solution. A precipitate forms at high pH values, and this precipitate is commonly referred to as "yellowboy".

$$FeS_2 + 14Fe^{3+} + 8H_2O \rightarrow 15Fe^{2+} + 2SO_4^{2-} + 16H^+ \quad \textbf{Step 4}$$

The final reaction (step 4) is the oxidation of additional pyrite by means of the ferric iron. The initial oxidation in steps 1 and 2 are responsible for generating the ferric iron. Here iron is the oxidising agent. This reaction takes place extremely rapidly and continues until either ferric iron or pyrite is used up. Oxygen is not required for step 4.

The overall pyrite reaction series is among the most acid-producing of all weathering processes in nature.

1.3 Existing Technology

Purifying acid mine drainage is not a new phenomenon, but ongoing methods have been around for many years. The problem in treating contaminated mine water is not only to reduce the dissolved salts to acceptable low levels, but to do this at costs which are bearable. Methods of purifying solutions from sulphates include precipitation with lime, precipitation with barium salts, co-precipitation with calcium carbonate, reverse osmosis, electrodialysis, and ion exchange and bacterial sulphate reduction.

1.3.1 Ion Exchange

It is a well-established technology for producing very pure water from water containing low levels of dissolved salts. Ion exchange is a reversible chemical reaction wherein an ion from solution is exchanged for a similarly charged ion attached to an immobile solid particle. There are two types of solid ion exchange particles, namely naturally occurring zeolites or synthetically produced organic resins. Predominant use is made of the synthetic organic resins because they are tailor made for specific applications. It is however necessary for the resin to be periodically regenerated. Regeneration takes place by eluting the cation-exchange resin with an acidic solution (e.g. hydrochloric acid), then rinsing it with clean water. A similar approach is applied to the anion exchange resin, except than an alkaline solution (e.g. sodium hydroxide) is used instead of an acidic one. The regeneration process therefore produces acidic and alkaline solutions containing all the dissolved minerals that were extracted from the incoming water, as well as an equal or even greater amount of additional salts from the acid and alkaline solutions used to regenerate the resins. The problem with mine water is that they contain significant larger quantities of dissolved salts than the water that is conventionally purified by ion exchange. Another disadvantage of this technique is that if ion exchange is used, the costs of the acid and alkali needed to regenerate the resins are relatively expensive. This approach leads to the production of brines, which contain more than twice the dissolved salts that were present in the original water, albeit in a reduced volume.

1.3.2 Membrane processes

1.3.2.1 Reverse Osmosis

Osmosis is the phenomenon of water flow through a semi permeable membrane that prevents the transport of salts or other solutes through it. When separation of two water (or other solvent) by a semi permeable membrane takes place, water will flow from the side of low solute concentration, to the side of high solute concentration. This flow may be halted or even reversed by applying an external pressure on the side of the higher concentration. When this takes place, the phenomenon is called reverse osmosis. If solute molecules are only present on one side of the system, then the pressure that stops the flow is called the osmotic pressure. Osmotic pressure π is described by the van't Hoff formula:

$$\pi = cRT \qquad (1.1)$$

where c is the molar solute concentration, R is the gas constant and T is the absolute temperature.

It is possible to use this technology to purify acid mine drainage, however the presence of soluble calcium sulphate would limit the water recovery by causing scaling, if allowed to become too concentrated in the brine. The dissolved salts could be concentrated into brine comprising up to fifty percent of the original volume of the polluted min water.

1.3.2.2 Electrodialysis

Electrodialysis removes contaminants from water by using an electric current to pull ionic impurities through ion selective membranes and away from the purified water. The impurities (cations and anions) are transported across these membranes and concentrated into brine streams. This results in a product stream of purified water. The following diagram, Figure 1.1, describes this process.

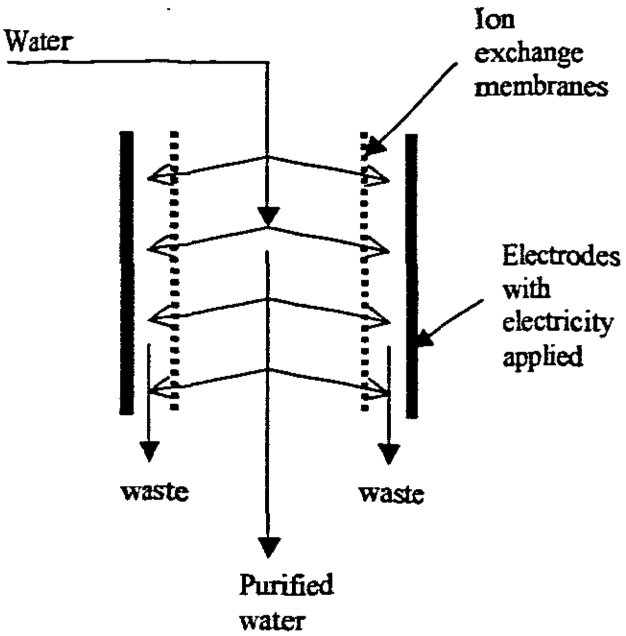

Figure 1.1 *Diagrammatical representation of the Electrodialysis Process*

Electrodialysis has the drawback in that it is limited in the contaminants it can remove. It cannot remove organics, pyrogens and elemental metals, which have weak or nonexistent surface charges because they are attached to the membranes. Secondly, the system requires a skilled operator and routine maintenance. Large membranes, which bear a significant charge, some colloids and detergents, can plug the membranes' pores reducing their ionic transport ability and requiring frequent cleaning. This means that the calcium in the AMD could give rise to scaling of the membranes thereby limiting the recovery of purified water. Even more problematically, electrodialysis releases hydrogen gas, which is potentially dangerous and liberates caustic soda, which can cause scaling. Last, and probably not least, it is relatively expensive. It requires more than the normal amount of electricity to produce, and purification beyond the potable level is not economically due to increased power costs and the extremely expensive material costs of the platinum and stainless steel materials needed to build it.

1.3.3 Bacterial sulphate reduction

This technology, still at its infant stage, entails the use of bacteria to catalyse a reaction between the sulphate ions and an appropriate reductant (hydrogen, ethanol and even raw sewage) has been proposed. Due to the vast amounts of chemical reactions taking place in a sulphate reducing bacteria system, it is practically impossible to document all of these. Some generally accepted reactions are presented below:

$$SO_4^{2-} + 4H_2 \rightarrow H_2S + 2OH^- + 2H_2O \quad (1.2)$$

$$SO_4^{2-} + \text{nutrients} + H_2O \rightarrow H_2S + HCO_3^- \quad (1.3)$$

$$M^{2+} + S^{2-} \rightarrow MS_{(ppt)} \quad (1.4)$$

Equation 1.2 shows the production of alkalinity (hydroxide) and hydrogen sulphide using hydrogen gas as an energy source. A carbonate gets formed from a generic nutrient source in equation 1.3. At equation 1.4, sulphide which was produced at 1.2 and 1.3, gets consumed by the reaction with a dissolved divalent metal (M^{2+}). The conventional sulphate reducing systems involves passing the entire flow of water to be treated through a bioreactor in which microbial sulphate reduction and sulphide precipitation occur together as shown in Figure 1.2.

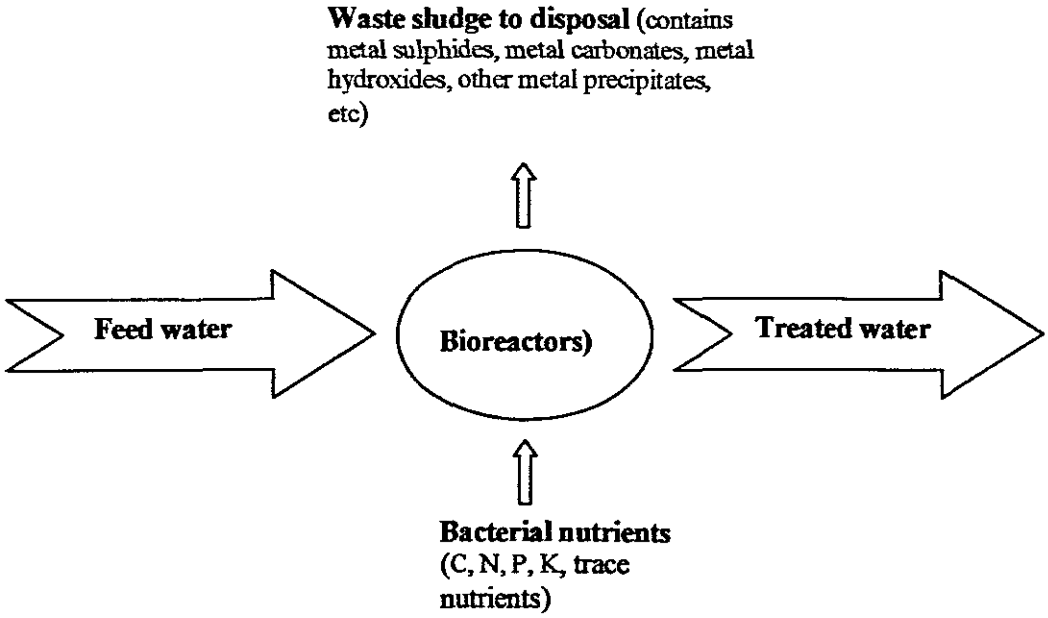

Figure 1.2 *Diagrammatic representation of Bacterial Sulphate reduction*

Presently, this technology does not appear to be able to reduce the levels of dissolved sulphate in polluted mine water sufficiently, on its own, so that potable water may be produced.

1.4 The Chemical Precipitation Process

This precipitation process to rid AMD of harmful Ca^{2+} and SO_4^{2-} was patented by Mintek and Savannah mining, involves the addition of lime to waste water to precipitate the metal hydroxides, and the subsequent formation of ettringite to remove the calcium and sulphates.

1.4.1 Process Description

The process consists of 5 main stages as described below and illustrated by Figure 1.3.

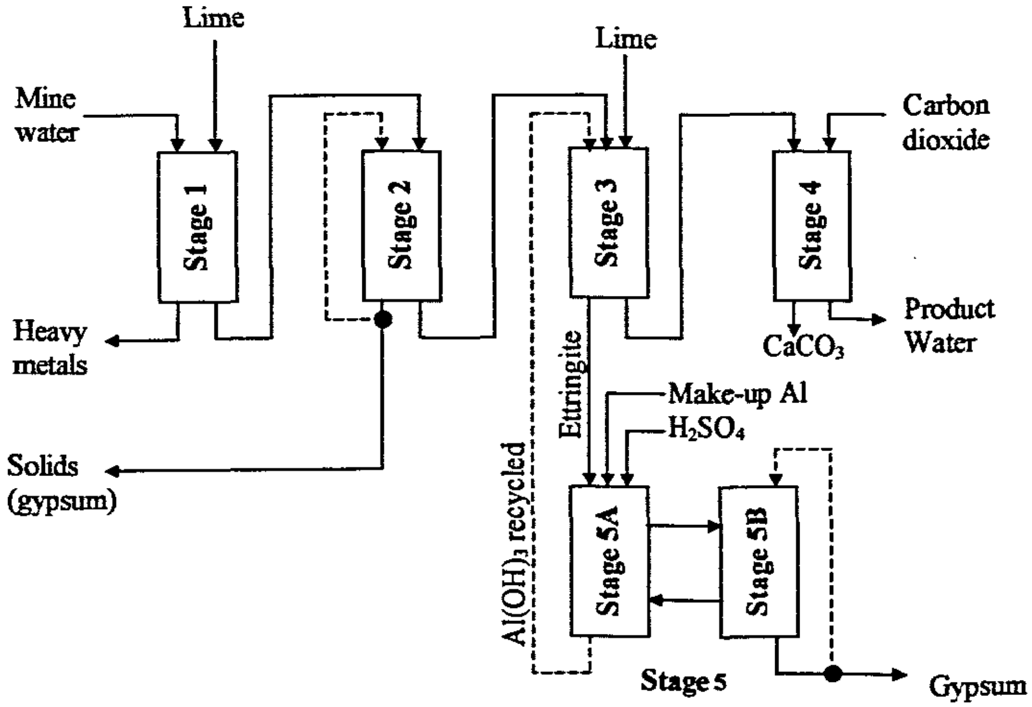

Figure 1.3. *The Chemical Precipitation Process*

1.4.1.1 Stage 1: *Precipitation of heavy metals*

Here the polluted mine water, at an approximate pH value of 6, is brought into contact with lime in order to raise the pH to greater than 11.5. These heavy metals are precipitated as hydroxides (reactions 1.5 and 1.6) and although most metal hydroxide species will precipitate at relatively low pH values (pH < 8), a higher pH is required to precipitate magnesium.

$$Me^{2+} + 2OH^- \rightarrow Me(OH)_2 \downarrow \tag{1.5}$$

$$Mg^{2+} + 2OH^- \rightarrow Mg(OH)_2 \downarrow \tag{1.6}$$

Where 'Me' refers to divalent heavy metals such as iron, nickel, magnesium, etc.

These hydroxides are sent away for land filling.

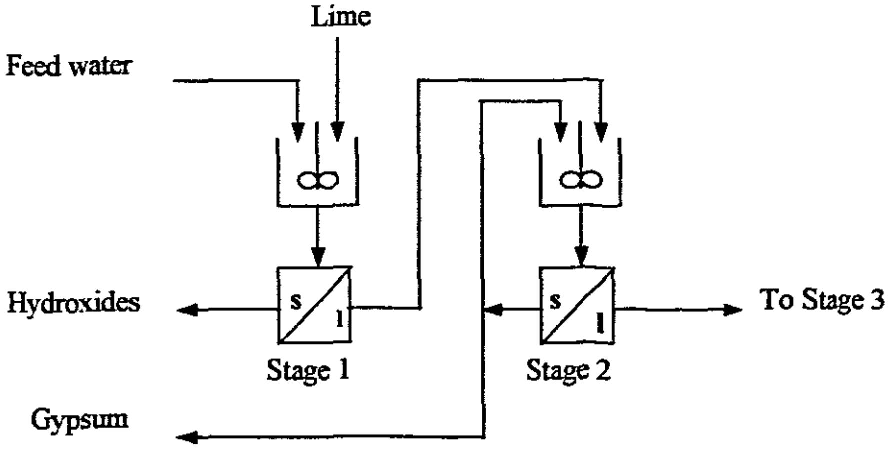

Figure 1.4 *Stages 1 and 2 of the Chemical Precipitation Process*

1.4.1.2 Stage 2: *Gypsum de-supersaturation*

The solution from stage 1 is contacted with gypsum crystals in stage 2. One of the characteristics of dissolved calcium sulphate, is that when a suitable surface such as gypsum is not present to crystallize on it, it can be short lived or metastable at concentrations that exceed it equilibrium solubility. During the addition of lime in stage 1, the solution phase may become supersaturated with respect to gypsum, depending on the amount of sulphate in the feed water. By separating the solids from the liquids, dissolved calcium sulphate is separated from the metal hydroxides.

The solution from stage 1 is contacted with gypsum crystals in stage 2 in order to provide active surfaces of gypsum, which acts as a catalyst for the precipitation of the 'supersaturated' gypsum. This precipitated gypsum is thickened and filtered, and leaves the process as waste or as a by-product, depending on the specific situation. Part of the precipitated gypsum is returned to the mixing tank of stage 2 to provide the seed crystals for the rapid crystallization of the supersaturated portion of the dissolved calcium sulphate.

The purpose of stage 2, is therefore, to ensure that in the absence of mono-valent cations (such as Na^+), the feed water entering stage 3 would be a saturated gypsum solution and therefore identical for different waste streams, even if their compositions vary substantially. If however, mono-valent cations are present in the feed water, the concentration of sulphates entering stage 3 may be substantially higher. This is due to the fact that sulphate associated with Na^+ and K^+ would not be available for precipitation, and would therefore be present in solution.

1.4.1.3 Stage 3: *Ettringite precipitation*

Stage 3 is the heart of the Ettringite process and involves the addition of aluminium hydroxide to the saturated gypsum solution from stage 2. This results in the formation of the insoluble salt known as ettringite thereby removing both calcium and sulphate from the solution. The stoichiometry for ettringite precipitation is given by the following reaction:

$$6Ca^{2+} + 2Al(OH)_4^- + 3SO_4^{2-} + 4OH^- + 26H_2O \rightarrow Ca[Al(OH)_6 2(SO_4)_3 . 26H_2O \qquad (1.7)$$

The ideal conditions for ettringite formation range between pH values 11.4 and 12.4. In order to keep the pH between these limits, lime is added resulting in the maximization of ettringite precipitation. The end product of stage 3 is filtered and the solid ettringite proceeds to stage 5 while the liquid goes to stage 4 as can be seen by Figure 3 below.

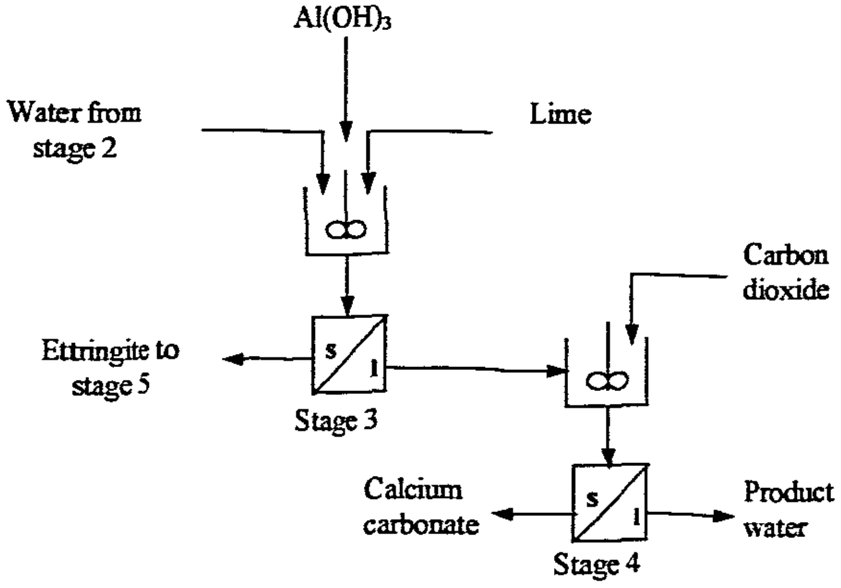

Figure 1.5 *Stages 3 and 4 of the Chemical Precipitation Process*

1.4.1.4 Stage 4: *Carbonation*

The solution from stage 3, which is now free from all heavy metals, calcium and sulphates is treated with carbon dioxide to reduce the pH to a suitable level. Pure calcium carbonate is precipitated, and can be separated from the resulting product water by filtration. The pH can however also be controlled so that calcium bicarbonate is formed instead of calcium carbonate, but this however depends on certain case specific factors.

1.4.1.5 Stage 5: *Regeneration of Aluminium Hydroxide*

Ettringite slurry is transported to stage 5 (as seen by Figure 4) so that it may decompose in order to regenerate the amorphous aluminium hydroxide for recycle. The decomposition of ettringite is achieved by bringing it into contact with sulphuric acid, which in turn lowers the pH of the slurry and thereby renders it unstable. Decomposition takes place in gypsum-saturated water, at a liquid to solid ratio that allows the calcium and sulphate ions to remain in solution as supersaturated calcium sulphate. The decomposition reaction stoichiometry is the reverse of that for ettringite formation. The end of this stage is characterised by thickening and filtration, which separates into an insoluble aluminium hydroxide and gypsum. The supersaturated solution of calcium sulphate is contacted with gypsum crystals, as in Stage 2, in order to crystallize the calcium sulphate, which is removed by thickening and filtration. The gypsum-saturated water is recycled to the beginning of stage 5 while the aluminium hydroxide is recycled as feed for stage 3.

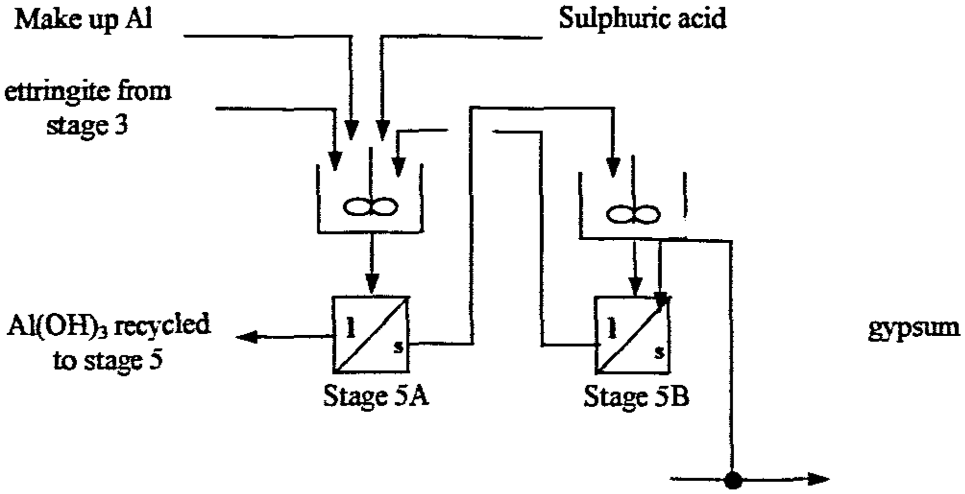

Figure 1.6 *Stage 5 of the Chemical Precipitation Process*

1.5 Objectives

A preliminary model was developed by Mintek to simulate the Savmin process. This simulation was done on an Aspen Plus simulation package. The main purpose of this project was to investigate this model and to subsequently modify the model if necessary. In order to get to that point, certain objectives need to be achieved, and they are outlined below as follows:

- Examine the formation of ettringite by forming it under laboratory conditions.

- Perform an extensive literature review on all the precipitation processes involved in the Savmin process with emphasis on the properties of ettringite, namely:

    - Crystal structure
    - Field of stability
    - Formation and decomposition of ettringite
    - Substitution of anions
    - Substitution of cations
    - Solubility

- Investigate the effect of non-ideal conditions on the formation of ettringite. This is achieved by altering operating parameters in the model, and evaluating the effects on the removal of calcium and sulphate.

- Performing a sensitivity analyses on the model by altering various physical parameters at the different stages. Investigate how these sensitivities affect the treatment of AMD as well as the reagent costs involved.

- Attempts to modify the existing ASPEN model.

CHAPTER 2

LITERATURE REVIEW

The functioning of the Chemical Precipitation process, which was described in chapter 1, is essentially based on precipitation processes. The main solids that are precipitated in this process are:

- Ettringite
- Metal hydroxides
- Gypsum and
- Calcium carbonate

Product water of different qualities can be produced. This purified water can be classed in three different groups depending on the requirement of the water. The resulting water is classed as follows: -

Agricultural water	($Ca^{2+} < 300$ ppm; $SO_4^{2-} < 500$ ppm)
Potable water	($Ca^{2+} < 150$ ppm; $SO_4^{2-} < 200$ ppm)
High quality industrial water	($Ca^{2+} < 50$ ppm; $SO_4^{2-} < 50$ ppm)

This literature study investigates these precipitates and the conditions under which they form.

2.1 Precipitation

According to Söhnel and Garside (1992), it is probably impossible to produce a precise definition of precipitation, at least in part because there is no clear dividing line between the two phenomena (i.e. 'precipitation' vs. 'crystallization'). They stated that it is perhaps best to think of precipitation as embodying fast crystallization and that the rapidity of the precipitation process is a consequence of the high supersaturation at which it takes place. This definition results in a number of consequences, most of which give rise to other characteristics of precipitation, namely:

- Materials that are relatively insoluble usually precipitate since the low solubility of these materials allows the development of high supersaturations.

- Primary nucleation rates are usually very high as a result of the high supersaturations at which nucleation takes place. This underlines the importance of nucleation in the precipitation processes.

- These high nucleation rates result in a large number of crystals being produced, which has a limiting effect on the average size to which the crystals can grow. Consequently, the concentration of particles is usually very high, normally between about 10^{11} and 10^{16} particles per cm^3, while the size of the crystals are usually relatively small, possibly between 0.1 and 10μm.

- A number of secondary processes, such as ripening, ageing, agglomeration and coagulation may occur if the precipitated crystals are sufficiently small, which could cause major changes in the precipitate size distribution.

- Precipitation is sometimes referred to as "reactive crystallization" because the supersaturation that is necessary for precipitation frequently results from a chemical reaction. Many of these reactions are fast, thus emphasizing the role of mixing in the precipitation processes.

- Precipitations are usually carried out at constant temperature and do not usually rely on cooling to produce supersaturation.

2.2 Crystal Growth kinetics

According to Benefield *et al.* (1982), precipitation can be thought of as a two-step process: nucleation and crystal growth. He states that nucleation is the generation of crystals (birth) in the solution, whereas growth is the process where atoms or molecules are transported to the individual crystal surface and are then orientated into the crystal lattice. Figure 2.1 has been constructed to explain what effect the degree of oversaturation has on the precipitation process. This graph represents a batch reactor system. When high degrees of supersaturation (the region labeled as "labile") take place, the solution will undergo rapid precipitation by means of spontaneous nucleation and crystal growth. However, when low degrees of supersaturation (the region labeled as "metastable") take place, no visible precipitation will take place for long periods of time. This upper value of the metastable region will differ depending on the salt and has been observed to be as high as 10 times the solubility value. In order to initiate rapid precipitation in the metastable region, certain seed crystals need to be added.

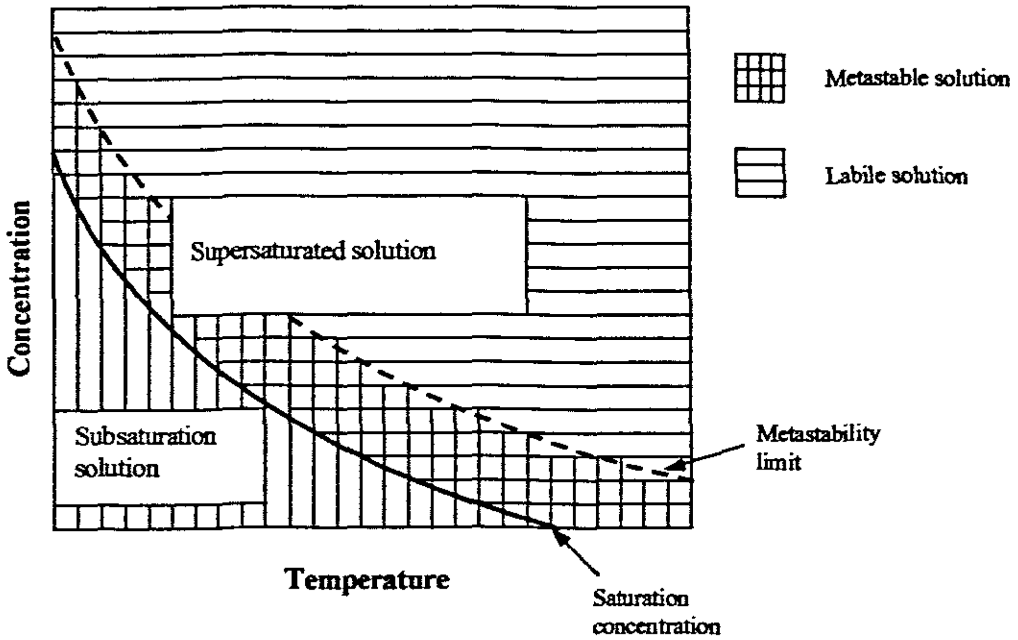

Figure 2.1
Solubility diagram showing subsaturated, labile and metastable supersaturated solutions.

2.3 Ettringite

Ettringite in its natural form has been known for more than 100 years. It was first discovered at the Ettringer Bellerberg in Eifel, West Germany. Candlot documented a compound with a similar composition in hardened cement stone in 1890. By 1892, Michaelis named this salt "cement bacillus" because of its deteriorating properties. Notable occurrences include several South African localities such as Hotazel and Kuruman District. It is commonly found in weathered cement, cement based solidification by-products and alkaline fly ashes (McCarthy *et al.*, 1992; Myneni *et al.*, 1997).

Ettringite, as we know it today, represents a whole group of acicular calcium aluminate hydrates which have the general composition:

$$3CaO.\ Al_2O_3 \cdot 3CaX_2 \cdot nH_2O$$

or

$$3CaO.\ Al_2O_3 \cdot 3CaY \cdot nH_2O$$

with $X = OH^-, NO_3^-, \ldots$ and $Y = SO_4^{2-}, CO_3^{2-}, \ldots$

There exists a series of related compounds, known as a mineral group or family, and they include the following minerals:

Charlesite	$Ca_6(Si,Al)_2(SO_4)_2(B[OH]_4)(OH)_{12}.26H_2O$
Sturmanite	$Ca_6Fe_2(SO_4)_2(B[OH]_4)(OH)_{12}.26H_2O$
Thaumasite	$Ca_6Si_2(SO_4)_2(CO_3)_2(OH)_{12}.24H_2O$
Jouravskite	$Ca_6Mn_2(SO_4)_2(CO_3)_2(OH)_{12}.24H_2O$
Bentorit	$Ca_6(Cr,Al)_2(SO_4)_2(OH)_{12}.26H_2O$

Ettringite is often called **Aft** by cement chemists. It forms in hydrated Portland cement from reactions of dissolved sulphate with tricalcium aluminate ($Ca_3Al_2O_6$) and "ferrite" ($Ca_4(Fe,Al)_4O_{10}$). **Aft indicates that the ettringite structural phase is an Aluminate Ferrite trisulphate.**

2.3.1 Crystal Structure of Ettringite

The minerals of the ettringite group form hexagonal prismatic or acicular crystals. According to Moore and Taylor (1970), its crystal structure consists of columns arranged parallel to the c-axis and channels between the columns. The ettringite structure is fairly significant and is made up of calcium aluminium hydroxide hydrate columns $(Ca_6Al_2[OH]_{12}.24H_2O)^{6+}$ (Figure 2.1(b)) with the intercolumn SO_4^{2-} holding the columns together through electrostatic interactions as is shown by Figure 2.1(a). The columnar Al is in octahedral coordination with 6 OH^-, and Ca atoms are in 8-fold coordination with 4 OH^- and 4 H_2O molecules. These Ca-coordinated water molecules are projected into the channels and surround the outer-sphere sulphate ions. Thus, ettringite surfaces consist of $\equiv CaOH_2$, $\equiv Ca_2OH$, and $\equiv AlOH$ functional groups and, of these, the $\equiv CaOH_2$ functional groups are predominant. The channels between the parallel columns consist of water molecules and anions. When this ettringite contains sulphates, the channel composition has a formula

$$\{3SO_3 \cdot nH_2O\}^{-6}$$

With n = 2 at 65% r.h.

Visible changes in the morphology of ettringite occur when ettringite crystals grow in the presence of organic additives, some of which are known to act as set-retarders in Portland cement (Pöllmann *et al.* (1989)).

2.3.2 Compounds with Ettringite structure

Ettringite has the capacity for uptaking other metals. Al^{3+} may be replaced by any trivalent cation of similar size by means of isomorphic substitution. It has also been discovered that the zeta potential, defined as the electric potential in the double layer at the interface between a particle which moves in an electric field and the surrounding liquid, of ettringite is −11.7 mV measured at a pH of 10.7 (Chen and Mehta, 1982). This makes ettringite a good absorbent for positively charged metal species. Moreover, in high pH regimes, dangling metal oxide bonds of phyllosilicates or multioxide feldspars, and ettringite surface sites are negatively charged (Mohamed *et al.*, 1995). This makes it possible for ettringite to be absorbed on the ettringite structure. Dangling metal oxide bonds at the edge of a polyhedron are possible surface complexation sites on ettringite.

Ettringite can withstand modest deviations in composition without a change in structure. This compositional change can occur on a crystal chemical level in the form of ionic substitution. Al^{3+} in ettringite can be substituted by Ti^{3+}, Cr^{3+}, Mn^{3+} and Fe^{3+} to form similar compounds of the type $Ca_6[M(OH)_6](SO_4)_3.26H_2O$ (Bensted and Varma,1972). According to McCarthy *et al.,* (1992), SO_4^{2-} can be replaced by CrO_4^{2-}, MnO_4^-, Cl^-, OH^-, CO_3^{2-} and NO_3^-.Similarly, Sr^{2+}, Ba^{2+}, Ni^{2+} and Zn^{2+} may replace Ca^{2+}.

2.3.2.1 Substitution of cations

Bensted and Varma (1971), did extensive investigation in replacing Al^{3+} with other cations, like Ti^{3+}, Cr^{3+}, Mn^{3+}, Fe^{3+}, to form other ettringite-like compounds. This led to similar compounds of the type, $Ca_6[M(OH)_6]_2(SO_4)_3{\cdot}26H_2O$, where M represents the appropriate metal in its trivalent oxidation state. What these metals have in common with Al^{3+} is that they have a similar ionic radii as well as third ionization potential, as indicated in Table 2.1. This accounts for there ability to form ettringite-like compounds. According to Bensted and Varma (1971), the formation of Cr^{3+} and Fe^{3+} derivatives can be understood by the stability of their +3 oxidation states in the presence of weak ligand fields such as those due to H_2O and OH^-. He stated that Ti^{3+}, which has a d^1 configuration, does not rapidly oxidize to Ti(IV) (having a stable d^0 configuration) which would destroy such a structure, but it is sufficiently stable to allow the formation of an ettringite. Other cationic substitutions that were successfully documented are the substitutions of Si^{4+} in an octahedral coordination.

Table 2.1 *Ionization potential and Ionic radii according to Bensted and Varma (1971)*

Element	3rd ionization potential (volts) $M \rightarrow M^{3+} + 3e^-$	Ionic radius (Å) of M^{3+} ion
Al	28.44	0.51
Ti	27.47	0.76
Cr	30.95	0.63
Mn	33.69	0.66
Fe	30.64	0.64

2.3.2.2 Substitution of anions

Anionic substitution also takes place as with the 3 SO_4^{2-} being replaced by 3 CrO_4^{2-}, 3 CO_3^{2-}, 6 NO_3^- (Pöllmann *et al.*, 1989) and 6 OH^- groups.

Pöllmann et al., (1989) investigated the synthesis of various ettringite compounds by means of the "saccharat method", which was first described by Carlson & Berman (1960). His investigation resulted in the synthesis of:

Sulphate ettringite	$3CaO \cdot Al_2O_3 \cdot 3CaSO_4 \cdot 32H_2O$
Carbonate ettringite	$3CaO \cdot Al_2O_3 \cdot 3CaCO_3 \cdot 32H_2O$
Hydroxide ettringite	$3CaO \cdot Al_2O_3 \cdot 3Ca(OH)_2 \cdot 32H_2O$
Nitrite ettringite	$3CaO \cdot Al_2O_3 \cdot 3Ca(NO_3)_2 \cdot 30H_2O$
Sulphite ettringite	$3CaO \cdot Al_2O_3 \cdot 3CaSO_3 \cdot 33H_2O$
Borate ettringite	
(High boron content)	$3CaO \cdot Al_2O_3 \cdot [B(OH)_4]_2 \cdot 2Ca(OH)_2 \cdot 36H_2O$
(Low boron content)	$3CaO \cdot Al_2O_3 \cdot 2[B(OH)_4]_2 \cdot Ca(OH)_2 \cdot 30H_2O$

Of these, the most stable compound was found to be sulphate ettringite. All these ettringite compounds became amorphous because they lost the molecular water of their channels at temperatures ranging between 70°C to 85°C. Crystallization and the stability of the ettringite compounds are largely affected by its shape and extension of the incorporated anions.

2.3.3 Formation of ettringite

Ettringite forms willingly in cementitious systems whenever there are components that contain large amounts of calcium, aluminium and sulphate that can be dissolved at pH values of about 12. A few examples of the formation of ettringite in cementitious systems based on solid wastes from coal conversion are:

i. High-calcium fly ash.
ii. Flue gas desulfurization (SO_2 scrubber) residues
iii. Fluidized bed combustion and other advanced coal combustion residues

These coal combustion residues are extremely reactive when they are exposed to natural waters, and are observed to modify soil element dissolution patterns and to control surface and sub-surface water quality in their vicinity (Mattigod *et al.*, 1990; Fowler *et al.*, 1993). When these materials weather, the pH increases to above 10 and dissolved Ca^{2+}, Al^{3+}, and SO_4^{2-} ion concentrations result in the formation of ettringite as one of the dominant secondary mineral phases (Mattigod *et al.*, 1990; Damidot *et al.*, 1992; Damidot and Glasser, 1993; Fowler *et al.*, 1993; Myneni, 1995). Fowler has also shown that ettringite formation takes place simultaneously with the reduction of leachate trace elements.

In order to synthesize ettringite, a water solution containing large enough quantities of Ca^{2+}, SO_4^{2-} and an aluminium-containing agent is required as is shown by the following stoichiometric reaction:

$$6Ca^{2+} + 3SO_4^{2-} + 2Al(OH)_3 + 37H_2O \rightarrow \underbrace{3CaO \cdot Al_2O_3 \cdot 3CaSO_4 \cdot 31H_2O}_{\textbf{ettringite}} + 6H_3O^+ \qquad (2.1)$$

For the purposes of this exercise, $Al(OH)_3$ is used as the aluminium-containing agent. The formation of ettringite takes place in an alkaline medium where it is most stable between pH values of 11.4 and 12.4 (Myneni *et al.*, 1997).

In solution at these pH values, aluminium exists largely as the amphoteric $Al(OH)_4^-$ species. The solubility curves (Figure 2.3) for aluminium hydroxide species show that below a pH of 10.3, aluminium exists largely as insoluble amorphous aluminium hydroxide ($Al(OH)_3(am)$). The aqueous formation of ettringite should therefore not be possible below a pH of 10.3, since it is assumed that the aluminium must be present as the amphoteric species for ettringite to form. In addition to this, once the synthesis of ettringite takes place, its stability is pH dependent. The stability of the mostly ettringite product is further enhanced if it contains additional alkaline components such as calcium hydroxide (portlandite), since the portlandite has additional acid-neutralizing potential

2.3.4 Decomposition of ettringite

Ettringite is an alkaline solid, which dissolves at a much lower pH. Solubility products vary and according to Reardon (1990), log $K_{sp} = -43.13$. Furthermore, temperature, dissolved CO_2, and H_2O activity can strongly influence ettringite stability. According to McCarthy *et al.* (1992), their experimentation suggested that ettringites cannot be considered "stable" phases below a pH of about 11, or in highly alkaline, pH > 12.5 solutions. Their results were largely in accord with pH stability relations described by Hampson & Bailey (1982) who proposed the following solubility equation:

$$Ca_6Al_2(SO_4)_3(OH)_{12} \cdot 26H_2O \rightarrow 6Ca^{2+} + 2Al(OH)_4^- + 3SO_4^{2-} + 4OH^- \qquad (2.2)$$

Hampson & Bailey (1982) suggested that in a system with sufficient sulphate activity, at pH values less than approximately 11, ettringite is unstable due to the low solubility of $Al(OH)_3$ (see Figure 2.2) and above approximately 12.5, its instability is because of the low solubility of $Ca(OH)_2$. In order to bring ettringite outside its range of stability, it should be treated with either acid, to drop the pH, or alkali, to raise the pH.

In order for the equilibrium of ettringite in an aqueous solution to exist, that solution should contain adequate activities of the appropriate species of calcium, aluminium and sulphate. Ettringite will therefore dissolve if other low solubility phases dominate the activities of Ca and Al at too low a value. When acid is added to a solution that is in equilibrium with ettringite, the activity of the OH^- is reduced and the activity of $Al(OH)_4^-$ falls off markedly as $Al(OH)_3$ precipitates.

Besides adjusting the pH of ettringite to get it outside its region of stability, various authors have investigated its decomposition by means of altering the temperature. Ettringite could therefore be thermally decomposed into calcium aluminate monosulphate and calcium sulphate hemihydrate at high temperatures, which exceed 110°C (Hall *et al.*, 1996). According to Damidot and Glasser (1992), monosulphoaluminate is more stable than ettringite at high temperatures. Nishikawa *et al.*, *1992, stated that at high* CO_2 *and low* H_2O *activity level, ettringite decomposed to aragonite* with vaterite as an intermediate phase.

2.3.5 Ettringite solubility

Jones (1944), studied the various mineral phases when Ca^{2+}, SO_4^{2-}, Al^{3+}, and water reacted under alkaline conditions. He concluded that the minerals that formed in this system are solid solutions of ettringite as well as monosulphoaluminate ($Ca_4Al_2(SO_4)(OH)_{12} \cdot 6H_2O$), and that these coexist with gibbsite, gypsum and portlandite (see Figure 2.2). Of these phases that were formed, ettringite was found to be the most stable in high alkaline and sulphate rich solutions [Jones (1944); Damidot and Glasser (1993)]. Myneni's (1995) work on the influence of pH on the solubility product constant of ettringite in the pH stability range (10.7 to 12.5) revealed that there was no change in the K_{sp}. Similar observations were also reported by Atkins *et al.* (1991), Damidot *et al.* (1992), and Warren and Reardon (1994). Standard free energies of formation was estimated as −15204.7 ± 23 kJ/mol (Myneni *et al.*, 1997) and −15207.0 kJ/mol (Warren and Reardon, 1994).

Ettringite can also exist at pH values < 10.7, but only in association with gypsum and $Al(OH)_3$, while it completely dissolves at near neutral pH (Myneni *et al.*, 1997).

2.4 Metal Hydroxides

Heavy metals such as zinc, copper, iron, magnesium, nickel and cadmium are often present in polluted water systems. Various methods exist to remove these metals, i.e. precipitation, sorption and ion exchange. The preferred method of removal of heavy metals, using this process, is precipitation.

2.4.1 Removal by precipitation

The concentration of metal in solution can be lowered by precipitation to a point dictated by the solubility of the various species of that metal. Most metals are usually precipitated as hydroxides, carbonates and sulphides because they are relatively insoluble in this form. The precipitation of metals as hydroxides is achieved by adjusting the pH to between 8 and 11. Many metal hydroxides are amphoteric in nature and exhibit an optimum pH for the removal by precipitation. This optimum pH is synonymous with the associated minimum solubility of the metal concerned.

2.4.2 Effect of hydrolysis on solubility

Metal ions exist in solution as hydrated ions. In an aqueous solution, hydrated metal ions react with hydroxyl ions to form hydro complexes, which will contain one or more mteal ions (mono or polynuclear complexes). Benefield *et al.* (1982) uses the following generalized equations to describe the hydro complex formation reactions for a trivalent metal ion when only mononuclear complexes are formed:

$$Me_{(aq)}^{3+} + OH^- \leftrightarrow Me(OH)_{(aq)}^{2+} \quad (2.3)$$

$$Me_{(aq)}^{3+} + 2OH^- \leftrightarrow Me(OH)_{2(aq)}^{+} \quad (2.4)$$

$$Me_{(aq)}^{3+} + 3OH^- \leftrightarrow Me(OH)_{3(aq)}^{0} \quad (2.5)$$

$$Me_{(aq)}^{3+} + 4OH^- \leftrightarrow Me(OH)_{4(aq)}^{-} \quad (2.6)$$

These complex formation reactions can be used to construct solubility diagrams, as has been done in Figures 2.2, 2.3, 2.4, and 2.5. The associated hydro complex reactions are tabulated in the appendix. These curves indicate how the solubility's of $Al(OH)_3$, $Fe(OH)_2$, $Fe(OH)_3$, and $Mg(OH)_2$ change with a change in the pH. The solubility of $Al(OH)_3$ and $Fe(OH)_3$ is increased under both acidic and basic conditions. At low pH's (acidic conditions), both form cationic species which increase the solubility of the solid phase, while at high pH's (alkaline conditions), they form anionic species which increase the solubility of the solid phase. These curves also show that $Fe(OH)_2$, $Fe(OH)_3$, and $Mg(OH)_2$ will precipitate at fairly high pH ranges.

2.5 Gypsum

The formation of gypsum is described by the reaction of Ca^{2+} with SO_4^{2-} and water as represented by this stoichiometric reaction:

$$Ca^{2+} + SO_4^{2-} + H_2O \rightarrow CaSO_4 \cdot 2H_2O \qquad (2.7)$$

It is a relatively insoluble solid that has a low solubility product (log K_{sp}= -4.64)

2.6 Calcium carbonate

The principle reason for bubbling carbon dioxide gas into the ettringite treated water, is to reduce the pH to a suitable level. This can be seen be the following reaction:

$$H_2O + CO_2 \rightarrow CO_3^{2-} + 2H^+ \qquad (2.8)$$

A carbonate ion (CO_3^{2-}) is formed as well as 2 hydrogen ions. The presences of the H+ ions will inevitable lower the pH. The CO_3^{2-} ions will now react with the Ca^{2+} ions in solution in solution to form calcium carbonate as shown below.

$$Ca^{2+} + CO_3^{2-} \rightarrow CaCO_3\,(s) \qquad (2.9)$$

$CaCO_3$ is a relatively insoluble solid with a low solubility product (log K_{sp} = -8.35).

Besides altering the pH, by precipitating $CaCO_3$, small quantities of calcium are also removed from the solution.

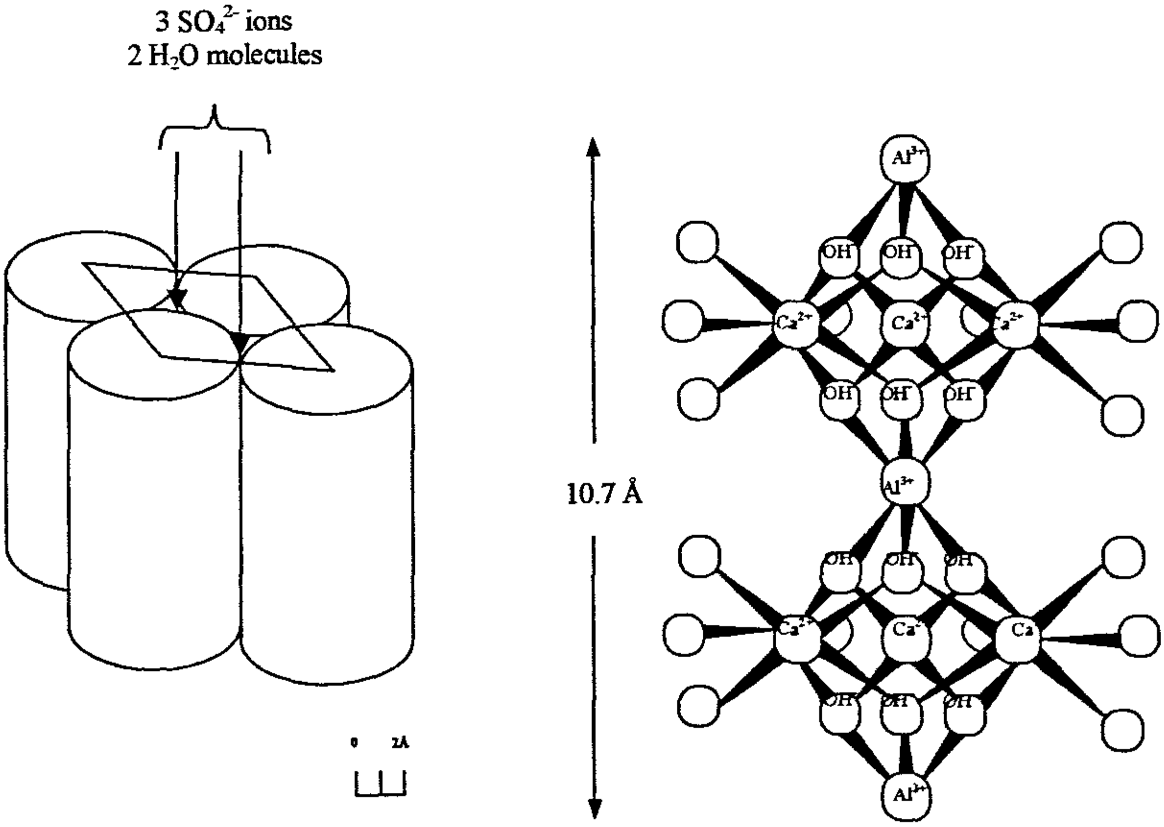

(a) (b)

Figure 2.2
Structure of Ettringite according to Moore and Taylor(1970)

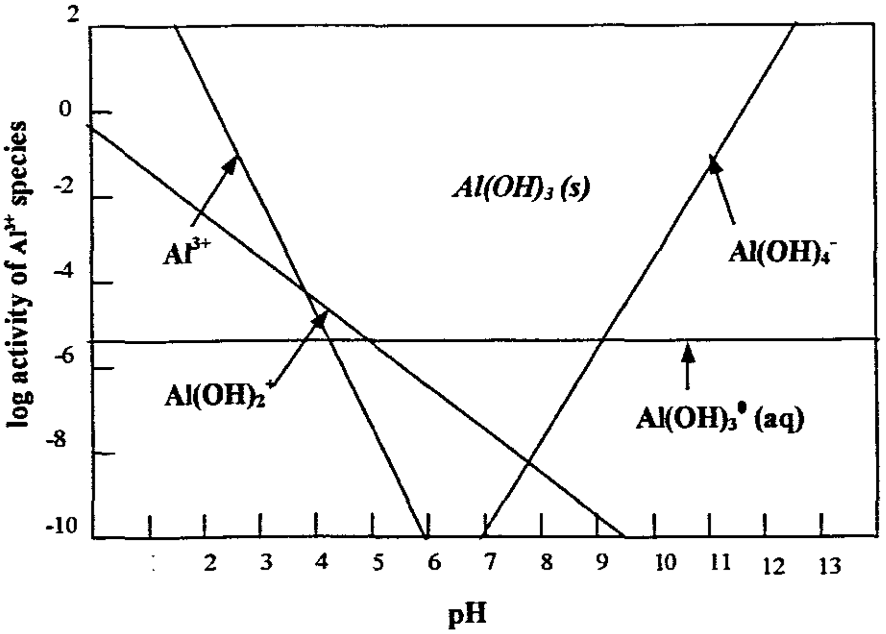

Figure 2.3
Solubility diagram for aluminium hydroxide

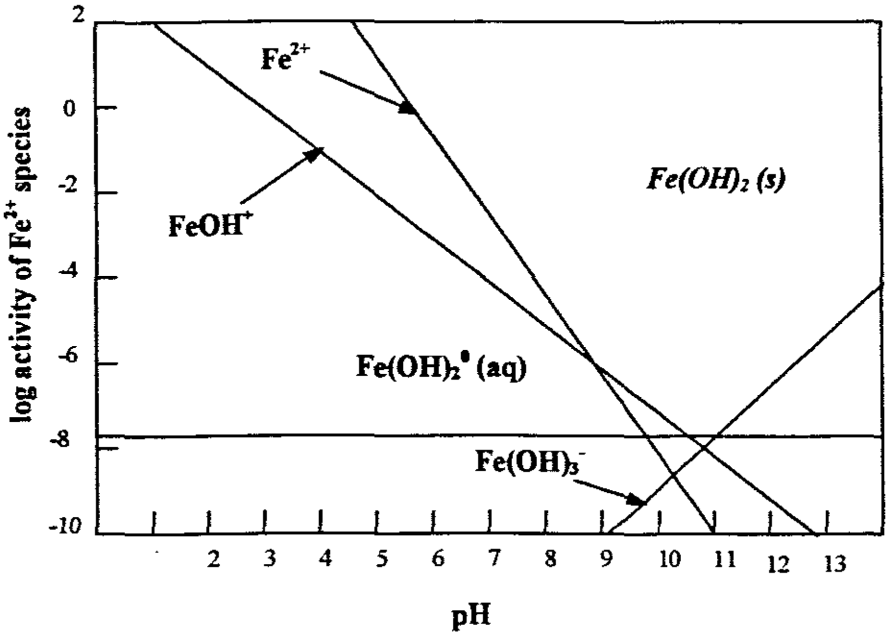

Figure 2.4
Solubility diagram for iron (II) hydroxide

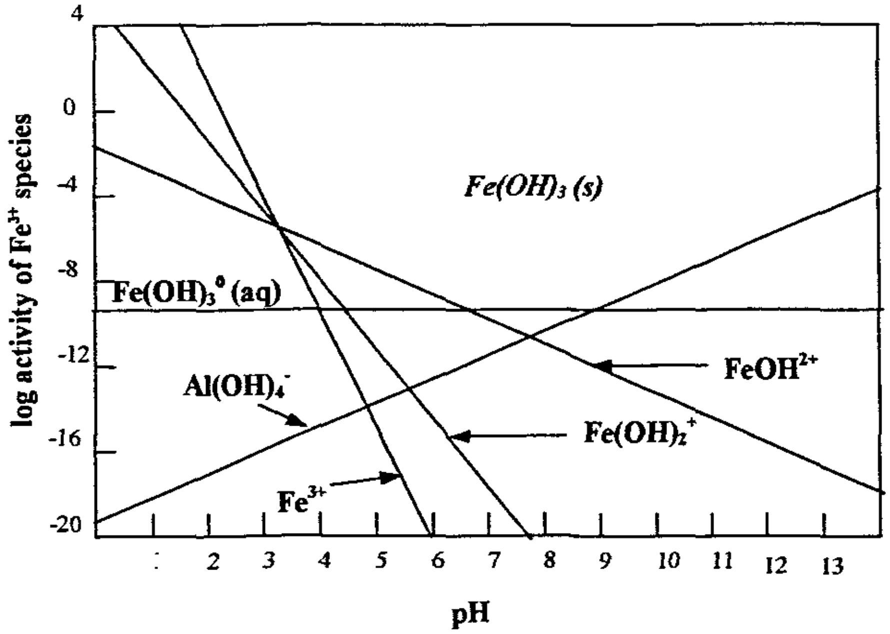

Figure 2.5
Solubility diagram for iron (III) hydroxide

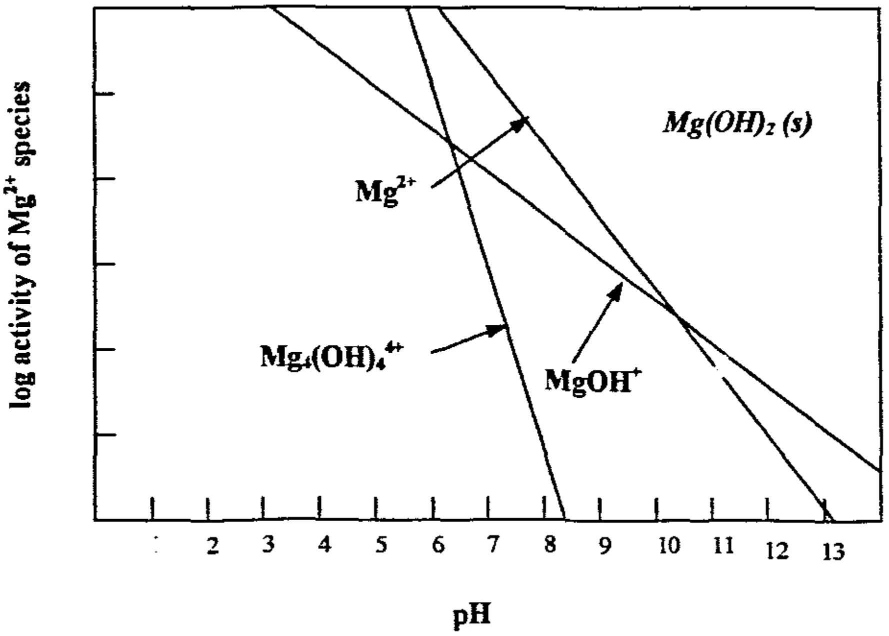

Figure 2.6
Solubility diagram for magnesium hydroxide

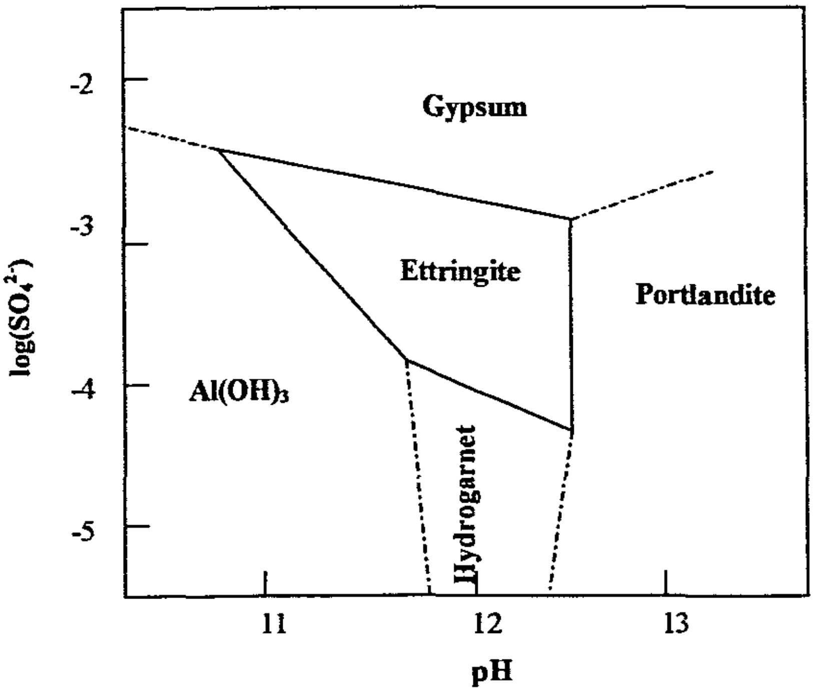

Figure 2.7
Ettringite stability in alkaline environments (Hampson and Bailey, 1982)

CHAPTER 3

EXPERIMENTAL

This chapter describes the experimental procedure used to produce and decompose ettringite under laboratory conditions. The purpose of the experiment is to confirm the formation (and break down) of ettringite under conditions specified in literature. The experiment was also used to investigate the removal of both calcium and sulphate.

3.1 Reagents

In addition to normal tap water being used to perform this experiment, a number of other reagents that were obtained by Associated Chemical Enterprises c.c. were also used. These include: -

- calcium sulphate dihydrate (gypsum), $CaSO_4 \cdot 2H_2O$
- Amorphous aluminium hydroxide, $Al(OH)_3$
- Calcium hydroxide, $Ca(OH)_2$
- Sulphuric acid, H_2SO_4

The chemicals used to perform this experiment were all of AR grade.

3.2 Experimental method

The explanation of the experimental procedure is best decribed with reference to Figure 3.1. A synthetic solution was prepared by dissolving 2.7 g of calcium sulphate dihydrate in one liter of distilled water to yield a saturated calcium sulphate solution. This solution was agitated and a sample was taken and named sample 1. To the saturated solution 0.6g of amorphous $Al(OH)_3$ was added. In order to raise the pH in the beaker, and thereby set the correct conditions for the formation of ettringite, $Ca(OH)_2$ powder was added. This was done until the pH stabilised at 11.9.

The stability of the pH was done over a period of approximately 30 minutes. The solution was then filtered off leaving behind a white cake-like substance, which was dried. Another sample, sample 2, was taken from the supernatant, which resulted from the filtration. The dried cake was the added to 1 liter of a 30% H_2SO_4 solution. This allowed the ettringite to be broken down again. A final sample, sample 3, was taken from the decomposed ettringite solution. All 3 samples were tested by ICP analysis in order to determine the relevant calcium, aluminium and sulphate contents. A mass balance was done over the whole system to determine the amount of calcium, sulphate and aluminium removed. The dried cake was analyzed by means of XRD analysis to verify the formation of ettringite.

3.3 Equipment used

This experiment was performed in a batch configuration, using a 1000 ml glass beaker with a magnetic stirrer. The pH was measured by means of an HANNA HI8314 membrane pH meter, calibrated by using buffer solutions of pH 7 and 10 respectively. Filtration was performed by means of a 1000 ml erlen Meyer flask with a small Buckner funnel. 90mm WHATMAN filter paper was used to filter the synthetic solution. Sample solutions were analyzed for calcium, sulphate and aluminium by means of ICP analysis and solids were analyzed by means of X-Ray diffractometry (XRD) to test for the formation of ettringite.

3.4 Observation and Results

The pH of the synthetic calcium sulphate solution was recorded as 8.45 but as soon as the aluminium hydroxide was added, the pH started to rise as a result of the presence of OH^- ions. Lime was added and after approximately 2 minutes a decline in the pH was observed. This signaled the formation of ettringite. The pH was kept constant at 11.9. The results obtained by means of the ICP are tabulated in Table 3.1 and were used to determine the amount of calcium and sulphate removed when this precipitate is formed.

Table 3.1

Sample results from experimentation

	Sample 1	Sample 2	Sample 3
Ca^{2+} (ppm)	794	425	1295
SO_4^{2-} (ppm)	1900	133	2200
Al^{3+} (ppm)	-	6.2	212

This experiment yielded results which showed that 68% of calcium was removed while 92% of sulphate was removed on a mass basis. The product water also yielded only 6.2 ppm of aluminium as shown in sample 2.

Testing of the solid cake by X-ray diffractometry indicated that ettringite definitely was formed under these conditions. Besides ettringite being formed, these tests also showed that portlandite as well as calcite had also formed (see XRD spectrum Figure 3.2).

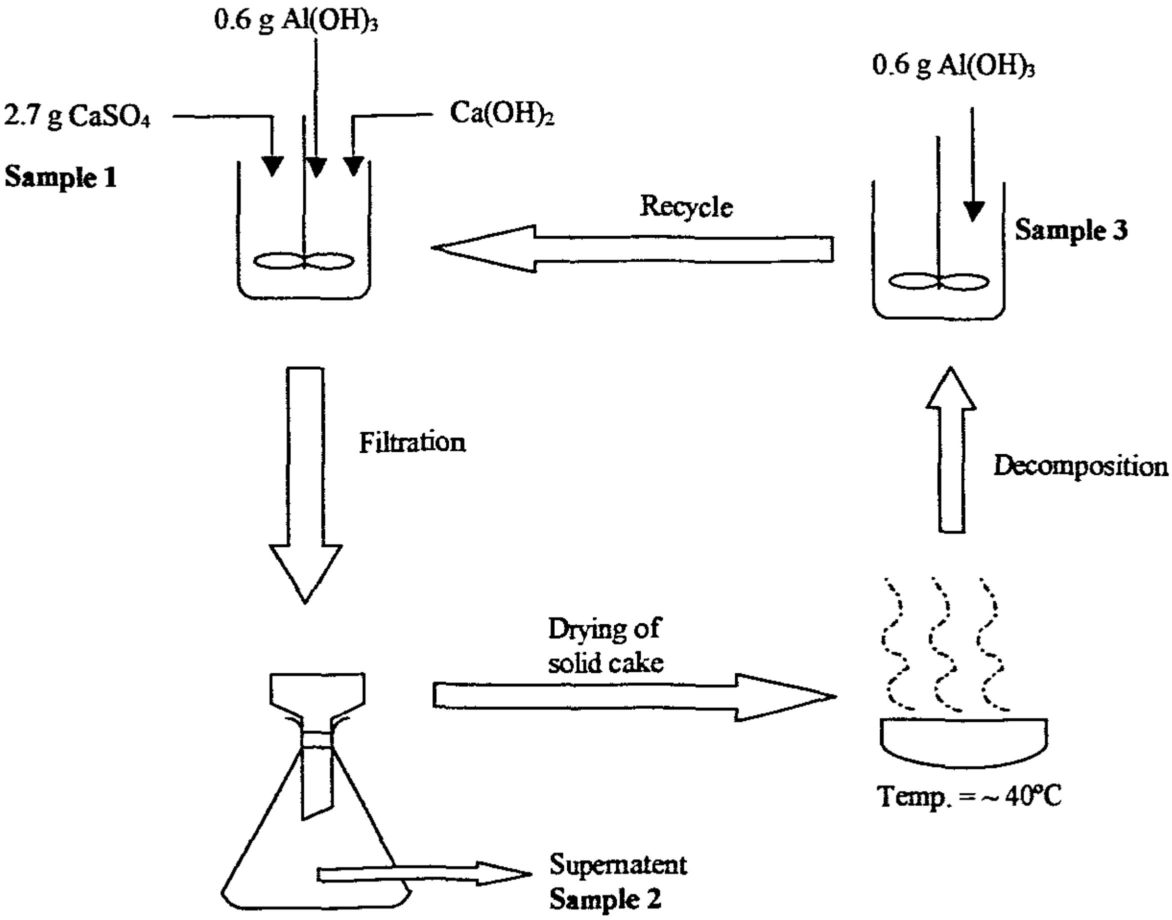

Figure 3.1
Diagrammatic representation of the experimental process.

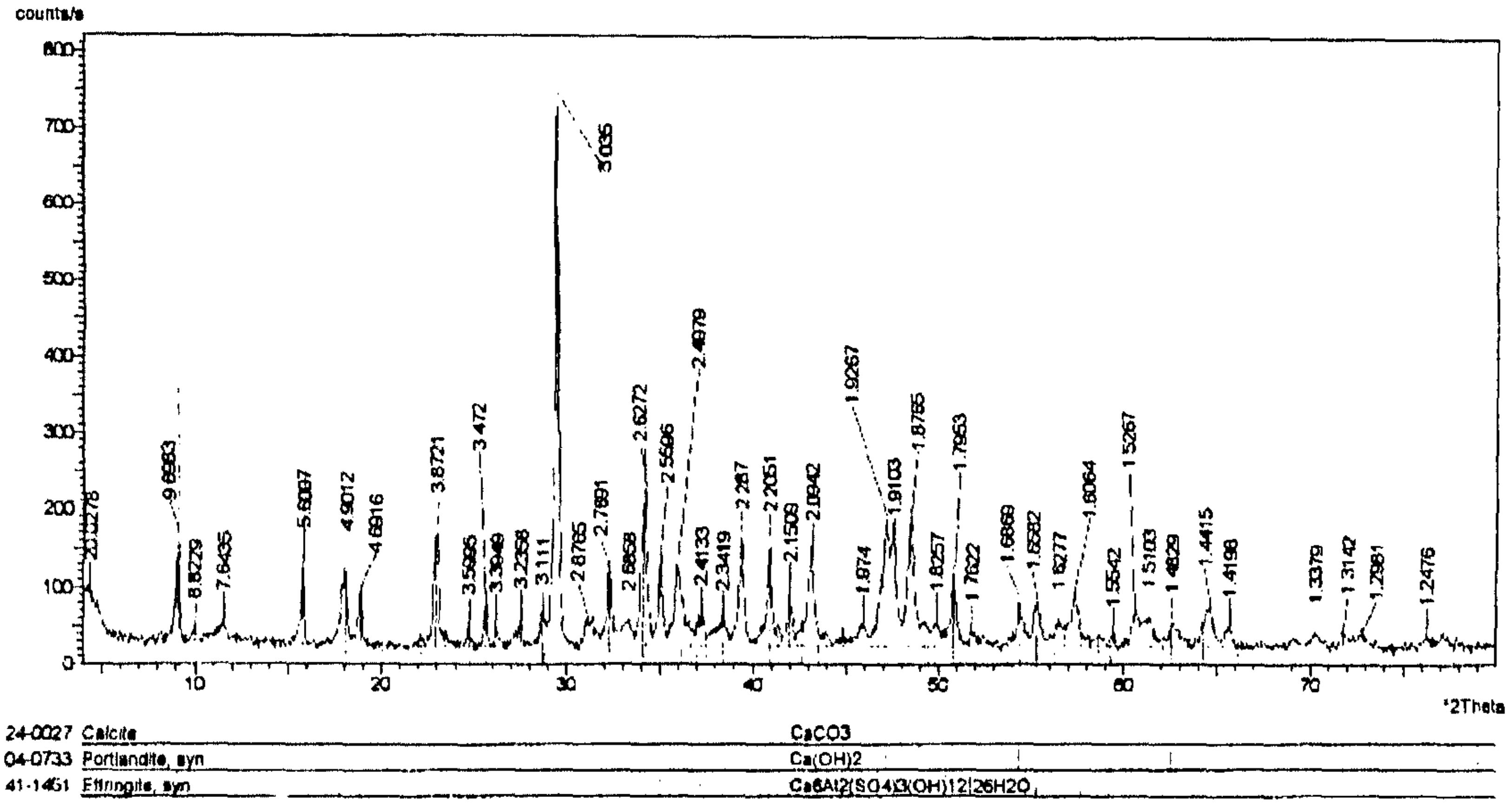

Figure 3.2

Diffractogram indicating the presence of ettringite

CHAPTER 4

THEORY

4.1 Introduction

The essence of this paper is based on simulating the Chemical Precipitation process by means of a computer-generated simulation program. The program used to perform this intricate task is known as the ASPEN PLUS *simulation package. In order to fully utilize this tool, one needs to* understand how it works and on which principles the simulator performs its relevant calculations.

A preliminary model was completed by MINTEK and Figure 4.1 illustrates its flowsheet.

The modeling of this process is based on: -

- Mass balance principles
- Chemical reactions
- Thermodynamics
- Design specifications

In addition to these, the program uses various convergence techniques to solve the many recycle loops present.

4.1.1 Relevance of a Process Simulator

The question may arise as to why this process or any process for that matter needs to be simulated. A number of reasons have been stipulated to answer that question, namely: -

- Simulating the Savmin Process on an Aspen Plus simulation package serves as a useful tool to predict the behaviour of the process.
- It is a cost effective means of examining how the process is affected by using certain quantities of chemicals, using various grades of polluted water, changing flow rates, and altering the split fractions at separators.
- Simulators are often used at the laboratory and pilot plant stages of plant design, and it is no different for this process.
- This simulation acts is a guideline as to how this process will react under actual conditions.
- Aspen Plus makes it possible to determine the effects of non-ideal conditions on ettringite formation and serves as a guide for the trends that are obtained when analyzing various sensitivities.

4.1.2 Chemical Reactions

When setting up a process flowsheet on Aspen, and after inserting all the reactors, separators, streams etc; the various chemical reactions need to be specified. Aspen contains a large database, which is useful when determining what type of reactions will take place when certain chemicals react. When the Chemical Precipitation process was constructed, the chemical reactions were inserted without the use of the database. These reactions have been specified in Table 4.1. When reactions are specified, Aspen checks whether they are possible and will not run if the reactions are unlikely to take place. The formations of products from reactants by means of chemical reactions are calculated using conventional chemistry where moles of reacts are converted to moles of products. From here the relevant masses and concentrations can also be determined.

4.1.3 Mass balance principles

As with all chemical engineering processes, material balancing over a system is of paramount importance. Mass balances can take place around one unit (i.e. reactor, separator, flash drum, and heat exchanger etc) or over the entire process. A material balance is simply comparing the amount of material entering a unit or process to what is exiting. Even in chemical reactions, there is the law of conservation of mass, which states that the mass remains constant during a chemical change (chemical reaction). Therefore, over the entire process, all volumes, energy, masses, and specific component masses should be in balance, whether it is over one unit or over the entire process. Aspen operates on the same principle and the process will only run to completion once all the material balances have been completed.

4.1.4 Thermodynamics

Thermodynamics is the study of the relationship between heat and other forms of energy involved in a chemical or physical process (Ebbing (1987)). This branch of science is not only useful in determining enthalpies, entropies, heat of reaction and formation, but for the purposes of this project its main use is found in the spontaneity of reactions. The spontaneity of a reaction is measured by means of Gibbs free energy, G, which is a thermodynamic quantity defined by the equation $\Delta G^\circ = \Delta H^\circ - T\Delta S^\circ$. Here, ΔH° denotes the standard enthalpy, which is simply the heat of reaction at constant pressure. T is the temperature and S° denotes the standard entropy, which is a measure of the randomness or disorder in the system. Standard enthalpies of formation, standard entropies of formation as well as free energies of formation (ΔG°) for selected substances and ions are found in the databases in Aspen. For a given reaction, the standard enthalpy change for a reaction is $\Delta H^\circ = \Sigma n\Delta H^\circ_f$ (products) - $\Sigma m\Delta H^\circ_f$ (reactants). Similarly, the standard entropy change and the standard free energy change have the same form. When $\Delta G^\circ < 0$, then the reaction takes place spontaneously and reactants transform almost entirely to products when equilibrium is reached. If, however $\Delta G^\circ > 0$, then the reaction does not take place spontaneously and reactants do not give significant amounts of products at equilibrium. When $\Delta G^\circ = 0$ then the reaction gives an equilibrium mixture with significant amounts of both reactants and products.

4.1.5 Design Specifications

When setting up an Aspen flowsheet, various inputs need to be included in order for the program to run. These inputs include feed flow rates, feed component concentrations, split fractions at separators and chemical reactions at reactors, etc. Occasionally, the need arises to provide specifications for variables or parameters that are not permitted by any unit (i.e. separators, reactors, etc). To accomplish this, Aspen provides a facility for iterative adjustments of the variables and parameters that are permitted to be specified so as to achieve the desired specifications. Simulation calculations are performed after guesses are made of the so-called manipulated variables and a control subroutine makes a comparison between the calculated value and the desired specification, or set point. As soon as significant differences are detected, new guesses are prepared by the control subroutine, by means of numerical methods, and the simulation calculation is repeated. This procedure is similar to feedback control subroutines in a chemical plant, which is designed to reject disturbances during dynamic operations.

4.1.6 Convergence

For Aspen to solve the unknown stream variables in the recycling loops, it uses a solution technique, which is based on tear stream guesses. In the recycle loop, a guess is taken of the variables of one of the streams (tear stream) in the loop and information is passed from unit to unit until new values of the variables in the tear stream are computed. These new values are used to repeat the calculations until the convergence tolerances are satisfied. This is the principle behind the method of successive substitutions for convergence. Upon satisfying the convergence criteria, control is transferred to the unit following the recycle loop in the calculation order.

Aspen uses a number of convergence methods to converge recycle loops. Two methods are specified in this particular program, namely the Wegstein and Secant methods respectively (see Appendix D)

4.2 ASPEN MODELLING

The design specifications of the model in question together with the convergence and computational order are explained in Appendix C and D.

The Aspen simulation flowsheet is illustrated in Figure 4.1. The feed water (stream 1) enters at a flow rate of 300 m^3/h and has the following composition.

Table 4.2 *Aspen feed water components*

$MgSO_4$(ppm)	$FeSO_4$(ppm)	H_2SO_4(ppm)	$CaSO_4$(ppm)
148	100	10	2200

This amounts to 567 ppm calcium and 1697 ppm sulphate in the feed water. A 40% lime concentration was made-up at streams 2 and 15, and enters at a flow rate of 108 kg/hr and 369 kg/hr respectively, thereby adjusting the pH at stages 1 and 3 respectively. 90 % Sulphuric acid is added at stream 25 at a flow rate of 502 kg/hr in order to decompose the ettringite from stage 3.

The chemical reactions that take place at the various reactors (i.e. R1, R2, R3, R4, R5A, R5B) are tabulated in Table 4.1. This process is modeled with metal hydroxides being removed at stream 8 and gypsum being removed at stream 36. In order for supersaturated calcium sulphate to precipitate as gypsum at stage 2, large quantities of gypsum needs to be in the system. Similarly, in order to prevent scaling with the recycle of aluminium hydroxide, stage 5B also has another recycle which already contains gypsum. This also allows calcium and sulphate ions in solutions to be contacted with gypsum in order to form gypsum.

The program has a number of separators as seen in Figure 4.1. Table 4.3 illustrates the percentage solids being separated into their respective streams e.g. at separators S1A, 99% of the solids in stream 3 is now sent to stream 5.

TABLE 4.3. *Separation of solids from liquids at various separators of the Aspen model.*

Separator	Split percentage
S1A	99% solids to stream 5
S1B	99% solids to stream 7
F1	99% solids to stream 8
S2	99% solids to stream S2
F2	99% solids to stream 36
S3	100% solids to stream 20
S5A	99% solids to stream 30
S5B	99% solids to stream S5B

To further enhance the model, certain design specifications were inserted into the system. These are tabulated in Table 4.4. Design specifications indicate to the program which variable needs to be changed in order to achieve a certain set point for another variable e.g. in order to keep the pH in stream 3 at 11.7, the composition of lime at stream 2 needs to be varied. This means that even though the composition and acidity of the feed water may change, the pH of 3 will remain constant.

TABLE 4.4. *Design Specifications of the ASPEN model.*

Design specification of set point	**Vary variable to achieve set point**
flow rate of feed water =300 m^3/hr	mass flow of feed (stream 1)
pH (stream 1) = 9.5	mass flow of CO_2 (stream AA)
pH (stream 3) = 11.7	mass flow of lime (stream 2)
% solids entering reactor R2 = 5%	flow fraction of stream 12
pH (stream R3) = 11.95	mass flow of lime (stream 15)
[SO_4^{2-}] at stream R3 = 200ppm	conversion of SO_4^{2-} to ettringite (stage 3)
pH (stream R4) = 8.5	mass flow of CO_2 (stream 22)
pH (stream R5A1) = 9	mass flow of H_2SO_4 (stream 25)
% solids entering reactor R5B = 5%	flow fraction of stream 34
very kg of SO_4^{2-} fed to stage 3, ~ 1 kg of $Al(OH)_3$ is fed to stage 5)	mass flow of stream 26
Metal hydroxides(stream 8) = 25% solids	flow fraction of stream 8
Gypsum(stream 36) = 60% solids	flow fraction of stream 36
% solids in stream 5 = 1.5%	flow fraction of stream 5
% solids in stream 7 = 5%	flow fraction of stream 7
% solids in stream S2 = 30%	flow fraction of stream S2
% solids in stream 20 = 15%	flow fraction of stream 20
% solids in stream 29 = 15%	flow fraction of stream 29
% solids in stream S5B = 30%	flow fraction of stream S5B
[Ca^{2+}] at stream R5A =1.5kg/m^3	flow fraction of stream 27

Potable water (Ca^{2+} < 150 ppm; SO_4^{2-} < 200 ppm) was recovered by treating AMD using the Aspen modeling approach. The results for the production of potable water obtained may be seen in Appendix B. A table (Table 4.5) depicting the amount of species removed from solution shows that for a supersaturated calcium sulphate feed solution, 87% of the sulphate was removed and 97% of the calcium was removed. The removal of the heavy metals was 100%, while no sodium ions were removed from the system.

TABLE 4.5. *Percentage removal of species from solution as predicted by Aspen.*

species	Ca^{2+}	SO_4^{2-}	Na^+	Mg^{2+}
Feed water (ppm)	567	1697	14.89	29.7
Product water (ppm)	17.2	199.8	14.83	0.01
% removal	97	88	0	100

Virtually all the magnesium in the form of magnesium hydroxide is removed at stage 1 (stream 8). The continues process allows for 17 809 kg/hr of gypsum to be recycled at stage (stream 10). The gypsum is contacted with Ca^{2+} and SO_4^{2-} ions from streams 4, 6 and 9 respectively, resulting in 17 911 kg/hr leaving reactor R2 at stream 11. Stage 3 produced 3997 kg/hr of ettringite while 373 kg/hr of gibbsite was recycled. The product water (stream 23) has a calcium and sulphate concentration of 17 ppm and 200 ppm respectively, and has a pH of 8.5.

4.3 Summary

This model is able to treat AMD with varying quantities of calcium and sulphate. At stage 1, it removes metals in the form of hydroxides (i.e. $Mg(OH)_2$) at a pH of 11.7. Calcium and sulphate is first removed at stage 1, where gypsum is precipitated and removed, provided the $CaSO_4$ in the feed water is at a supersaturated level. Gypsum is also formed and recycled at stage 2 to provide the seed crystals for gypsum precipitation when $CaSO_4$ is fed to stage 2. Stage 3 is where the precipitation of ettringite takes place. Here, large portions of calcium and sulphate are removed as well as aluminium hydroxide. The process is designed to produce potable water as stated by the design specifications at stage 3. In order to produce ettringite, gibbsite needs to be rercycled. The recycled gibbsite is formed when ettringite is decomposed at stage 5A. Stage 5B is set in place to prevent scaling by converting excess calcium and sulphate in the recycle to gypsum. This gypsum is then removed at the separator of stage 2. The purified solution entering stage 4 now gets treated with carbon dioxide to alter the pH to 8.5. This produces calcium carbonate which remains in solution in the product water.

TABLE 4.1 *Chemical reactions at different stages of the process*

Stage 1

1. $FeSO_4 \rightarrow Fe^{2+} + SO_4^{2-}$
2. $Al_2(SO4)_3 \rightarrow 2Al^{3+} + 3SO_4^{2-}$
3. $Fe_2(SO4)_3 \rightarrow 2Fe^{3+} + 3SO_4^{2-}$
4. $MgSO_4 \rightarrow Mg^{2+} + SO_4^{2-}$
5. $Al^{3+} + 12H_2O \rightarrow Al_2(OH)_6\ (s) + 6H_3O^+$
6. $Fe^{3+} + 6H_2O \rightarrow Fe(OH)_3\ (s) + 3H_3O^+$
7. $Fe^{2+} + 4H_2O \rightarrow Fe(OH)_3\ (s) + 2H_3O^+$
8. $CaSO_4 \rightarrow Ca^{2+} + SO_4^{2-}$
9. $Ni^{2+} + Ca(OH)_2 \rightarrow Ni(OH)_2\ (s) + Ca^{2+}$
10. $Mg^{2+} + Ca(OH)_2 \rightarrow Mg(OH)_2\ (s) + Ca^{2+}$
11. $H_3O^+ + OH^- \rightarrow 2H_2O$
12. $Ca(OH)_2 \rightarrow Ca^{2+} + 2OH^-$
13. $Zn^{2+} + Ca(OH)_2 \rightarrow Zn(OH)_2\ (s) + Ca^{2+}$
14. $Ca^{2+} + 2F^- \rightarrow CaF_2\ (s)$

Stage 2

$Ca^{2+} + SO_4^{2-} + 2H_2O \rightarrow \text{gypsum}$

Stage 3

1. $CaOH^+ \rightarrow Ca^{2+} + OH^-$
2. $Ca(OH)_2\ (s) \rightarrow Ca^{2+} + 2OH^-$
3. $\text{gypsum}\ (s) \rightarrow Ca^{2+} + SO_4^{2-} + 2H_2O$
4. $6Ca^{2+} + 3SO_4^{2-} + Al_2(OH)_6\ (s) + 37H_2O \rightarrow \text{ettringite}\ (s) + 6\ H_3O^+$
5. $H_3O^+ + OH^- \rightarrow 2H_2O$

Stage 4

$Ca^{2+} + CO_2 + 2OH^- \rightarrow CaCO_3 + H_2O$

Stage 5

Reactor 5A

1. ettringite (s) → $3Ca(OH)_2 + Al_2(OH)_6$ (s) + $3CaSO_4 + 25\ H_2O$
2. $CaSO_4 \rightarrow Ca^{2+} + SO_4^{2-}$
3. $Ca(OH)_2 \rightarrow Ca^{2+} + 2OH^-$
4. $H_2SO_4 + H_2O \rightarrow HSO_4^- + H_3O^+$
5. $HSO_4^- + H_2O \rightarrow SO_4^{2-} + H_3O^+$
6. $H_3O^+ + OH^- \rightarrow 2\ H_2O$

Reactor 5B

$Ca^{2+} + SO_4^{2-} + 2H_2O \rightarrow$ gypsum

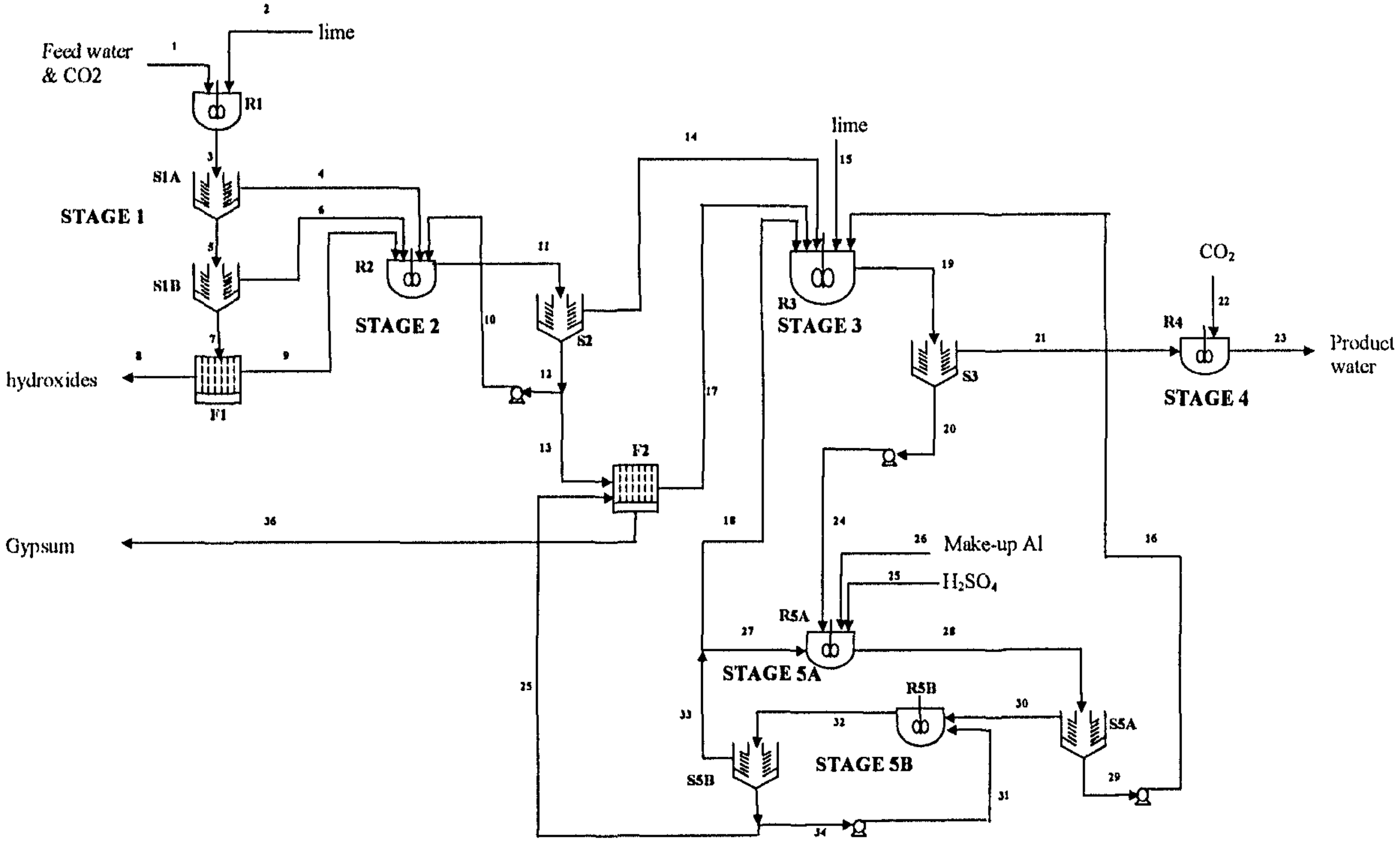

Figure 4.1.
Aspen simulation flowsheet

CHAPTER 5

EFFECTS OF NON-IDEAL CONDITIONS ON ETTRINGITE FORMATION

5.1 Introduction

Under ideal conditions, the Aspen model behaves as described in Chapter 4. For a feed water solution containing 567 ppm Ca^{2+} and 1697 ppm SO_4^{2-}, some of the important results that are obtained are as follows:

- Metals are precipitated as hydroxides at a high pH (i.e. 11.7) at stage 1.
- Gypsum is recycled at stage 2 to be brought into contact with calcium and sulphate in solution to form more gypsum, which is removed.
- Ca^{2+} and SO_4^{2-} is therefore first removed from stage 2 as gypsum. These removal quantities are however very small. The main purpose for the formation of gypsum at stage 2 is to release a constant amount of Ca^{2+} and SO_4^{2-} to stage 3, whenever supersaturated quantities of $CaSO_4$ is present in the feed water.
- The heart of this process is however at stage 3 where ettringite is formed. The formation of this ettringite (1915 kg/hr) results in the removal of 66% calcium and 88% sulphate on a mass basis.
- To form this amount of ettringite, 373 kg/hr of gibbsite is recycled, as a result of decomposition at stage 5A, of which 146 kg/hr is converted to ettringite.
- Excess calcium and sulphate from stage 5A is sent to stage 5B in order to prevent scaling in the recycling stage.

- At stage 4, the pH of the treated water is adjusted to 8.5 by the addition of carbon dioxide. The result is the formation of calcium carbonate, which results in the conversion of more calcium into another form.
- The product water now contains 200 ppm SO_4^{2-} and 17.2 ppm Ca^{2+}, which means a total removal of 88% and 97% respectively.

In order to gain a better understanding of this model, it needs to run under various non-ideal conditions. Changes in the following parameters were investigated:

- Quality of the product water
- Amount of sulphate that is converted to ettringite at stage 3
- Amount of ettringite decomposed at stage 5
- Amount of mono-valent cations in the feed water
- Ratio of calcium to sulphate fed to stage 3
- Amount of solids fed to the decomposition stage

5.2 Quality of product water

3 different qualities of water were investigated using the Aspen model. This analysis involved producing agricultural, potable and high quality industrial water. The composition of these different qualities of water is as follows:

Agricultural water	($Ca^{2+} < 300$ ppm; $SO_4^{2-} < 500$ ppm)
potable water	($Ca^{2+} < 150$ ppm; $SO_4^{2-} < 200$ ppm)
High quality industrial water	($Ca^{2+} < 150$ ppm; $SO_4^{2-} < 50$ ppm)

The results of these 3 runs are tabulated in Appendix A (Tables A1, A2, and A3).

As the quality of the water is improved, more ettringite is produced at stage 3 (i.e. 1407 kg/hr, 1815 kg/hr, and 2044 kg/hr for agricultural, potable and industrial water respectively). If more ettringite is produced, more calcium, sulphate and gibbsite are removed from the polluted water. This is illustrated in Figure 5.1, which shows increasing removals of the species in question as the product water quality improves. The amount of gibbsite recycled does not change much for the 3 grades of water, but the amount converted to ettringite does change.

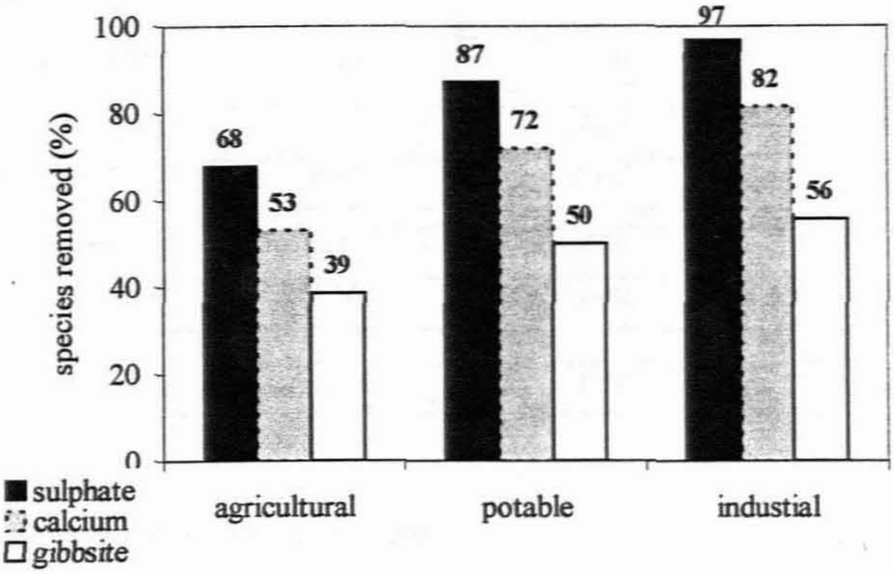

Figure 5.1. *Aspen results of varying product water quality vs. the percentage species removed*

By producing improved qualities of water, so the reagent costs will also be affected. The amount of reagents used at stage 1 remains constant for all 3 grades of water, but changes are evident for the reagents used at stages 3, 4 and 5 (see Table 5.1).

The amount of lime used at stage 3 increases as water quality improves, because more ettringite is being formed. An increase in the amount of ettringite formed, results in more H_3O^+ ions being formed and therefore a drop in the pH. To compensate for this decrease in pH, more lime needs to be added, therefore increasing the cost.

Similarly, the amount of sulphuric acid used also increases as water quality improves, because now more ettringite is decomposed. When decomposition takes place, OH^- ions are produced, which causes the pH to increase. This increase results in an increase in H_2SO_4 being added to drop the pH to the specified value.

Table 5.1. *Reagents used and their costs for different product water grades*

	Agricultural	Potable	Industrial
Lime (stage 1), kg/hr	108	108	108
Lime (stage 3), kg/hr	303	370	408
Cost of lime, R/m^3	0.430	0.497	0.538
CO_2 (stage 4), kg/hr	77.6	79.9	94.1
Cost of CO_2, R/m^3	0.124	0.127	0.146
H_2SO_4, kg/hr	342	437	480
Cost of H_2SO_4, R/m^3	0.364	0.466	0.512
Total reagent costs	0.92	1.09	1.20

5.3 Conversion of sulphate to ettringite

The formation of ettringite takes place due to the stoichiometric reaction at stage 3 :

$$6\,Ca^{2+} + 3SO_4^{2-} + \text{gibbsite (s)} + 37\,H_2O \rightarrow \text{ettringite (s)} + 6H_3O^+ \qquad (5.1)$$

These results are tabulated in Appendix A (Table A4 (i)). By varying the mole conversion of SO_4^{2-} in reaction 5.1, it was possible to ascertain how the system would react to different quantities of sulphate being used to form ettringite. This leads to a linear relationship between the sulphate converted to ettringite and the ettringite being formed. Figure 5.2. represents this relationship between the conversion of sulphate and the formation of ettringite. When 90% of the sulphate available at stage 3 takes part in reaction 5.1, then 2014 kg/hr of ettringite is formed. The conversion of sulphate also has a linear effect on the conversion of calcium and recycled gibbsite, which is clear from the reacting relationship in reaction 5.1. An increase in the conversion of sulphate yields an increase in both the amount of calcium being removed from the contaminated water, as well the gibbsite from the recycle stream. A linear increase in the amount of ettringite being formed will result in a linear increase in the amount of aluminium in the form of gibbsite being produced when the ettringite is decomposed. Figure 5.3. shows the linear relationship between the conversion of sulphate at stage 3 and the formation of gibbsite, as well as the recycling of gibbsite, when ettringite is decomposed. As more ettringite is formed, so less gibbsite is left unreacted (stream 20). When more ettringite is decomposed, more gibbsite is formed but this quantity is small compared with the unreacted amount entering stage 5 (stream 19). This results in a decrease in the amount of gibbsite recycled.

The reagent costs incurred when varying the conversion of sulphate to ettringite is largely affected by the lime to stage 3 and the sulpharic acid at stage 5 (see Table A4 (ii), Appendix A). When the conversion of sulphate increases, ettringite formation increases, and therefore more lime is required to meet the conditions necessary for ettringite formation. As more ettringite is formed, more ettringite will be decomposed. As increasing amounts of ettringite are decomposed, therefore more acid is required to meet the conditions stipulated for decomposition. The increased lime and acid consumption will affect the total reagent costs as illustrated by Figure 5.4. This graph shows an almost linear increase in the total reagent costs from R 0.41 /m^3 to R1.20 /m^3 as the conversion of sulphate to ettringite increases from 10% to 100%.

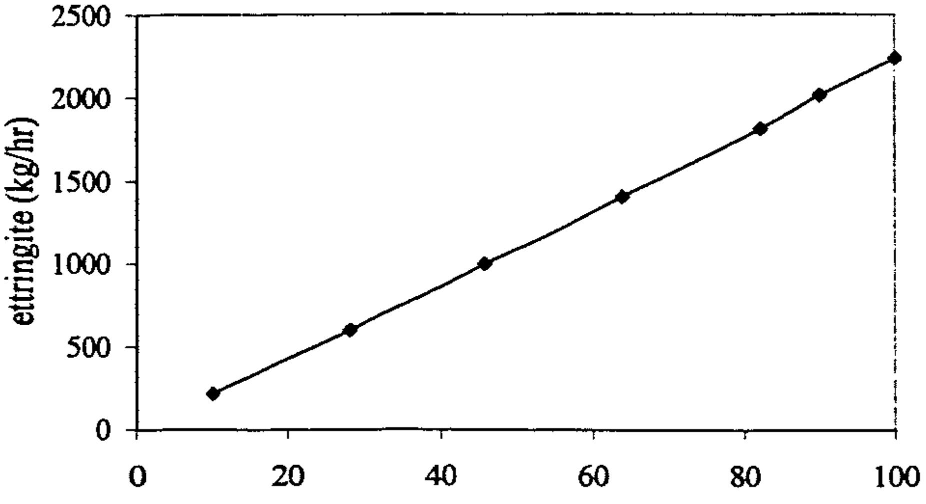

Figure 5.2. *Aspen results showing the conversion of sulphate to ettringite vs.ettringite produced*

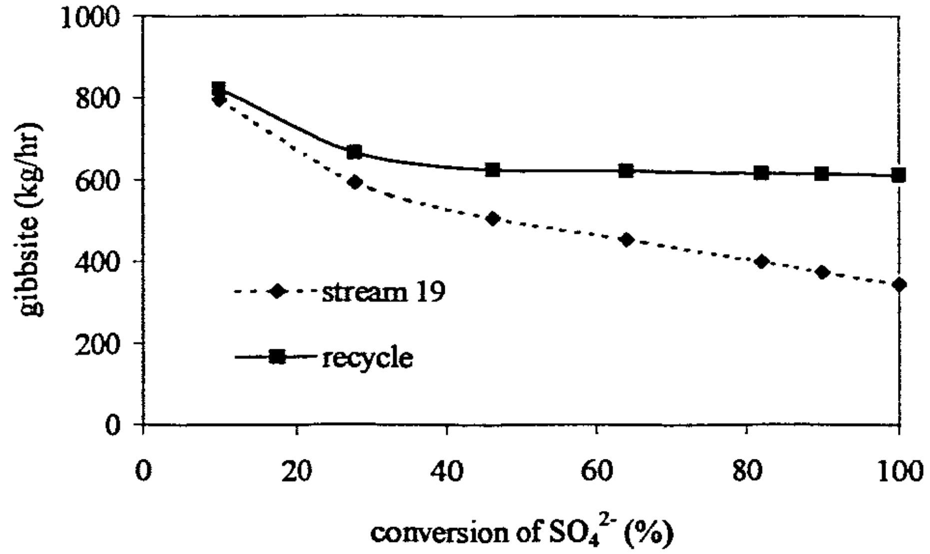

Figure 5.3. *Aspen results showing the conversion of sulphate to ettringite vs.gibbsite quantities*

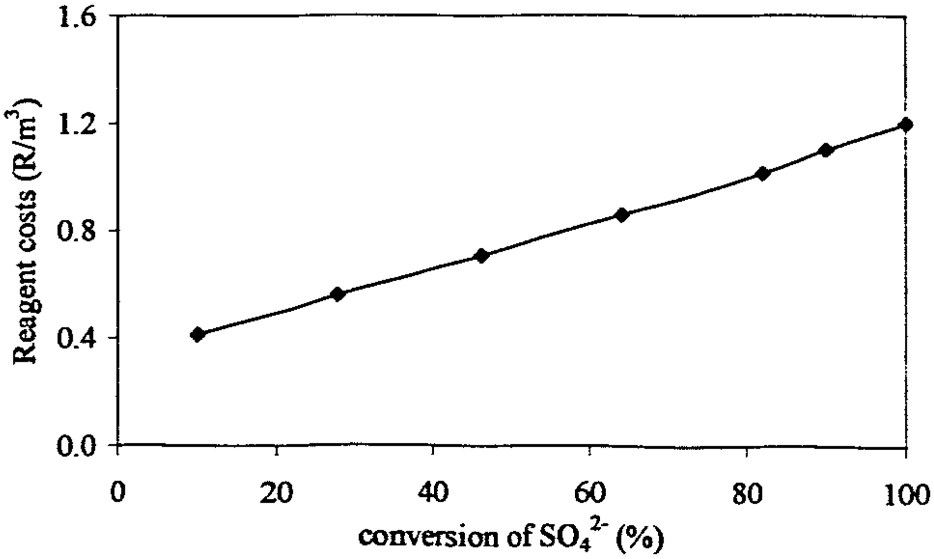

Figure 5.4. *Aspen results showing the conversion of sulphate to ettringite vs.total reagent costs*

5.4 Decomposition of ettringite

The decomposition of ettringite takes place due to the stoichiometric reaction 5.2 at stage 5:

$$\text{ettringite (s)} \rightarrow 3Ca(OH)_2 + \text{gibbsite (s)} + 3CaSO_4 + 25\ H_2O \qquad (5.2)$$

Results for this run are tabulated in Table A5(i) in Appendix A. As more ettringite decomposes, more gibbsite will be formed and ultimately more gibbsite will be recycled as shown by Figure 5.5. In order to meet all the conditions of the recycle loop, a large amount of ettringite needs to be made available to be decomposed when very little decomposition of ettringite takes place. This also means that that when very little ettringite is decomposed, a large amount of ettringite will be recycled (Figure 5.5). It would therefore not make economic sense if decomposition is very low. When the decomposition of ettringite is between 10% and 43%, all the gibbsite that is formed and recycled is again used to form ettringite at stage 3. This results in a 100% removal of gibbsite when ettringite is formed as shown by Figure 5.7. As more ettringite is decomposed between these decomposition ranges, more sulphate and calcium is also recycled and ultimately reacts to form ettringite (Figure 5.6 & 5.7). When more than 43% of ettringite is decomposed, enough gibbsite is formed and recycled in order to meet the demand set for ettringite formation. From this point onwards, the amount of sulphate entering stage 3 remains constant and therefore a constant removal of sulphate to form ettringite takes place. The increasing amount of gibbsite recycled as more ettringite is decomposed means that less of this gibbsite will react to form ettringite when the amount of sulphate reacting at stage 3 remains constant (Figure 5.7). This results in a fairly constant formation of ettringite as seen by Figure 5.6.

The trend for the total reagent costs (Figure 5.8) is very similar to the graph showing the formation of ettringite (Figure 5.5). Reagent costs results are tabulated in Table A5 (ii) in Appendix A. As the decomposition of ettringite increases from 10% to 48%, so the lime as well as acid consumption increases from R 0.47 /m^3 to R 0.83 /m^3 respectively. When decomposition exceeds 48%, lime and acid consumption gradually decrease resulting in a decrease in the reagent costs.

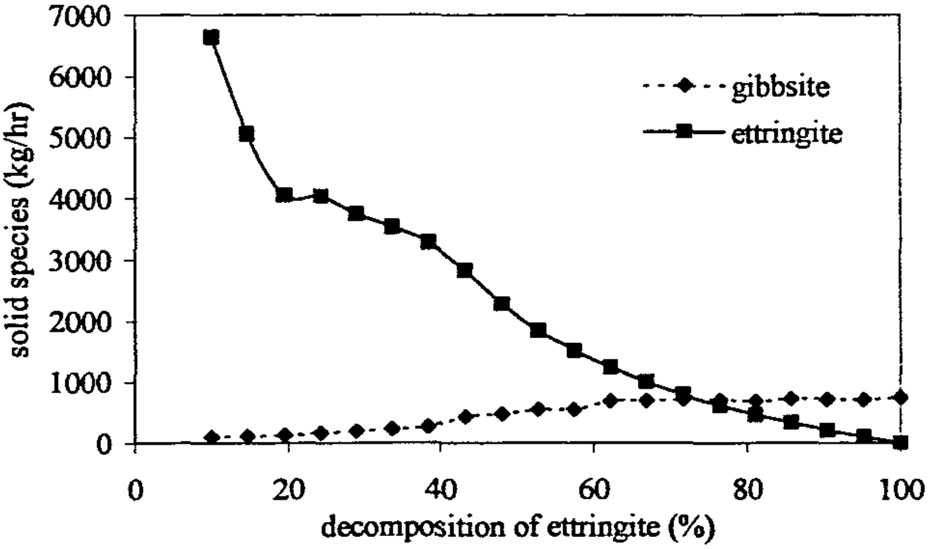

Figure 5.5 *Aspen results showing the decomposition of ettringite vs. solid species recycled.*

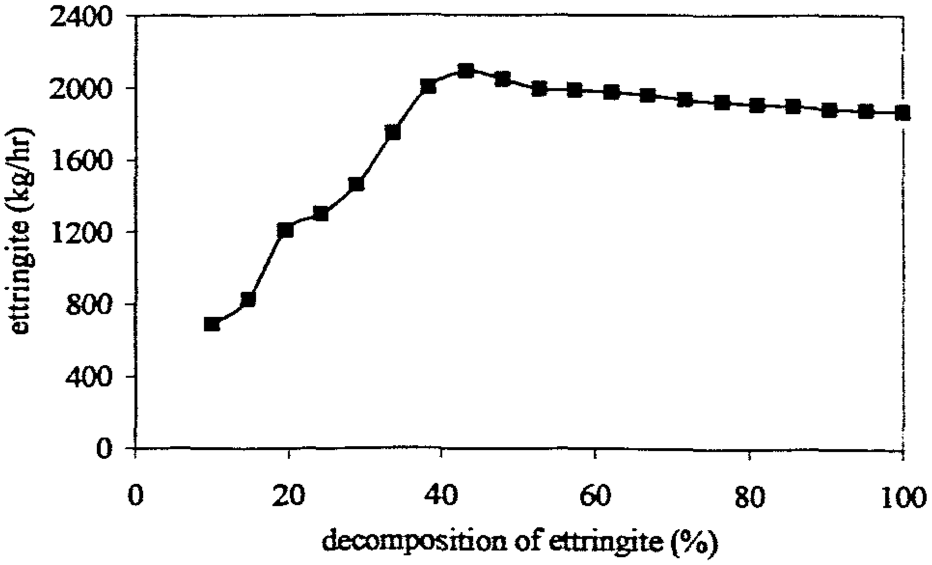

Figure 5.6. *Aspen results showing the decomposition of ettringite vs. ettringite produced*

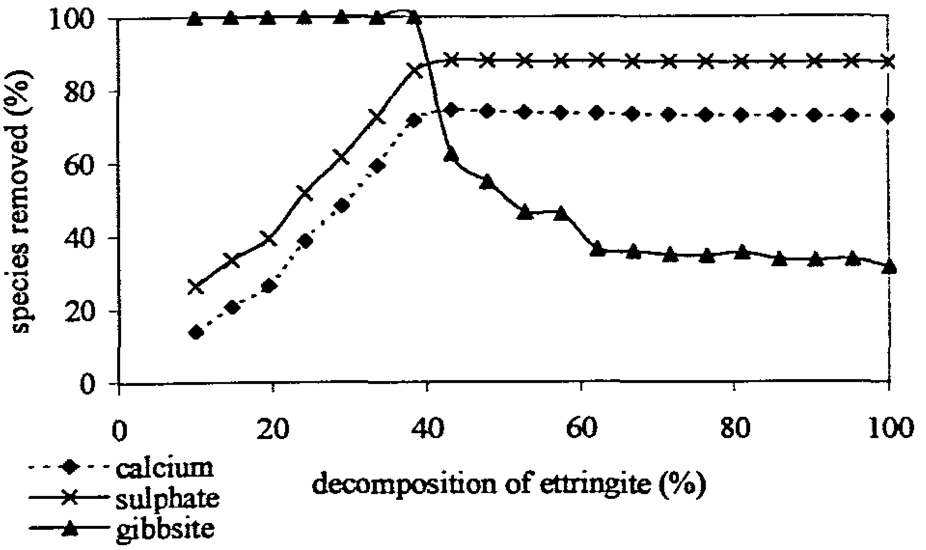

Figure 5.7. *Aspen results showing the decomposition of ettringite vs. species removed at stage 3*

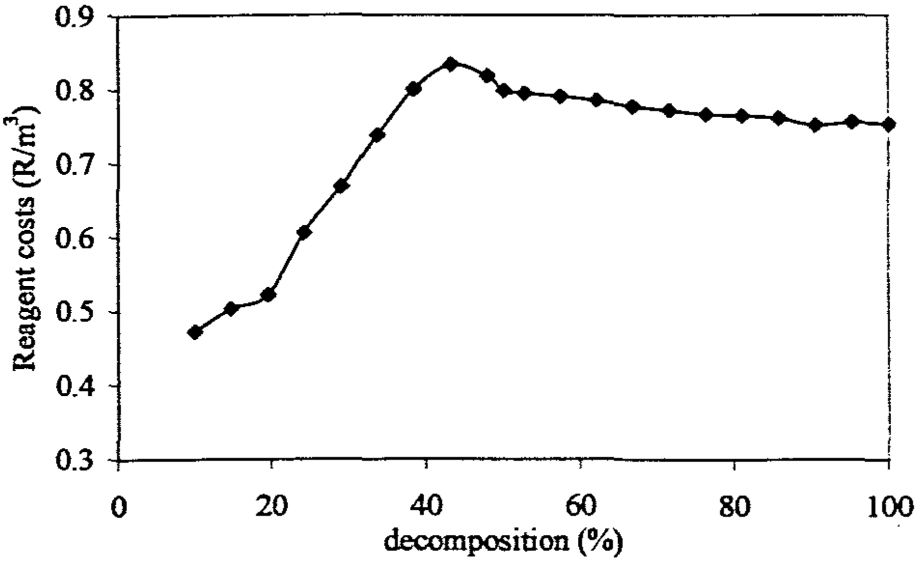

Figure 5.8. *Aspen results showing the decomposition of ettringite vs. total reagent costs*

5.5 Mono-valent cations in feed water

The presence of Na^+ and K^+ in the feed water has the effect that alters the solubility of the sulphate in the water. The preliminary results contained 15 ppm Na^+, and showed that the solubility of sulphate at a pH of 9.5 at stream 1 was 1.697 g/l. As more sodium chloride was added to the feed water, the solubility of calcium and sulphate increased as can be seen in Table A6(i) of Appendix A. The increase in the solubility of sulphate with an increase in NaCl in the feed water is also illustrated in Figure 5.9. Here, the concentration of sulphate increases from 1697 ppm to 1775 ppm as the NaCl increases from 15 ppm to 415 ppm. This increase in sulphate solubility at stage 1 results in the amount of gypsum precipitated at stream 8 to decrease.

The consequence of an increase in the presence of mono-valent cations is an increase in the concentration of sulphate and calcium entering and ultimately leaving stage 2. As larger amounts of sulphate and calcium are fed to stage 3, more ettringite will be produced and would leave stage 3. Figure 5.10 shows an increase in ettringite at stage 3 from 1919 kg/hr to 2062 kg/hr as the amount of NaCl in the feed water increases. An increase in ettringite results in a invrease in the amount of gibbsite recycled (see Figure 5.11).

An increase in ettringite formation leads to an increase in lime as well as acid consumption, which results in an increase in the total reagent costs (see Table A6 (ii), Appendix A). Figure 5.12 illustrated how an increase in NaCl in the feed from 15 ppm to 415 ppm causes the reagent costs to increase from R 1.09 /m^3 to R 1.15 /m^3.

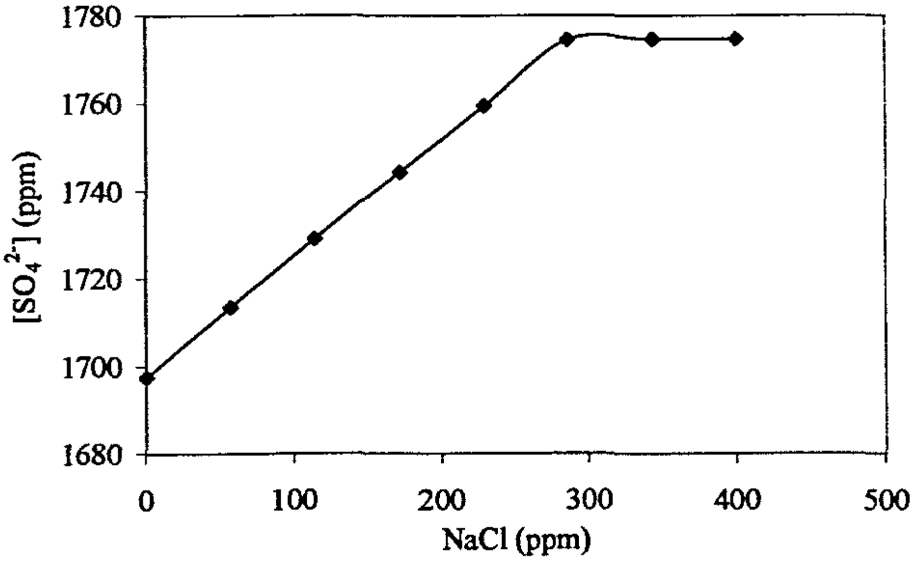

Figure 5.9. *Aspen results showing NaCl in the feed water vs. the solubility of sulphate at stage 1*

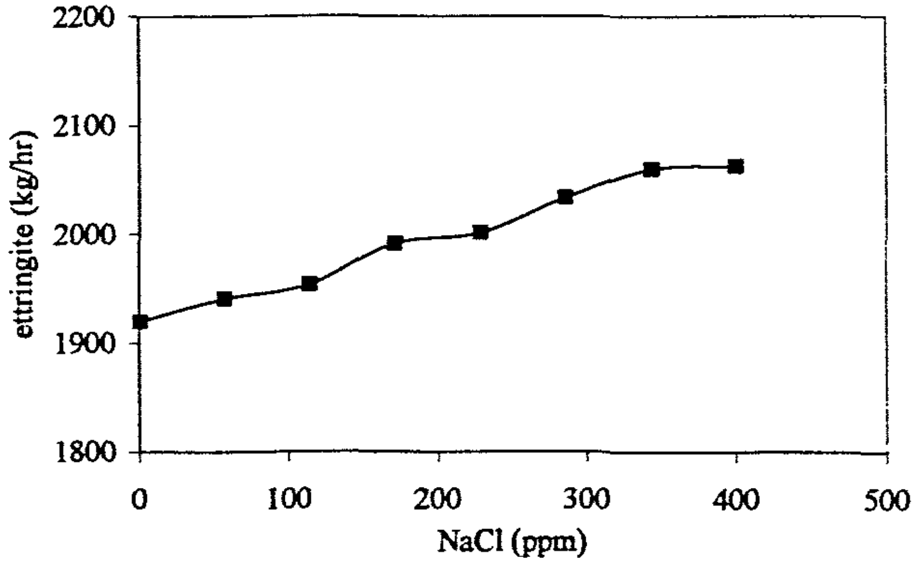

Figure 5.10. *Aspen results showing NaCl in the feed water vs. the ettringite leaving stage 3*

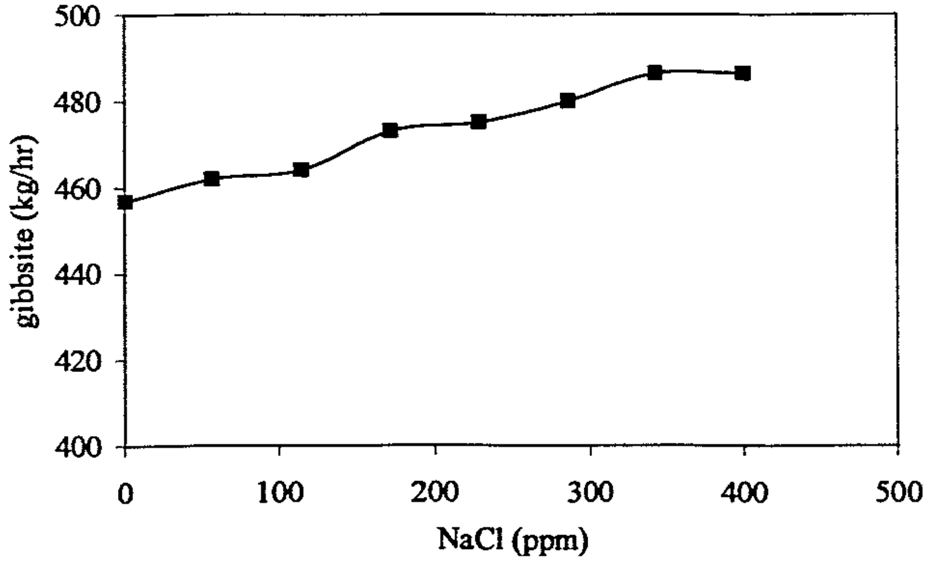

Figure 5.11. *Aspen results showing NaCl in the feed water vs. the gibbsite recycled*

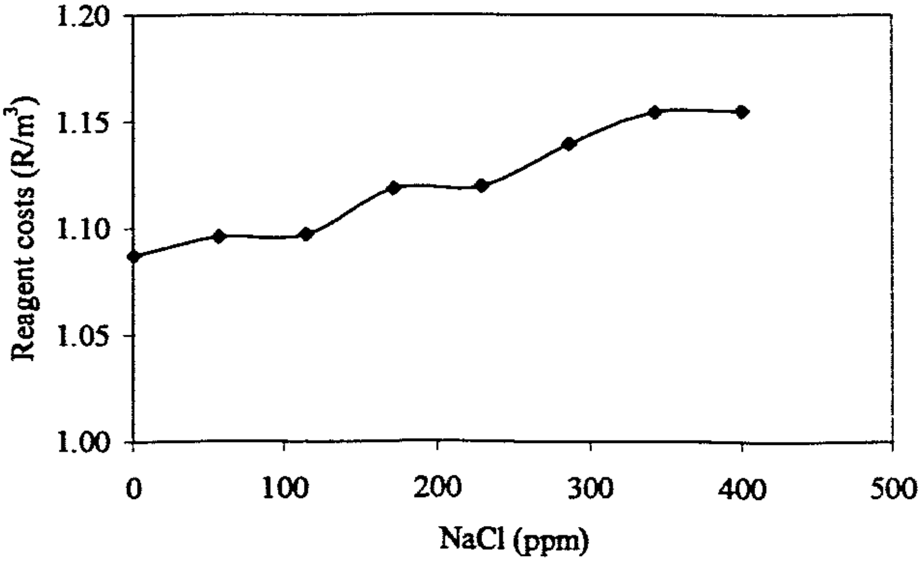

Figure 5.12. *Aspen results showing NaCl in the feed water vs. the total reagent costs*

5.6 $[Ca^{2+}]/[SO_4^{2-}]$ ratio at stage 3

These results are tabulated in Table A7 of Appendix A.

At stage 3, the formation of ettringite is dependent on the conversion of sulphate in the ettringite formation reaction. This means that the mole flow of calcium taking part in this reaction is dependent on the sulphate participating in the reaction. An increase in the $[Ca^{2+}]/[SO_4^{2-}]$ ratio entering stage 3 (ettringite formation stage) therefore results in less ettringite being formed (Figure 5.13). The increase in ratio is due to an increase in calcium or otherwise a decrease in the amount of sulphate at this stage. Ettringite formation first uses the mole flow of sulphate at its disposal, and then calculates how much calcium, gibbsite and water is required for this reaction. Therefore, if less sulphate reacts, then less calcium, gibbsite and water will react, and hence less ettringite will be formed. This explains why more sulphate is always removed than calcium, as can be seen in Figure 5.14. This graph shows that an increase in the $[Ca^{2+}]/[SO_4^{2-}]$ ratio will result in a decrease in the removal of both calcium and sulphate as is expected. All the sulphate is not removed because the ettringite formation reaction converts 90% of the mole flow of sulphate into ettringite and this model also ensures that stream R3 contains 0.2 kg/m^3 of sulphate. A decrease in ettringite formation leads to a decrease in the amount of ettringite decomposed and therefore less gibbsite being formed at stage 5. Although less gibbsite is formed, an increase in the amount of gibbsite recycled takes place. This is because in order to meet all the design specifications in the recycle loop, a fairly large gibbsite residue is present at stage 3. Hence, more gibbsite enters stage 5, than gibbsite formed at stage 5. Figure 5.15 shows this increase in the $[Ca^{2+}]/[SO_4^{2-}]$ ratio results in an increase in the amount of gibbsite recycled.

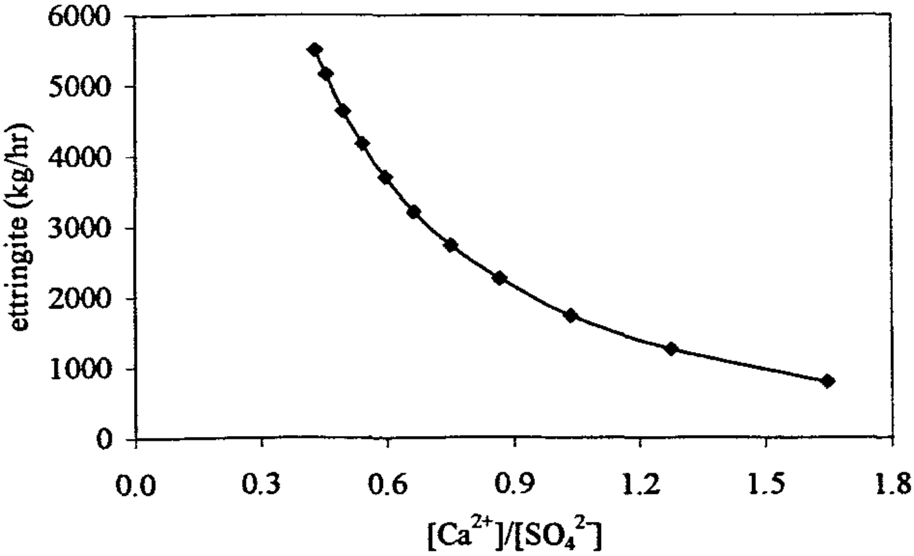

Figure 5.13. *Aspen results showing the calcium to sulphate ratio vs. ettringite produced*

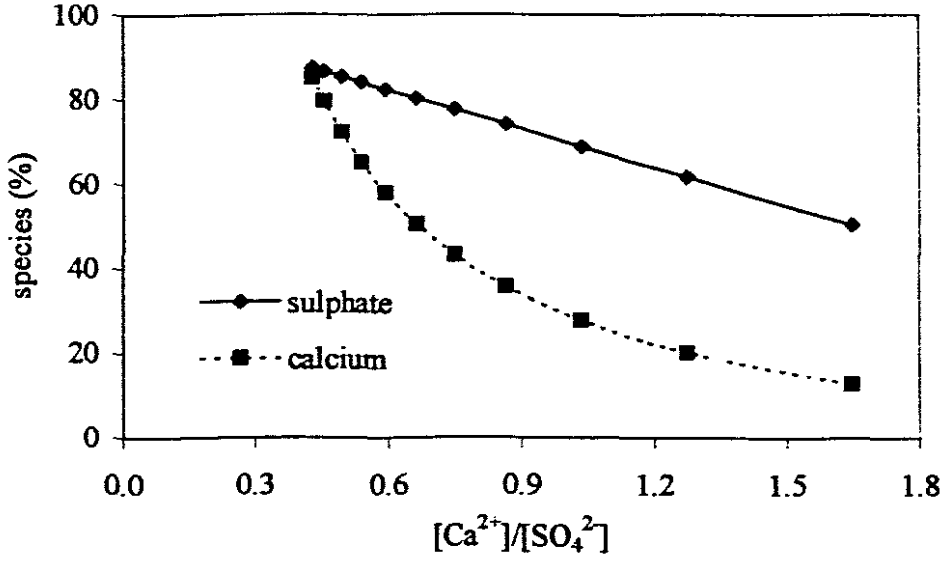

Figure 5.14. *Aspen results showing the calcium to sulphate ratio vs. percentage species removed at stage 3*

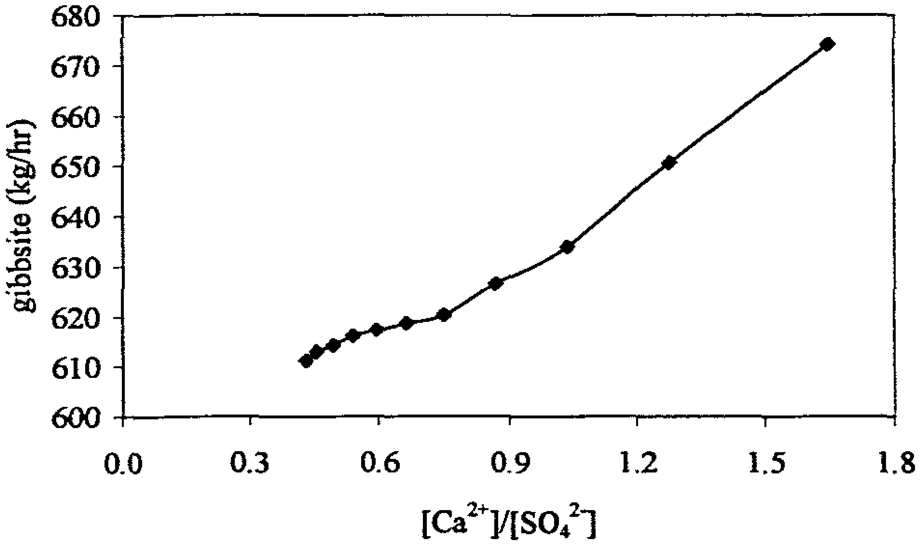

Figure 5.15. *Aspen results showing the calcium to sulphate ratio vs. gibbsite recycled*

CHAPTER 6

SENSITIVITY ANALYSIS

6.1 Introduction

In order to investigate how this process will react when changes are applied to it, a sensitivity analyses were completed. The following sensitivities were carried out:

- The concentration of $CaSO_4$ in the feed water
- The flow rate of the feed water
- The lime input to stage 1
- The lime input to stage 3

6.2 Sensitivities

6.2.1 *Concentration of $CaSO_4$ in the feed water*

By varying the $CaSO_4$ in the feed water means varying quantities of Ca^{2+} and SO_4^{2-} ions that will be available at stage 3 to react to form ettringite. An increase in the concentration of $CaSO_4$ in the feed water will lead to a linear increase in Ca^{2+} and SO_4^{2-} in solution at stage 1. The K_{sp} of $CaSO_4$ is 2.01×10^{-4}, making it soluble in water. However, for high degrees of oversaturation, the $CaSO_4$ solution will experience rapid precipitation through spontaneous nucleation and crystal growth. $CaSO_4$ is saturated in water at 1852 ppm. At this level and at fairly low degrees of oversaturation ("metastable" region), no noticeable precipitation will occur for long periods of time (Benefield *et al.*, 1982). $CaSO_4$ crystallizes as insoluble gypsum upon reaching a concentration of 2105 ppm, since it is outside the "metastable" region. The Ca^{2+} and SO_4^{2-} concentrations increase until crystallization takes place, after which it remains constant. When the Ca^{2+} and SO_4^{2-} concentration remains constant, precipitated gypsum is formed which is removed with the metal hydroxides at stream 8.

The dissolved $CaSO_4$ is contacted with gypsum crystals from stage 2. This is to enable the precipitation of $CaSO_4$. Virtually no gypsum is precipitated while the $CaSO_4$ concentration in the feed water is below 1930 ppm (see Figure 6.1). This is in contrast to gypsum first precipitating when the $CaSO_4$ was at 2105 ppm. This is because of the presence of gypsum crystals in stage 2 catalyses the precipitation of gypsum when dissolved $CaSO_4$ is saturated and "metastable". After the $CaSO_4$ is at a saturated level, there is a linear increase in the gypsum precipitated at stage 2.
A result of the precipitation of gypsum is that an increase in $CaSO_4$ in the feed water will lead to a linear increase in the Ca^{2+} and SO_4^{2-} concentration being fed to the ettringite formation stage (stage 3), until the $CaSO_4$ is at its saturation point. Once saturated $CaSO_4$ is present in the feed water, by the time it reaches stage 3, it has a feed of 1496 ppm SO_4^{2-} and 622 ppm Ca^{2+}. This means that whenever AMD containing supersaturated quantities of $CaSO_4$ is fed into this process to be treated, by the time the dissolved $CaSO_4$ reaches the ettringite formation stage; it will be at its saturation level. This inevitably means that a constant amount of ettringite will be formed when supersaturated quantities of $CaSO_4$ is fed to stage 1 (see Figure 6.2). When undersaturated quantities of $CaSO_4$ are fed to stage 1, this leads to a linear increase in the amount of ettringite formed.

The program is written in such a way that the amount of ettringite formed is dependent on the amount of sulphate given off, and the sulphate conversion increases as more sulphate is made available. The amount of sulphate converted to ettringite also affects the amount of calcium and gibbsite being removed at stage 3 by the formation of ettringite. Figure 6.3 shows that an increase in $CaSO_4$ into the feed water results in an increase in the amount of sulphate being converted to ettringite until it remains constant (~ 87%), while the calcium and aluminium hydroxide increase until saturation of $CaSO_4$ takes place. Thereafter, 72% and 39% are removed from the system respectively. As more ettringite is formed, so less calcium and gibbsite is left as residue exiting stage 3. However, by decomposing more ettringite, more gibbsite will be formed, but the trend shows a decrease in the recycle of gibbsite (see Figure 6.4). This is because the amount of gibbsite entering stage 5 is more than that being formed. As with the formation of ettringite, once supersaturated $CaSO_4$ is fed to stage 1, the gibbsite recycled will remain constant at 611 kg/hr.

Total reagent costs are directly related to the formation of ettringite. This is seen in the similarity of Figure 6.2 and Figure 6.5 (reagent cost curve). As the amount of ettringite formed increases, so the reagent costs also increase. Once the formation of ettringite is constant, the costs incurred also remain constant. An increase in the formation of ettringite leads to an increase in lime consumption at stage 3. This is due to a drop in pH when ettringite gets formed, and in order to stabilize the pH at 11.95, more lime is needed. This increasing amount of ettringite proceeds to stage 5 where it is decomposed. Decomposition results in an increase in pH and in order to maintain a constant decomposition pH of 7, more sulphuric acid needs to be consumed. Figure 6.5 shows an increase in reagent costs from approximately R 0.5 /m^3 to a constant value of R1.06 /m^3 when $CaSO_4$ in the feed water reaches its saturation point.

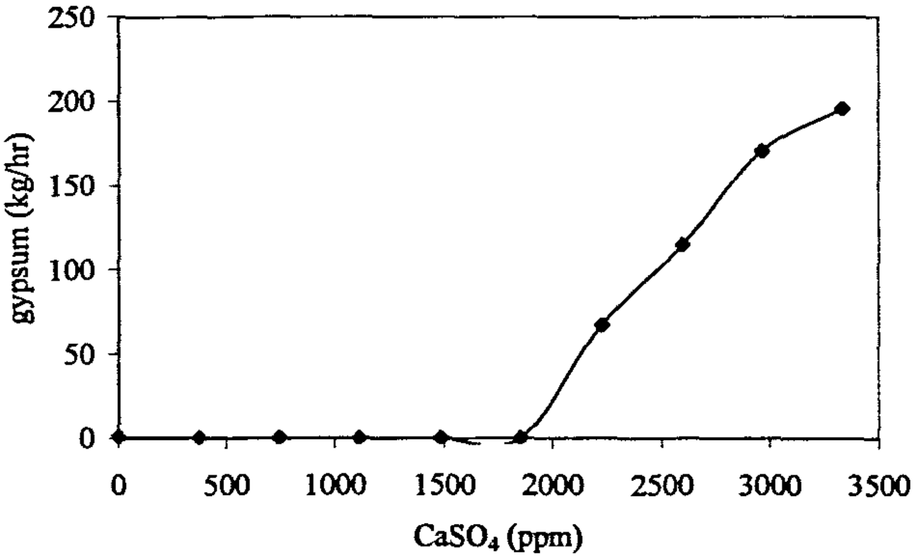

Figure 6.1 *Aspen results of $CaSO_4$ in the feed water vs. the gypsum removed at stage 2 (stream 36)*

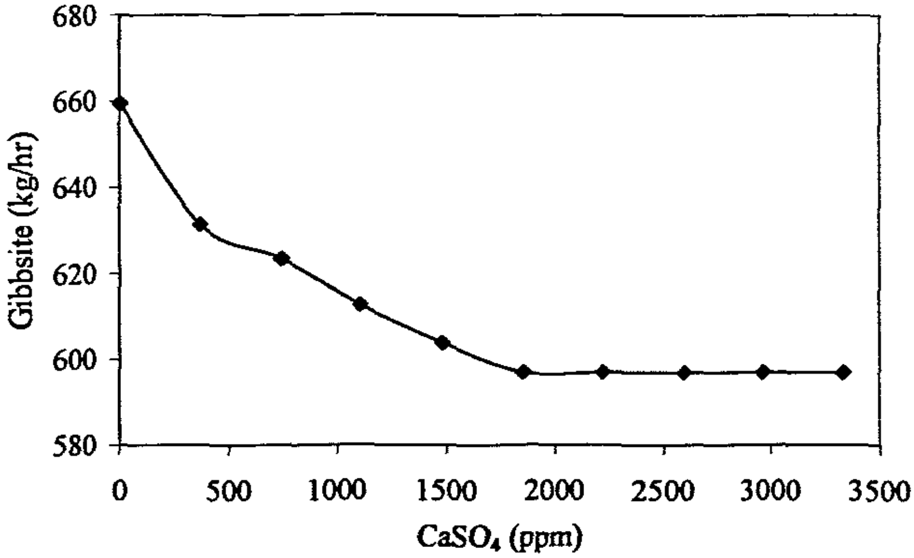

Figure 6.4. *Aspen results of $CaSO_4$ in the feed water vs. the amount of gibbite recycled*

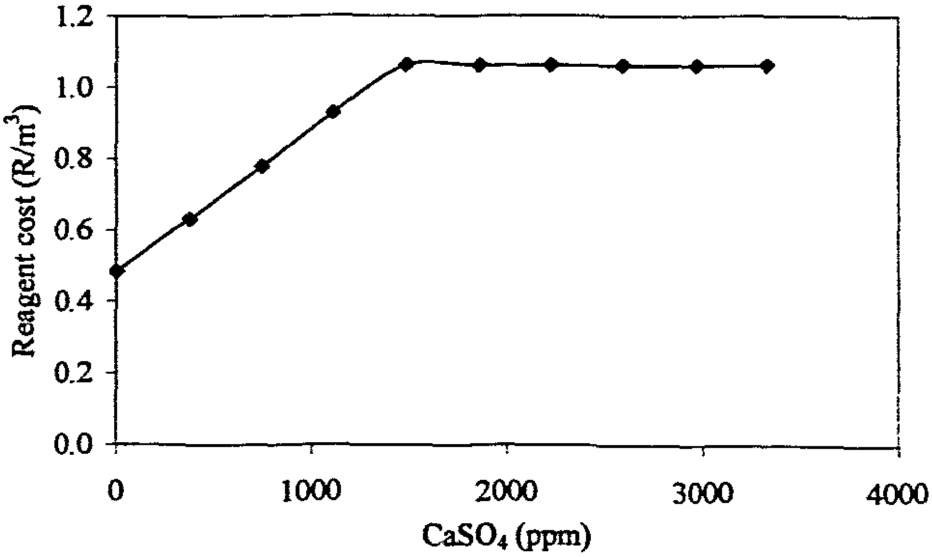

Figure 6.5. *Aspen results of $CaSO_4$ in the feed water vs. total reagent costs*

calcium fed to stage 3 as a result of increased lime usage at stage 1. By producing ettringite, a constant amount of sulphate is removed (i.e. ~ 96%), while an increasing amount of calcium is removed from 69% to 80%. As more sulphate is converted to ettringite, so more gibbsite is also used. This results in a drop in the amount of gibbsite residue leaving stage 3.

An increase in lime usage at stage 1 will alter the pH, so that it affects the amount of lime required at stage 3. This is seen in Table A10(ii) of Appendix A, where the lime usage decreases from 411 kg/hr to 0 kg/hr. This results in the total lime consumption, and therefore the cost of lime, decreasing while the $Ca(OH)_2$ is soluble at stage 1. Once the $Ca(OH)_2$ is insoluble at stage 1, then the amount of lime used increases. The cost of sulphuric acid decreases from R 0.47 /m^3 to R 0.39 /m^3 with an increase in pH at stage 1. This is because an increase in pH results in a decrease in ettringite production. This decrease in ettringite results in a decrease in ettringite decomposed and therefore less acid is required. Therefore, while the lime used at stage 1 is soluble, total reagent costs decrease from R 1.11 /m^3 to R 0.96 /m^3 and increases rapidly when the lime is insoluble. This is illustrated in Figure 6.11.

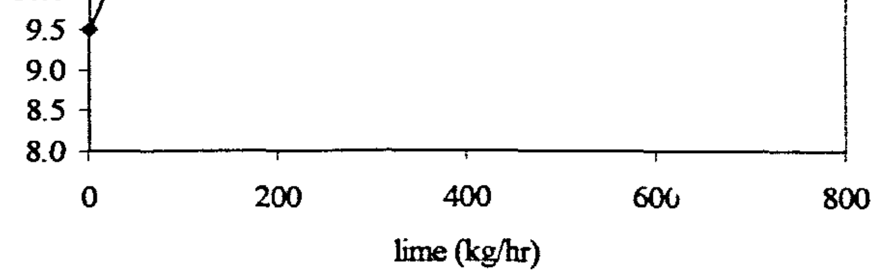

Figure 6.8. *Aspen results of lime input to stage 1 vs. pH at stage 1*

6.2.2 Flow rate of the feed water

The program reacts as expected, with linear increases in metal hydroxides removed, gypsum precipitated, and ettringite formed. Figure 6.6 shows how an increase in feed water flow rate leads to an almost linear increase in the amount of ettringite leaving in stage 3. Since the concentrations of the various components of the feed water remain constant, so an increase in flow rate will result in a linear increase of various components in the feed water. Therefore, the calcium and sulphate in solution at stage 1 will increase. This inevitably results in an increase in calcium and sulphate into the ettringite formation stage, which results in an increase in the formation of ettringite. Results are tabulated in Table A9 of Appendix A.

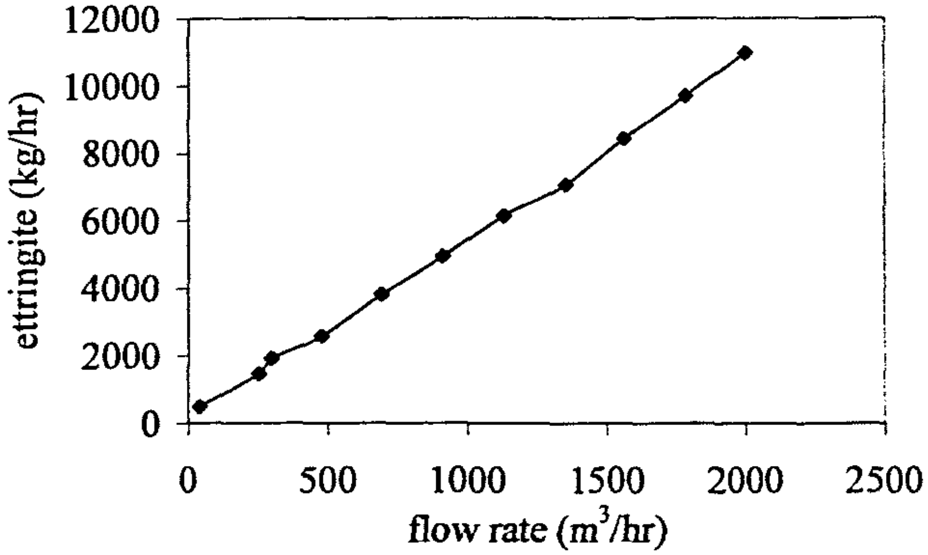

Figure 6.6. *Aspen results of varying feed water flow rate vs. ettringite formation*

Reagent costs are largely affected by the amount of lime used in the system. This is illustrated in Table A9(ii) of Appendix A as well as Figure 6.7. Reagent costs are measured in Rands per m^3 of feed water used. An increase in the feed water flow rate will result in increases in the flow rates of all the streams in the system. This means that in order to meet all the conditions specified, increasing quantities of reagents are required. These increasing quantities of reagents when compared with increasing quantities of feed water flow rates results in reagent cost, which remain fairly stable as depicted in Figure 6.7. At a small flow rate of 40 m^3/hr, the total reagent costs are at its highest (i.e. R 1.29 /m^3). This is because twice as much lime per m^3 of feed water is required at stage 3. From 258 m^3/hr, the reagent costs remain fairly constant with costs fluctuating between R 0.8 /m^3 and R 0.9 /m^3 (average about R 0.85 /m^3).

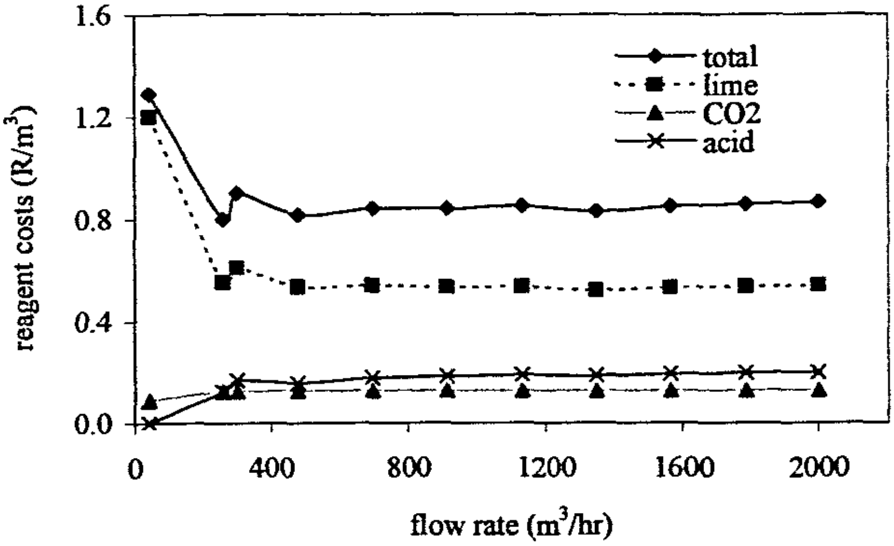

Figure 6.7. *Aspen results of varying feed water flow rate vs. Reagent costs*

6.2.3 Lime input to stage 1

All theses results are tabulated in Table A10(i) of Appendix A.

An increase in the amount of lime to stage 1 will result in an increase in the pH at this stage from 9.5 to 12.36. $Ca(OH)_2$ is insoluble at a pH of 12.36, and this is first achieved when 467 kg/hr of lime is consumed (see Figure 6.8). This increase in the pH at stage 1 until the lime is insoluble shows a similar trend at stage 2, with the pH ranging from 9.5 to 12.37.

At a pH of 9.5, no $Mg(OH)_2$ is precipitated, because magnesium only precipitates as a hydroxide from a pH of about 10.3. Beyond this pH, 21.5 kg/hr of $Mg(OH)_2$ is removed at stage 8, which constitutes virtually all the magnesium.

Probably the most important influence that an increase in the lime at stage 1 has, is that it results in a decrease in the solubility of sulphate at this stage. Therefore, less sulphate is fed to stage 2 and ultimately to stage 3. Figure 6.9 illustrates how an increase in pH at stage 1 leads to a decrease in the amount of sulphate fed from stage 2 to stage 3. This decrease in sulphate results in a decrease in the amount of ettringite formed, even though there is an increase in the amount of

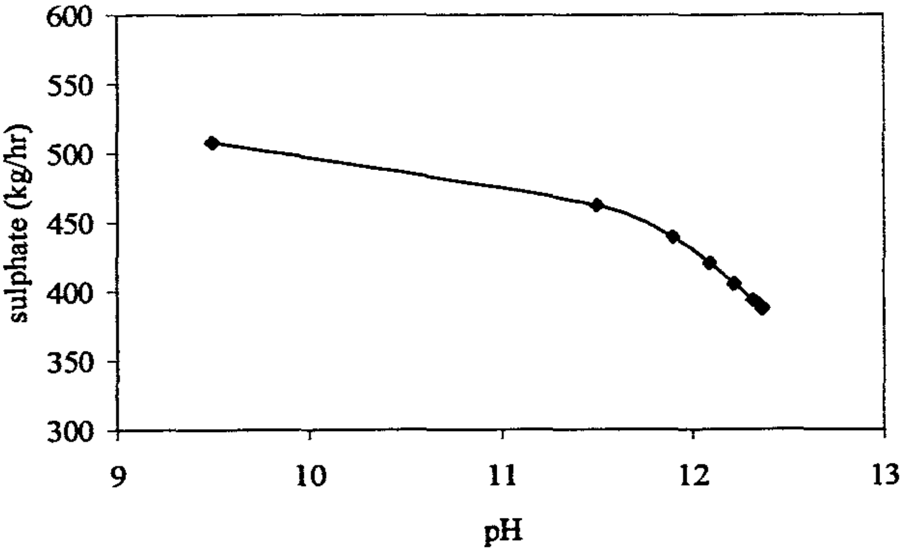

Figure 6.9. *Aspen results of lime input to stage 1 vs. sulphate exiting stage 2*

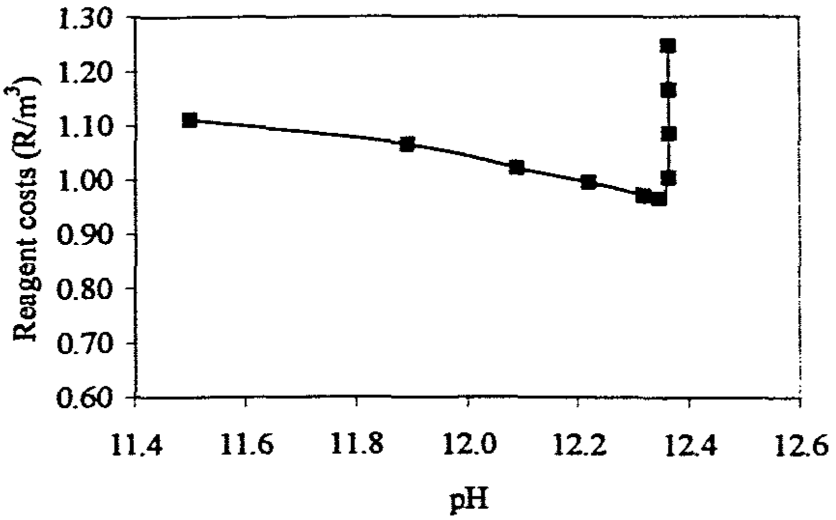

Figure 6.10. *Aspen results of lime input to stage 1 vs. Reagent costs*

6.2.4 Lime input to stage 3

The amount of lime fed to stage 3 does not have an effect on stage 1 and 2. The main reason for adding lime at this stage is to adjust the pH so that it will remain at 11.95. In order to form ettringite, the pH at stage 3 needs to be within the required range (i.e. 11.4 to 12.4). By increasing the lime from 400 to 700 kg/hr, the pH ranges from 11.6 to 12.44. An increase in lime would therefore have little effect on the amount of sulphate removed. It does however have an effect on the amount of calcium removed as can be seen in Table A11(i) of Appendix A. An increase in lime means that more calcium is fed to the system, and because the amount of sulphate fed to stage 3 remains relatively constant, the amount of sulphate not reacting to form ettringite increases. There is therefore a decrease in the amount of calcium removed as seen in Figure 6.11. This results in an increase in calcium in the product water. The amount of ettringite produced at this stage remains constant at about 1929 kg/hr and therefore a constant amount of ettringite and gibbsite is recycled.

The increase in lime usage results in an increase in the cost of lime from R 0.42 /m^3 to R 0.84 /m^3. As more lime is unreacted at this stage, so an increase in calcium proceeds to stage 4. The increase calcium at stage 4 requires an increasing amount of CO_2 in order to form $CaCO_3$. This means an increase in the cost of CO_2. The cost of sulphuric acid remains constant because the amount of ettringite decomposed remains constant. The overall result is an increase in the total reagent costs as the amount of lime increases at stage 3. This is illustrated in Figure 6.12, which shows that the reagent costs increase from R 0.95 /m^3 to R 1.7 /m^3.

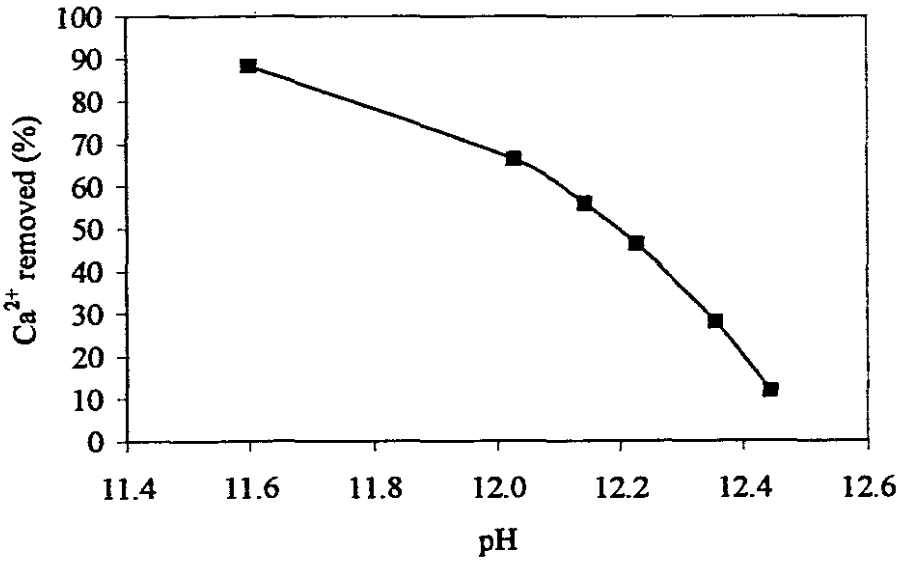

Figure 6.11. *Aspen results of lime input to stage 3 vs. calcium removed at stage 3*

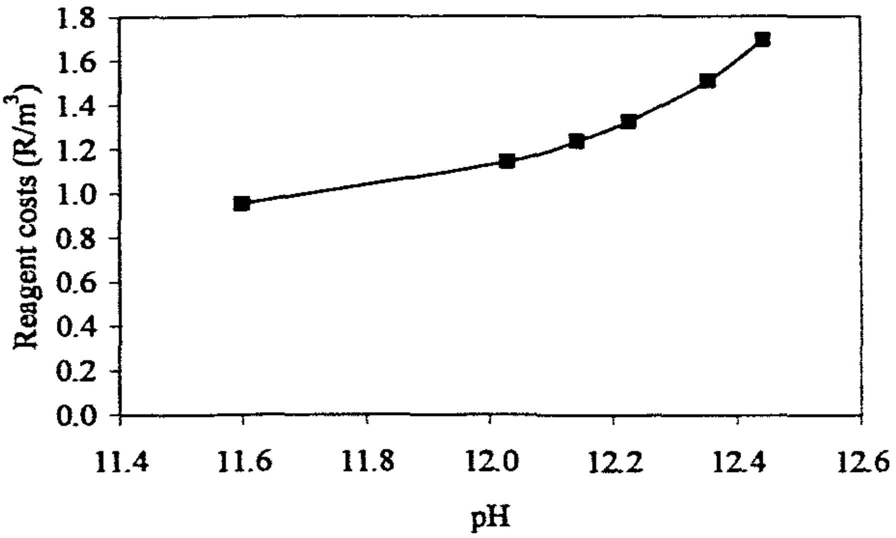

Figure 6.12. *Aspen results of lime input to stage 3 vs. Reagent costs*

6.3 Decomposition comparisons

It is realistic to assume that at varying decomposition pH's at stage 5, varying amount of ettringite is decomposed. All the previous results were carried out using a decomposition pH of 7, which resulted in 95% conversion of ettringite to gibbsite. This was done because optimum decomposition takes place at a pH of 6.5 (Petersen, 1998). To drop the pH of the streams entering stage 5 from a fairly high alkaline pH to a value of 7 required a substantial amount of sulphuric acid. An experimental run was therefore performed to determine how this process would perform at a decomposition pH of 9, assuming 50% of the ettringite is decomposed.

Table 6.1 shows a comparison of results when decomposition takes place at a pH of 7 and at 9. In order to meet all the design specifications, more ettringite is formed at stage 3 and therefore decomposed at stage 5 when half the ettringite is decomposed. For 95% decomposition, less ettringite is fed to stage 5. This results in smaller quantities of ettringite and gibbsite being recycled for the higher conversion compared with 2066 kg/hr and 693 kg/hr for the lower conversion respectively. For both degrees of decomposition, the amount of calcium and sulphate removed at stage 3 are more or less the same. It would therefore appear that 95% conversion is the better option simply because of the smaller quantities of ettringite and gibbsite recycled, since too large quantities could cause scaling.

What is however very important is the reagent costs incurred at the different conversion rates. Table 6.1 shows that the cost of lime and carbon dioxide is more or less the same for both degrees of decomposition. The big difference however is the amount of sulphuric acid used. For 50% conversion, 128 kg/hr is used, whereas for 95% conversion 437 kg is used. This amount to the cost of acid at 50% and 95% conversion to be R 0.14 /m^3 and R 0.47 /m^3 respectively. This results in total reagent costs of R 0.81 /m^3 and R 1.09 /m^3 respectively.

Table 6.1. *Decomposition at pH of 9 and 7 respectively*

	50% conversion		95% conversion	
Ettringite decomposed	4128		1915	
Ettringite recycled	2066		100	
Gibbsite recycled	693		456	
Sulphate removed (stage 3)	88%		87%	
Calcium removed (stage 3)	74%		72%	
Reagent Costs		R/m^3		R/m^3
Lime (stage 1)	108 kg/hr	0.11	108 kg/hr	0.11
Lime (stage 3)	421 kg/hr	0.44	369 kg/hr	0.39
CO_2 (stage 4)	78 kg/hr	0.10	80 kg/hr	0.11
H_2SO_4	128 kg/hr	0.14	437 kg/hr	0.47
total		**0.81**		**1.09**

6.4 Addition of aluminium sulphate

A reason for using aluminium sulphate at stage 5 is that it can supplement the use of sulphuric acid. Aluminium sulphate is a source of aluminium and sulphate and would help in droping the pH at stage 5.

An increase in the amount of $Al_2(SO_4)_3$ at stream 26 results in a linear decrease in the amount of H_2SO_4 at stream 25 (see Figure 6.13). This is because $Al_2(SO_4)_3$ decomposes into gibbsite and sulphuric acid. When 600 kg/hr of $Al_2(SO_4)_3$ is used, 0 kg/hr acid is required. No big changes are observed at Figure 6.14, which shows the amount of gibbsite recycled. The recycled gibbsite does decrease slightly from 635 kg/hr to 626 kg/hr as the amount of $Al_2(SO_4)_3$ increases from 0 to 600 kg/hr. This is in conjunction with an increase in the amount of ettringite leaving stage 3 (Figure 6.15). Ettringite leaving stage 3 increases from 1938 to 2003 kg/hr.

Reagent costs are most affected by the addition of $Al_2(SO_4)_3$. $Al_2(SO_4)_3$ is very expensive (R 1.3 /kg) when compared to lime, H_2SO_4 and CO_2; but less expensive when compared to $Al(OH)_3$. For this reason, an increase in reagent costs is anticipated as seen by Figure 6.16. This is largely due to the increasing amount of $Al_2(SO_4)_3$. Costs increase from R 1.06 / m^3 to R 3.25 /m^3.

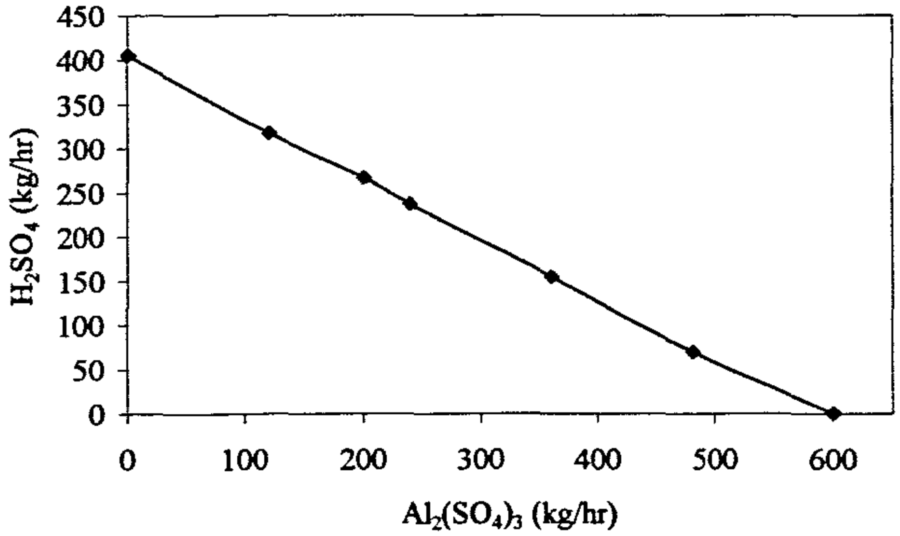

Figure 6.13. *Aspen results showing addition of $Al_2(SO4)_3$ used vs. H_2SO_4 used*

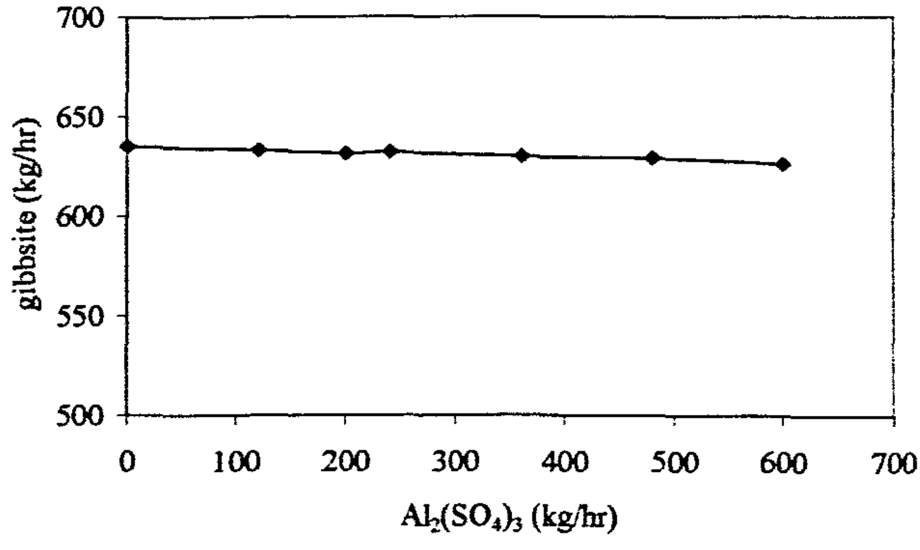

Figure 6.14. *Aspen results showing addition of $Al_2(SO4)_3$ used vs. gibbsite recycled*

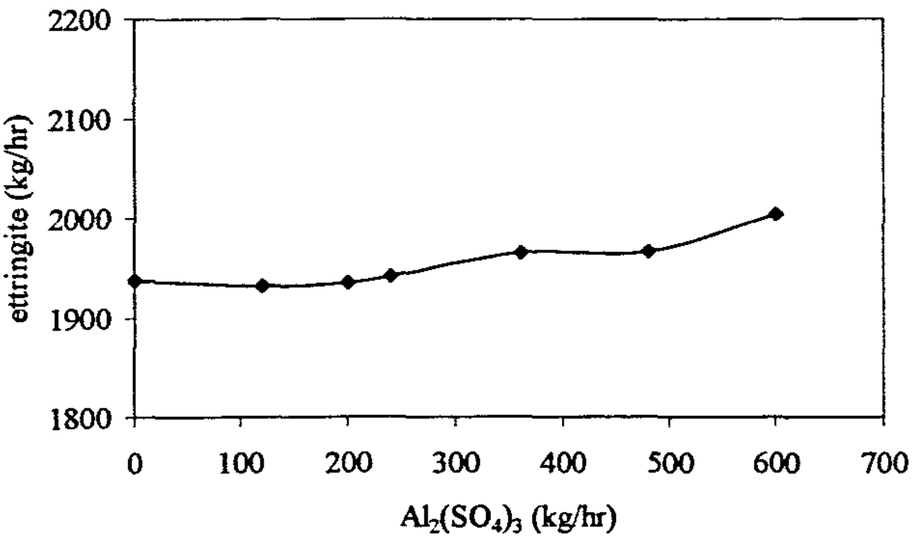

Figure 6.15. *Aspen results showing addition of $Al_2(SO4)_3$ used vs. ettringite at stage 3*

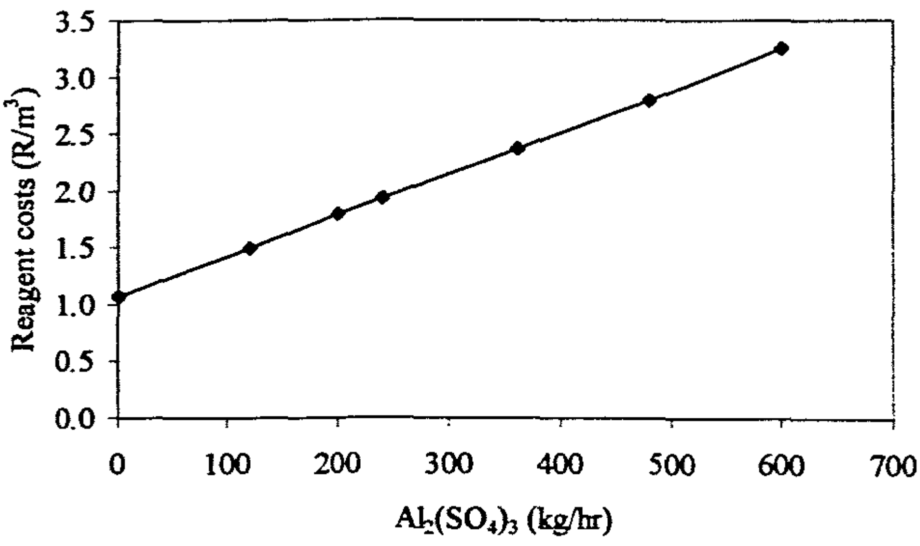

Figure 6.16. *Aspen results showing addition of $Al_2(SO4)_3$ used vs. total reagent costs*

CHAPTER 7

CONCLUSIONS AND RECOMMENDATIONS

7.1 CONCLUSIONS

According to the research performed in this thesis, the following conclusions could be made.

- Under alkaline conditions (pH ranging from 11.4 to 12.4), ettringite is formed when AMD, rich in $CaSO_4$, is contacted with sufficient amounts of an aluminium-containing agent.

- Laboratory experimental results showed that by forming ettringite from a synthetic $CaSO_4$ solution and $Al(OH)_3$, removals of calcium and sulphate equated to 68% and 92% respectively.

When simulating the Chemical Precipitation Process on an Aspen simulator, the following conclusions were obtained.

- The preliminary 5 stage model, containing 567 ppm Ca^{2+} and 1697 ppm SO_4^{2-} in the feed water, produced 1915 kg/hr of ettringite which amounted to the removal of 66% Ca^{2+} and 88% SO_4^{2-} at stage 3.

- This model produces product water of a potable quality (Ca^{2+} < 150 ppm, SO_4^{2-} < 200 ppm) by removing 97% Ca^{2+} and 88% SO_4^{2-} over the entire process.

- 99% of the metals ($Mg(OH)_2$) are removed at stage 1, while virtually no Na^+ is removed from the system.

- By decomposing 95% of the ettringite at stage 5, 456 kg/hr of gibbsite ($Al(OH)_3 \cdot 2H_2O$) is recycled for re-use in ettringite formation.

- To prevent a build up of $CaSO_4$ in the process, stage 5B converts the calcium and sulphate in solution to gypsum, which is removed from the system.

- Reagents used include lime ($Ca(OH)_2$), carbon dioxide and sulphuric acid. The reagent costs incurred over the preliminary model amounted to R 1.09 / m^3 of feed water used.

- Investigation was performed to produce 3 different grades of product water, namely: Agricultural water ($Ca^{2+} < 300$ ppm, $SO_4^{2-} < 500$ ppm), potable water, and high quality industrial water ($Ca^{2+} < 50$ ppm, $SO_4^{2-} < 50$ ppm). This led to the formation of 1407 kg/hr, 1815 kg/hr, and 2044 kg/hr of ettringite respectively.

- Reagent costs totalled R 0.92 / m^3 for agricultural water, R1.09 /m^3 for potable water and R 1.09 /m^3 for high quality industrial water.

- An increase in the conversion of sulphate to ettringite, results in a linear increase in the formation of ettringite, and a decrease in the amount of gibbsite recycled. This increase in ettringite formation from 10% to 100% results in a linear increase in total reagent costs from R 0.41 /m^3 to R 1.2 /m^3 respectively.

- An increase in the decomposition of ettringite results in an increase in the formation of gibbsite. However, at low decomposition rates of ettringite (between 10% and 48%), there needs to be fairly large amounts of gibbsite in the system to compensate for the little gibbsite being formed. This results in an increase in the formation of ettringite, until maximum formation of ettringite takes place when the decomposition is at 48%. As the decomposition of ettringite ranges from 48% to 100%, so the formation of ettringite gradually decreases. The reagent costs follow the same trend, with the maximum cost R 0.83/m^3 when decomposition is at 48%.

- When the NaCl concentration in the feed water is increased from 15 ppm to 415 ppm, the solubility of calcium and sulphate increases. This results in an eventual increase in the amount of ettringite being produced at stage 3 from 1919 kg/hr to 2062 kg/hr. This increase results in an increase in the total reagent costs from R 1.09 /m^3 to R 1.15 /m^3 respectively.

- An increase in the ratio of calcium to sulphate into stage 3 results in a decrease in sulphate available and therefore a decrease in the formation of ettringite.

- The process is best described when varying quantities of $CaSO_4$ are present in the feed water. For high degrees of oversaturation, $CaSO_4$ will precipitate as gypsum at stage 1. The presence of recycled gypsum at stage 2 causes the $CaSO_4$ to precipitate as gypsum for low degrees of supersaturation. The outcome of the removal of gypsum at stage 2 is that for supersaturated $CaSO_4$ in the feed water, the amount of calcium and sulphate entering stage 3 remains at 622 ppm and 1496 ppm respectively. Therefore, when supersaturated calcium sulphate is present in the feed, the amount of ettringite formed as well as gibbsite recycled remains unchanged.

- When the flow rate of the feed water is varied, a linear increase in the formation of ettringite is noted. Reagent costs are most affected by an increase in flow rate. When the flow rate increases from 258 m^3/hr to 2000 m^3/hr, the reagent costs fluctuate between R 0.8 /m^3 and R 0.9 /m^3.

- An increase in the amount of lime to stage 1 causes an increase in the pH at this stage from 9.5 to 12.36. Magnesium does not precipitate as $Mg(OH)_2$ at a pH of 9.5, only once it reaches a pH of 10.3. An increase in pH results in a drop in the solubility of sulphate, which eventually leads to a drop in the amount of ettringite produced at stage 3. A drop in lime consumption will result in a drop in reagent costs from R 1.11 /m^3 to R 0.96 /m^3.

- An increase in the amount of lime added to stage 3, in order to adjust the pH within its ettringite formation range, results in a constant formation of ettringite. This means that there is a constant decomposition of ettringite and therefore an unchanging amount of ettringite and gibbsite is recycled. The biggest effect that this addition of lime has is on the increasing amount of calcium in the product water. An increase in lime consumption will result in an increase in reagent costs from R 0.95 /m^3 to R 1.7 /m^3.

- Decomposition ettringite at a pH of 7 (95% decomposition) as compared with 9 (50% decomposition) results in larger quantities of ettringite and gibbsite flowing through the main recycle. Reagent costs however play the largest role, with comparative costs of R 1.09 /m^3 and R 0.81 /m^3 respectively.

- The addition of aluminium sulphate to stage 3 causes a linear decrease in the amount of sulphuric acid used to decompose ettringite. This decomposition, when between 0 to 600 kg/hr of $Al_2(SO_4)_3$ is added, results in a slight decrease in the recycling of gibbsite from 635 kg/hr to 636 kg/hr respectively. This leads to a slight increase in the amount of ettringite leaving stage 3 from 1938 to 2003 kg/hr for the same conditions. The amount of calcium and sulphate however remains fairly constant. Reagent costs increase from R 1.06 /m^3 to R 3.25 /m^3, largely because $Al_2(SO_4)_3$ is so much more expensive than all the other reagents involved. $Al_2(SO_4)_3$ however is a lot cheaper than $Al(OH)_3$, and would probably be a better alternative if the system needed to be fed with some aluminium-containing agent.

7.2 RECOMMENDATIONS

Changing the design specifications at stage 3 would probably complicate the model and would therefore be advisable to leave that stage of the process unchanged.

At stage 4, $CaCO_3$ is formed when calcium is contacted with carbon dioxide gas. This $CaCO_3$ is therefore present in the product water. It would therefore be advisable to remove this $CaCO_3$ by means of a separator. This could be added at the end of stage 4 and would release product water now free of all $CaCO_3$.

REFERENCES

Atkins, M., Macphee, D., Glasser, F.P. and Kindness, A., (1991). Solubility Properties of Ternary and Quatenary Compounds in the CaO-Al_2O_3-SO_3-H_2O system, Cement and Concrete Research, Volume 21, no. 6.

Benefield, L.D., Judkins, J.F. and Weand, B.L., (1982). Process Chemistry for water and wastewater treatment, Prentice Hall, Inc.

Bensted, J. and Varma, S.P., (1971). Ettringite and its derivatives. *Cem. Technol.*, Volume 2, pp. 73 -76, 100.

Bensted, J. and Varma, S.P., (1972). Ettringite and its derivatives II: Chromate substitution. *Silicates Ind.*, Volume 37, pp. 315 - 318.

Chen, S.S. and Mehta, P.K., (1982). Zeta potential and surface area measurements on ettringite. *Cement and Concrete Research*, Volume 12, pp. 257 – 259.

Damidot, D. and Glasser, F.P., (1992). *Cement and Concrete Research*, Volume 22, pp. 1179.

Damidot, D. and Glasser, F.P., (1993). Thermodynamic investigation of the CaO-Al_2O_3-$CaSO_4$-H_2O at 25°C and the influence of Na_2O. *Cement and Concrete Research*, Volume 23, pp. 221 – 238.

Damidot, D., Atkins, M., Kindness, A., Glasser, F.P., (1992). Sulphate attack on concrete: limits of the Aft stability domain. *Cement and Concrete Research*, Volume 22, pp. 229 – 234.

Dry, M.J. (1998). The Purification of polluted mine water. *Mintek Technical Memorandum.*, Reg. No. 98/14967/07

Ebbing D.D. (1987). General Chemistry, Second Edition. Houghton Mifflin Company, Boston. Chapter 20, pp 678 – 703.

Folwer, R.K., Traina, S.J., Bighan, J.M. and Soto, U.I., (1993). Solution chemistry and mineralogy of clean coal technology by-products in a long term equilibration study., *Agric. Abstr.*, Volume 30.

Hall, C., Barnes, P., Billimore, A.D., Jupe, A.C. and Turrilas, X. (1996). Thermal Decomposition of ettringite $Ca_6[Al(OH)_6]_2(SO_4)_3 \cdot 26H_2O$, *Journal Chem. Soc.*, Faraday Trans., volume 92, no. 12, pp 2125 – 2129.

Hampson, C.J. and Bailey, J.E., (1982). On the Structure of some precipitated calcium alumino-sulphate hydrates., *J.Mater.Sci.*, pp. 3341 – 3346.

Hoffman, J.D.; Numerical methods for Engineers and Scientists; McGraw-Hill, Inc; pp. 101 – 102.

Jones, F.E., (1994). The quaternary system $CaO\text{-}Al_2O_3\text{-}CaSO_4\text{-}H_2O$ at 25°C: equilibria with $Al_2O_3 \cdot 3H_2O$ alumina gel, and solid solution., *J. Phys. Chem.*, Volume 48, pp. 311 – 378.

Mattigod, S.C.B., Rai, D., Eary, L.E. and Aintsworth, C.C., (1990). Geochemical factors controlling the mobilization of inorganic constituents from fossil fuel combustion residues: I. Review of the major elements., *J. Environ. Qual.*, Volume 19, pp. 187 – 202.

McCarthy, G.J., Hassett, D.J. and Bender, J.A., (1992). Synthesis, crystal chemistry and stability of ettringite, a material with potential applications in hazardous waste immobilization. *Advanced Cementitious Systems: Mechanisms and Properties*, Materials. Research Society Symposium Proceedings, 245, pp. 129 –149.

Mohammed, A.M.O.; Boiley, J.F.; Hossein, M.; Hassani, F.P., (199ʳ). Ettringite formation in lime remediated lime tailings: I. *Thermodynamic modeling; CIM Bulletin*,; Volume 88, no. 995, pp 69 – 75.

Moore, A.E. and Taylor, H.F.W., (1968). Crystal structure of ettringite. *Nature*. Volume 218, pp. 1048 – 1049.

Moore, A.E. and Taylor, H.F.W., (1970). Crystal structure of ettringite. *Acta Cryt.* B26, pp. 386 – 393.

Myneni, S.C.B., (1995). Oxyanion-mineral sulphate interactions in alkaline environments: AsO_4 and CrO_4 sorption and desorption in ettringite. *PhD Dissertation*, The Ohio State University, Columbus, OH.

Myneni, S.C.B., Traina, S.J., Logan, T.J. and Waychunas, G.A., (1997). Oxyanion behaviour in alkaline environments: sorption and desorption of arsenate in ettringite., *Environ. Sci. Technol.*, Volume 31, p 1761.

Nishikawa, T., Suzuki, K. and Ito, S., (1992). Decomposition of synthesized ettringite by carbonation, *Cement and Concrete Research*, Volume 22, pp. 6 – 14.

Perry, R.H., Chilton, C.H; Chemical Engineers' Handbook, Fifth edition; International Student edition; Chapter 2; p 99 – 100.

Petersen, F.W., (1998). The fundamentals of the ettringite process., *Mintek Technical Memorandum.*, 18707

Pöllmann, H.; Kuzel, H.-J.; Erlangen & Wenda, R.; Neusäss (1989). Compounds with ettringite structure; *Neues Jahrbüch Miner. Abh,*; volume 160, no 2; pp133 –158.

Reardon, E.J., (1990). An ion interaction model for the determination of chemical equilibrium in cement/water systems. *Cement and Concrete Research*, Volume 20, pp. 175 – 192.

Seider, W.D., Seader, J.D. and Lewin. D.R., (1999). Process Design Principles: Synthesis, Analysis and Evaluation, *John Wiley & Sons, Inc.*

Söhnel, O. and Garside, J. (Published 1992). Precipitation: Basic Principles and Industrial applications, Butterworth-Heinemann Ltd.

Warren, C.J. and Reardon, E.J., (1994). The solubility of ettringite at 25°C., *Cement and Concrete Research*, pp. 1515 – 1524.

APPENDIX A.

TABULATION OF ASPEN RESULTS

Table A1. *Aspen results for the production of potable water*

Stream	1	2	3	4	5	6
State	liquid	slurry	slurry	liquid	slurry	liquid
Temperature °C	25	25	25	25	25	25
Pressure bar	0.86	0.86	0.86	0.86	0.86	0.86
Vapor Fraction	0	0	0	0	0	0
Solid Fraction		1	1		1	
Mass Flow kg/hr	299962	163	300135	293701	6434	4573
Volume Flow m^3/hr	300	0.2	300.2	293.7	6.4	4.6
pH	9.5	12.4	11.7	11.7	11.7	11.7

Component mass flows, kg/hr

H_2O	299146	163	299309	292892	6417	4560
CO_2	<0.001		trace	trace	trace	trace
H_2SO_4						
H_3O^+	trace	trace	trace	trace	trace	trace
OH^-	0.204	0.093	32.699	31.998	0.701	0.498
HCO_3^-	0.137		0.001	0.001	<0.001	<0.001
CO_3^{2-}	0.04		0.034	0.033	0.001	0.001
K^+	46.41		46.41	45.415	0.995	0.707
Na^+	4.467		4.467	4.371	0.096	0.068
Ca^{2+}	170.31	0.094	217.703	213.036	4.667	3.317
$CaOH^+$	0.082	0.043	15.958	15.616	0.342	0.243
Mg^{2+}	8.913		0.004	0.004	<0.001	<0.001
$MgOH^+$	0.089		0.007	0.006	<0.001	<0.001
Cl^-						
HSO_4^-	trace					
SO_4^{2-}	509.235		509.235	498.318	10.917	7.758
Gypsum(aq)	41.59					
$CaCO_3$(aq)	34.668					
Gibbsite						
$Mg(OH)_2$			21.492		21.492	
$Ca(OH)_2$		108.168				
Ettringite						
Gypsum			41.59		41.59	
$CaCO_3$(S)			34.901		34.901	

Continue...

Table A1. *Aspen results for the production of potable water*

Stream	7	8	9	10	11	12
State	slurry	slurry	liquid	slurry	slurry	slurry
Temperature °C	25	25	25	25	25	25
Pressure bar	0.86	0.86	0.86	0.86	0.86	0.86
Vapor Fraction	0	0	0	0	0	0
Solid Fraction	1	1		1	1	1
Mass Flow kg/hr	1862	294	1568	41559	341298	41559
Volume Flow m^3/hr	1.9	0.3	1.6	41.6	341.4	41.6
pH	11.7	11.7	11.7	11.7	11.7	11.7

Component mass flows, kg/hr

H_2O	1857	293	1563	41455	340449	41455
CO_2	trace	trace	trace	trace	trace	trace
H_2SO_4						
H_3O^+	trace	trace	trace	trace	trace	trace
OH^-	0.203	0.032	0.171	4.572	37.534	4.572
HCO_3^-	trace	trace	trace	<0.001	0.001	<0.001
CO_3^{2-}	<0.001	<0.001	<0.001	0.005	0.039	0.005
K^+	0.288	0.045	0.242	6.428	52.792	6.428
Na^+	0.028	0.004	0.023	0.63	5.092	0.63
Ca^{2+}	1.35	0.213	1.137	27.109	221.56	27.109
$CaOH^+$	0.099	0.016	0.083	2.073	17.024	2.073
Mg^{2+}	<0.001	trace	<0.001	0.001	0.005	0.001
$MgOH^+$	<0.001	trace	<0.001	0.001	0.007	0.001
Cl^-				0.015	0.015	0.015
HSO_4^-						
SO_4^{2-}	3.159	0.499	2.66	62.996	514.84	62.996
Gypsum(aq)						
$CaCO_3$(aq)						
Gibbsite						
$Mg(OH)_2$	21.492	21.492		0.085	0.086	0.085
$Ca(OH)_2$						
Ettringite						
Gypsum	41.59	41.59		17809.996	17911.959	17809.996
$CaCO_3$(S)	34.901	34.901		0.055	0.055	0.055

Continue...

Table A1. *Aspen results for the production of potable water*

Stream	13	14	15	16	17	18
State	slurry	liquid	slurry	slurry	liquid	liquid
Temperature °C	25	25	25	25	25.003764	25
Pressure bar	0.86	0.86	0.86	1	0.86	1
Vapor Fraction	0	0	0	0	0	0
Solid Fraction	1		1	1		
Mass Flow kg/hr	231	299505	556	3204	1969	6345
Volume Flow m^3/hr	0.2	299.6	0.6	3.2	2.0	6.3
pH	11.7	11.7	12.4	7.0	7.1	8.1

Component mass flows, kg/hr

H_2O	230	298760	556	3186	1962	6320
CO_2		trace		0.007	0.014	0.004
H_2SO_4						
H_3O^+		trace	trace	trace	trace	trace
OH^-	0.025	32.938	0.317	trace	0.019	<0.001
HCO_3^-	trace	0.001		0.057	0.018	0.055
CO_3^{2-}	<0.001	0.034		<0.001	<0.001	0.001
K^+	0.036	46.328		0.474	0.294	0.941
Na^+	0.003	4.469		0.207	0.123	0.413
Ca^{2+}	0.151	194.43	0.322	4.789	1.906	6.304
$CaOH^+$	0.012	14.94	0.146	trace	0.009	<0.001
Mg^{2+}	trace	0.004		0.001	0.001	0.002
$MgOH^+$	trace	0.006		trace	trace	trace
Cl^-	<0.001	0.013		0.269	0.153	0.534
HSO_4^-				trace	trace	trace
SO_4^{2-}	0.35	451.797		12.05	4.921	16.368
Gypsum(aq)						
$CaCO_3$(aq)						0.118
Gibbsite				456.539		
$Mg(OH)_2$	<0.001			0.422		
$Ca(OH)_2$			369.689			
Ettringite				100.421		
Gypsum						
$CaCO_3$(S)	<0.001			8.006		

Continue...

Table A1. *Aspen results for the production of potable water*

Stream	19	20	21	22	23	24
State	slurry	slurry	liquid	liquid	slurry	slurry
Temperature °C	25	25	25	25	25	25
Pressure bar	0.86	0.86	0.86	0.86	0.86	0.86
Vapor Fraction	0	0	0	1	0	0
Solid Fraction	1	1			1	1
Mass Flow kg/hr	310362	12196	298166	80	298102	12196
Volume Flow m^3/hr	311.0	12.2	298.8	52.1	298.8	12.2
pH	12.0	12.0	12.0		8.5	11.95

Component mass flows, kg/hr

H_2O	310123	12187	297936		297962	12187
CO_2	trace	trace	trace	79.93	0.107	trace
H_2SO_4						
H_3O^+	trace	trace	trace		<0.001	trace
OH^-	54.649	2.148	52.502		0.018	2.148
HCO_3^-	0.001	<0.001	0.001		22.581	<0.001
CO_3^{2-}	0.062	0.002	0.06		0.433	0.002
K^+	48.037	1.888	46.15		46.15	1.888
Na^+	5.212	0.205	5.007		5.007	0.205
Ca^{2+}	58.182	2.286	55.895		5.159	2.286
$CaOH^+$	10.191	0.4	9.79		<0.001	0.4
Mg^{2+}	0.001	<0.001	0.001		0.003	<0.001
$MgOH^+$	0.003	<0.001	0.003		trace	<0.001
Cl^-	0.969	0.038	0.931		0.931	0.038
HSO_4^-					trace	
SO_4^{2-}	62.2	2.444	59.755		59.755	2.444
Gypsum(aq)						
$CaCO_3$(aq)	trace	trace	trace			trace
Gibbsite	227.592	227.592				227.592
$Mg(OH)_2$	0.441	0.441				0.441
$Ca(OH)_2$						
Ettringite	1915.906	1915.906				1915.906
Gypsum						
$CaCO_3$(S)	8.348	8.348			143.873	8.348

Continue...

Table A1. *Aspen results for the production of potable water*

Stream	25	26	27	28	29	30
State	liquid	solid	liquid	slurry	slurry	slurry
Temperature °C	25		25	25	25	25
Pressure bar	0.86	0.86	1	0.86	0.86	0.86
Vapor Fraction	0		0	0	0	0
Solid Fraction		1		1	1	1
Mass Flow kg/hr	502	0	750196	764091	3204	760887
Volume Flow m^3/hr	0.3	0.0	749.3	761.9	3.2	758.7
pH	-2.603		8.073	7.001	7.001	7.001

Component mass flows, kg/hr

H_2O	0		747271	759832	3186	756646
CO_2			0.484	1.574	0.007	1.567
H_2SO_4	437.356					
H_3O^+	10.601		< 0.001	0.002	trace	0.002
OH^-			0.02	0.002	trace	0.002
HCO_3^-			6.539	13.585	0.057	13.528
CO_3^{2-}			0.081	0.016	< 0.001	0.016
K^+			111.3	113.119	0.474	112.645
Na^+			48.817	49.412	0.207	49.205
Ca^{2+}			745.377	1142.247	4.789	1137.457
$CaOH^+$			0.012	0.001	trace	0.001
Mg^{2+}			0.217	0.22	0.001	0.219
$MgOH^+$			< 0.001	trace	trace	trace
Cl^-			63.114	64.048	0.269	63.779
HSO_4^-	54.094		< 0.001	< 0.001	trace	< 0.001
SO_4^{2-}	< 0.001		1935.43	2873.92	12.05	2861.87
Gypsum(aq)						
$CaCO_3$(aq)			13.935			
Gibbsite				480.568	456.539	24.028
$Mg(OH)_2$				0.444	0.422	0.022
$Ca(OH)_2$						
Ettringite		196.518		105.706	100.421	5.285
Gypsum						
$CaCO_3$(S)				8.427	8.006	0.421

Continue...

Table A1. *Aspen results for the production of potable water*

Stream	31	32	33	34	35	36
State	slurry	slurry	liquid	slurry	slurry	slurry
Temperature °C	25	25	25	25	25	25.003764
Pressure bar	0.86	1	1	1	1	0.86
Vapor Fraction	0	0	0	0	0	0
Solid Fraction	1	1		1	1	1
Mass Flow kg/hr	106517	866120	756541	106517	2434	695
Volume Flow m^3/hr	106.4	865.1	755.7	106.4	2.4	0.7
pH	7.056	8.073	8.073	7.056	7.056	7.094

Component mass flows, kg/hr

H_2O	106101	862742	753591	106101	2424	693
CO_2	0.838	0.559	0.489	0.838	0.019	0.005
H_2SO_4						
H_3O^+	<0.001	<0.001	<0.001	<0.001	trace	trace
OH^-	<0.001	0.023	0.02	<0.001	trace	0.007
HCO_3^-	1.09	7.549	6.594	1.09	0.025	0.006
CO_3^{2-}	0.001	0.093	0.081	0.001	<0.001	<0.001
K^+	15.853	128.498	112.241	15.853	0.362	0.104
Na^+	7.155	56.36	49.23	7.155	0.163	0.044
Ca^{2+}	106.295	860.556	751.681	106.295	2.429	0.673
$CaOH^+$	<0.001	0.013	0.012	<0.001	trace	0.003
Mg^{2+}	0.031	0.25	0.218	0.031	0.001	<0.001
$MgOH^+$	trace	<0.001	<0.001	trace	trace	trace
Cl^-	9.087	72.867	63.648	9.087	0.208	0.054
HSO_4^-	<0.001	<0.001	<0.001	<0.001	trace	trace
SO_4^{2-}	276.099	2234.501	1951.798	276.099	6.308	1.738
Gypsum(aq)						
$CaCO_3$(aq)		16.088	14.052			
Gibbsite	825.874	849.902		825.874	18.869	18.869
$Mg(OH)_2$	0.554	0.577		0.554	0.013	0.013
$Ca(OH)_2$	trace	trace		trace	trace	trace
Ettringite	184.975	190.26		184.975	4.226	4.226
Gypsum						
$CaCO_3$(S)						<0.001

Table A2. *Aspen results for the production of Agricultural water*

Stream	1	2	3	4	5	6
State	liquid	slurry	slurry	liquid	slurry	liquid
Temperature °C	25	25	25	25	25	25
Pressure bar	0.86	0.86	0.86	0.86	0.86	0.86
Vapor Fraction	0	0	0	0	0	0
Solid Fraction		1	1		1	
Mass Flow kg/hr	299962.19	162.825	300135.2	293700.97	6434.235	4572.543
Volume Flow m^3/hr	300	0.163	300.151	293.717	6.435	4.573
pH	9.5	12.436	11.7	11.7	11.7	11.7

Component mass flows, kg/hr

H_2O	299146.05	162.596	299308.69	292892.17	6416.516	4559.951
CO_2	< 0.001		trace	trace	trace	trace
H_2SO_4						
H_3O^+	trace	trace	trace	trace	trace	trace
OH^-	0.204	0.093	32.699	31.998	0.701	0.498
HCO_3^-	0.137		0.001	0.001	< 0.001	< 0.001
CO_3^{2-}	0.04		0.034	0.033	0.001	0.001
K^+	46.41		46.41	45.415	0.995	0.707
Na^+	4.467		4.467	4.371	0.096	0.068
Ca^{2+}	170.31	0.094	217.703	213.036	4.667	3.317
$CaOH^+$	0.082	0.043	15.958	15.616	0.342	0.243
Mg^{2+}	8.913		0.004	0.004	< 0.001	< 0.001
$MgOH^+$	0.089		0.007	0.006	< 0.001	< 0.001
Cl^-						
HSO_4^-	trace					
SO_4^{2-}	509.235		509.235	498.318	10.917	7.758
Gypsum(aq)	41.59					
$CaCO_3$(aq)	34.668					
Gibbsite						
$Mg(OH)_2$			21.492		21.492	
$Ca(OH)_2$		108.168				
Ettringite						
Gypsum			41.59		41.59	
$CaCO_3$(S)			34.901		34.901	

Continue...

Table A2. *Aspen results for the production of Agricultural water*

Stream	7	8	9	10	11	12
State	slurry	slurry	liquid	slurry	slurry	slurry
Temperature °C	25	25	25	25	25	25
Pressure bar	0.86	0.86	0.86	0.86	0.86	0.86
Vapor Fraction	0	0	0	0	0	0
Solid Fraction	1	1		1	1	1
Mass Flow kg/hr	1861.692	293.955	1567.737	41558.573	341297.86	41558.573
Volume Flow m^3/hr	1.862	0.294	1.568	41.572	341.41	41.572
pH	11.7	11.7	11.7	11.706	11.708	11.706

Component mass flows, kg/hr

H_2O	1856.565	293.146	1563.42	41454.745	340448.95	41454.745
CO_2	trace	trace	trace	trace	trace	trace
H_2SO_4						
H_3O^+	trace	trace	trace	trace	trace	trace
OH^-	0.203	0.032	0.171	4.572	37.534	4.572
HCO_3^-	trace	trace	trace	<0.001	0.001	<0.001
CO_3^{2-}	<0.001	<0.001	<0.001	0.005	0.039	0.005
K^+	0.288	0.045	0.242	6.428	52.792	6.428
Na^+	0.028	0.004	0.023	0.63	5.092	0.63
Ca^{2+}	1.35	0.213	1.137	27.109	221.56	27.109
$CaOH^+$	0.099	0.016	0.083	2.073	17.024	2.073
Mg^{2+}	<0.001	trace	<0.001	0.001	0.005	0.001
$MgOH^+$	<0.001	trace	<0.001	0.001	0.007	0.001
Cl^-				0.015	0.015	0.015
HSO_4^-						
SO_4^{2-}	3.159	0.499	2.66	62.996	514.84	62.996
Gypsum(aq)						
$CaCO_3$(aq)						
Gibbsite						
$Mg(OH)_2$	21.492	21.492		0.085	0.086	0.085
$Ca(OH)_2$						
Ettringite						
Gypsum	41.59	41.59		17809.996	17911.959	17809.996
$CaCO_3$(S)	34.901	34.901		0.055	0.055	0.055

Continue...

Table A2. *Aspen results for the production of Agricultural water*

Stream	**13**	**14**	**15**	**16**	**17**	**18**
State	slurry	liquid	slurry	slurry	liquid	liquid
Temperature °C	25	25	25	25	25.017854	25
Pressure bar	0.86	0.86	0.86	1	0.86	1
Vapor Fraction	0	0	0	0	0	0
Solid Fraction	1		1	1		
Mass Flow kg/hr	230.928	299505.42	457.001	3113.648	2176.178	5489.766
Volume Flow m^3/hr	0.231	299.604	0.458	3.105	2.174	5.484
pH	11.707	11.708	12.436	7	7.577	7.532

Component mass flows, kg/hr

H_2O	230.352	298760.46	456.356	3096.427	2168.107	5468.805
CO_2		trace		0.013	0.015	0.043
H_2SO_4						
H_3O^+		trace	trace	trace	trace	trace
OH^-	0.025	32.938	0.26	trace	0.019	<0.001
HCO_3^-	trace	0.001		0.115	0.059	0.165
CO_3^{2-}	<0.001	0.034		<0.001	<0.001	0.001
K^+	0.036	46.328		0.454	0.319	0.801
Na^+	0.003	4.469		0.126	0.086	0.223
Ca^{2+}	0.151	194.43	0.264	4.654	2.091	5.431
$CaOH^+$	0.012	14.94	0.12	trace	0.008	<0.001
Mg^{2+}	trace	0.004		0.002	0.001	0.003
$MgOH^+$	trace	0.006		trace	trace	trace
Cl^-	<0.001	0.013		0.13	0.084	0.23
HSO_4^-				trace	trace	trace
SO_4^{2-}	0.35	451.797		11.727	5.377	14.04
Gypsum(aq)						
$CaCO_3$(aq)					0.013	0.024
Gibbsite				457.323		
$Mg(OH)_2$	<0.001			0.498		
$Ca(OH)_2$			303.593			
Ettringite				79.918		
Gypsum						
$CaCO_3$(S)	<0.001			11.728		

Continue...

Table A2. *Aspen results for the production of Agricultural water*

Stream	19	20	21	22	23	24
State	slurry	slurry	liquid	liquid	slurry	slurry
Temperature °C	25	25	25	25	25	25
Pressure bar	0.86	0.86	0.86	0.86	0.86	0.86
Vapor Fraction	0	0	0	1	0	0
Solid Fraction	1	1			1	1
Mass Flow kg/hr	309815.25	10085.622	299729.63	77.612	299637.42	10085.622
Volume Flow m^3/hr	310.315	10.102	300.213	50.618	300.262	10.102
pH	11.95	11.95	11.95		8.5	11.95

Component mass flows, kg/hr

H_2O	309438.03	10073.343	299364.69		299395.27	10073.343
CO_2	trace	trace	trace	77.612	0.018	trace
H_2SO_4						
H_3O^+	trace	trace	trace		<0.001	trace
OH^-	56.246	1.831	54.415		0.019	1.831
HCO_3^-	0.001	<0.001	0.001		4.006	<0.001
CO_3^{2-}	0.048	0.002	0.046		0.087	0.002
K^+	47.902	1.559	46.342		46.342	1.559
Na^+	4.904	0.16	4.745		4.745	0.16
Ca^{2+}	97.029	3.159	93.87		36.376	3.159
$CaOH^+$	15.472	0.504	14.969		0.002	0.504
Mg^{2+}	0.001	<0.001	0.001		0.003	<0.001
$MgOH^+$	0.004	<0.001	0.003		trace	<0.001
Cl^-	0.457	0.015	0.442		0.442	0.015
HSO_4^-					trace	
SO_4^{2-}	155.159	5.051	150.108		150.108	5.051
Gypsum(aq)						
$CaCO_3$(aq)	trace	trace	trace			trace
Gibbsite	279.886	279.886				279.886
$Mg(OH)_2$	0.525	0.525				0.525
$Ca(OH)_2$						
Ettringite	1486.944	1486.944				1486.944
Gypsum						
$CaCO_3$(S)	12.461	12.461			169.826	12.461

Continue...

Table A2. *Aspen results for the production of Agricultural water*

Stream	25	26	27	28	29	30
State	liquid	solid	liquid	slurry	slurry	slurry
Temperature °C	25		25	25	24.981167	24.981167
Pressure bar	0.86	0.86	1	0.86	0.86	0.86
Vapor Fraction	0		0	0	0	0
Solid Fraction		1		1	1	1
Mass Flow kg/hr	392.215	0	586426.88	598805.98	3113.648	595692.33
Volume Flow m^3/hr	0.215	0	585.806	597.093	3.105	593.985
pH	-2.603		7.532	7	7	7

Component mass flows, kg/hr

H_2O	0.001		584187.79	595494.06	3096.427	592397.64
CO_2			4.557	2.566	0.013	2.553
H_2SO_4	341.672					
H_3O^+	8.281		< 0.001	0.002	trace	0.002
OH^-			0.004	0.001	trace	0.001
HCO_3^-			17.653	22.113	0.115	21.998
CO_3^{2-}			0.062	0.026	< 0.001	0.026
K^+			85.584	87.246	0.454	86.792
Na^+			23.871	24.253	0.126	24.127
Ca^{2+}			580.125	895.108	4.654	890.454
$CaOH^+$			0.003	0.001	trace	0.001
Mg^{2+}			0.367	0.374	0.002	0.372
$MgOH^+$			< 0.001	trace	trace	trace
Cl^-			24.528	24.997	0.13	24.867
HSO_4^-	42.26		< 0.001	< 0.001	trace	< 0.001
SO_4^{2-}	< 0.001		1499.797	2255.231	11.727	2243.504
Gypsum(aq)						
$CaCO_3$(aq)			2.536			
Gibbsite				481.393	457.323	24.07
$Mg(OH)_2$				0.524	0.498	0.026
$Ca(OH)_2$						
Ettringite		193.049		84.124	79.918	4.206
Gypsum						
$CaCO_3$(S)				12.345	11.728	0.617

Continue...

Table A2. *Aspen results for the production of Agricultural water*

Stream	31	32	33	34	35	36
State	slurry	slurry	liquid	slurry	slurry	slurry
Temperature °C	25	25	25	25.016477	25.016477	25.017854
Pressure bar	0.86	1	1	1	1	0.86
Vapor Fraction	0	0	0	0	0	0
Solid Fraction	1	1		1	1	1
Mass Flow kg/hr	83049.44	677718.51	591916.65	83049.44	2727.354	782.104
Volume Flow m^3/hr	82.963	677.001	591.29	82.963	2.725	0.781
pH	7.542	7.532	7.532	7.542	7.542	7.577

Component mass flows, kg/hr

H_2O	82732.882	675130.85	589656.6	82732.882	2716.958	779.203
CO_2	0.611	5.266	4.6	0.611	0.02	0.005
H_2SO_4						
H_3O^+	<0.001	<0.001	<0.001	<0.001	trace	trace
OH^-	0.001	0.005	0.005	0.001	<0.001	0.007
HCO_3^-	2.439	20.402	17.819	2.439	0.08	0.021
CO_3^{2-}	0.009	0.072	0.063	0.009	<0.001	<0.001
K^+	12.115	98.907	86.385	12.115	0.398	0.115
Na^+	3.46	27.587	24.094	3.46	0.114	0.031
Ca^{2+}	81.955	670.436	585.556	81.955	2.691	0.751
$CaOH^+$	<0.001	0.003	0.003	<0.001	<0.001	0.003
Mg^{2+}	0.053	0.425	0.371	0.053	0.002	<0.001
$MgOH^+$	trace	<0.001	<0.001	trace	trace	trace
Cl^-	3.48	28.347	24.758	3.48	0.114	0.03
HSO_4^-	trace	<0.001	<0.001	trace	trace	trace
SO_4^{2-}	211.897	1733.277	1513.837	211.897	6.959	1.932
Gypsum(aq)						
$CaCO_3$(aq)	0.538	2.931	2.56	0.538	0.018	0.005
Gibbsite	749.564	773.633		749.564	24.616	24.616
$Mg(OH)_2$	0.605	0.631		0.605	0.02	0.02
$Ca(OH)_2$	trace	trace		trace	trace	trace
Ettringite	143.543	147.75		143.543	4.714	4.714
Gypsum						
$CaCO_3$(S)						<0.001

Table A3. *Aspen results for the production of High Quality Industrial water*

Stream	1	2	3	4	5	6
State	liquid	slurry	slurry	liquid	slurry	liquid
Temperature °C	25	25	25	25	25	25
Pressure bar	0.86	0.86	0.86	0.86	0.86	0.86
Vapor Fraction	0	0	0	0	0	0
Solid Fraction		1	1		1	
Mass Flow kg/hr	299962.19	162.825	300135.2	293700.97	6434.235	4572.543
Volume Flow m^3/hr	300	0.163	300.151	293.717	6.435	4.573
pH	9.5	12.436	11.7	11.7	11.7	11.7

Component mass flow, kg/hr

H_2O	299146.05	162.596	299308.69	292892.17	6416.516	4559.951
CO_2	< 0.001		trace	trace	trace	trace
H_2SO_4						
H_3O^+	trace	trace	trace	trace	trace	trace
OH^-	0.204	0.093	32.699	31.998	0.701	0.498
HCO_3^-	0.137		0.001	0.001	< 0.001	< 0.001
CO_3^{2-}	0.04		0.034	0.033	0.001	0.001
K^+	46.41		46.41	45.415	0.995	0.707
Na^+	4.467		4.467	4.371	0.096	0.068
Ca^{2+}	170.31	0.094	217.703	213.036	4.667	3.317
$CaOH^+$	0.082	0.043	15.958	15.616	0.342	0.243
Mg^{2+}	8.913		0.004	0.004	< 0.001	< 0.001
$MgOH^+$	0.089		0.007	0.006	< 0.001	< 0.001
Cl^-						
HSO_4^-	trace					
SO_4^{2-}	509.235		509.235	498.318	10.917	7.758
Gypsum(aq)	41.59					
$CaCO_3$(aq)	34.668					
Gibbsite						
$Mg(OH)_2$			21.492		21.492	
$Ca(OH)_2$		108.168				
Ettringite						
Gypsum			41.59		41.59	
$CaCO_3$(S)			34.901		34.901	

Continue...

Table A3. *Aspen results for the production of High Quality Industrial water*

Stream	7	8	9	10	11	12
State	slurry	slurry	liquid	slurry	slurry	slurry
Temperature °C	25	25	25	25	25	25
Pressure bar	0.86	0.86	0.86	0.86	0.86	0.86
Vapor Fraction	0	0	0	0	0	0
Solid Fraction	1	1		1	1	1
Mass Flow kg/hr	1861.692	293.955	1567.737	41558.573	341297.86	41558.573
Volume Flow m^3/hr	1.862	0.294	1.568	41.572	341.41	41.572
pH	11.7	11.7	11.7	11.706	11.708	11.706

Component mass flow, kg/hr

H_2O	1856.565	293.146	1563.42	41454.745	340448.95	41454.745
CO_2	trace	trace	trace	trace	trace	trace
H_2SO_4						
H_3O^+	trace	trace	trace	trace	trace	trace
OH^-	0.203	0.032	0.171	4.572	37.534	4.572
HCO_3^-	trace	trace	trace	<0.001	0.001	<0.001
CO_3^{2-}	<0.001	<0.001	<0.001	0.005	0.039	0.005
K^+	0.288	0.045	0.242	6.428	52.792	6.428
Na^+	0.028	0.004	0.023	0.63	5.092	0.63
Ca^{2+}	1.35	0.213	1.137	27.109	221.56	27.109
$CaOH^+$	0.099	0.016	0.083	2.073	17.024	2.073
Mg^{2+}	<0.001	trace	<0.001	0.001	0.005	0.001
$MgOH^+$	<0.001	trace	<0.001	0.001	0.007	0.001
Cl^-				0.015	0.015	0.015
HSO_4^-						
SO_4^{2-}	3.159	0.499	2.66	62.996	514.84	62.996
Gypsum(aq)						
$CaCO_3$(aq)						
Gibbsite						
$Mg(OH)_2$	21.492	21.492		0.085	0.086	0.085
$Ca(OH)_2$						
Ettringite						
Gypsum	41.59	41.59		17809.996	17911.959	17809.996
$CaCO_3$(S)	34.901	34.901		0.055	0.055	0.055

Continue...

Table A3. *Aspen results for the production of High Quality Industrial water*

Stream	13	14	15	16	17	18
State	slurry	liquid	slurry	slurry	liquid	liquid
Temperature °C	25	25	25	25	24.997633	25
Pressure bar	0.86	0.86	0.86	1	0.86	1
Vapor Fraction	0	0	0	0	0	0
Solid Fraction	1		1	1		
Mass Flow kg/hr	230.928	299505.42	613.608	3337.392	2879.362	8067.101
Volume Flow m^3/hr	0.231	299.604	0.615	3.328	2.877	8.059
pH	11.707	11.708	12.436	7	7.599	7.586

Component mass flow, kg/hr

H_2O	230.352	298760.46	612.743	3319.072	2868.764	8036.82
CO_2		trace		0.013	0.017	0.049
H_2SO_4						
H_3O^+		trace	trace	trace	trace	trace
OH^-	0.025	32.938	0.349	trace	0.019	< 0.001
HCO_3^-	trace	0.001		0.113	0.074	0.214
CO_3^{2-}	< 0.001	0.034		< 0.001	< 0.001	0.001
K^+	0.036	46.328		0.483	0.419	1.17
Na^+	0.003	4.469		0.088	0.075	0.213
Ca^{2+}	0.151	194.43	0.355	4.992	2.773	7.918
$CaOH^+$	0.012	14.94	0.161	trace	0.008	< 0.001
Mg^{2+}	trace	0.004		0.001	0.001	0.002
$MgOH^+$	trace	0.006		trace	trace	trace
Cl^-	< 0.001	0.013		0.062	0.051	0.149
HSO_4^-				trace	trace	trace
SO_4^{2-}	0.35	451.797		12.569	7.145	20.498
Gypsum(aq)						
$CaCO_3$(aq)					0.015	0.065
Gibbsite				462.295		
$Mg(OH)_2$	< 0.001			0.404		
$Ca(OH)_2$			407.63			
Ettringite				111.962		
Gypsum						
$CaCO_3$(S)	< 0.001			14.291		

Continue...

Table A3. *Aspen results for the production of High Quality Industrial water*

Stream	19	20	21	22	23	24
State	slurry	slurry	liquid	liquid	slurry	slurry
Temperature °C	25	25	25	25	25	25
Pressure bar	0.86	0.86	0.86	0.86	0.86	0.86
Vapor Fraction	0	0	0	1	0	0
Solid Fraction	1	1			1	1
Mass Flow kg/hr	313022.84	13467.494	299555.35	94.091	299548.75	13467.494
Volume Flow m^3/hr	313.734	13.498	300.236	61.365	300.302	13.498
pH	11.95	11.95	11.95		8.5	11.95

Component mass flow, kg/hr

H_2O	312853.61	13460.213	299393.4		299411.87	13460.213
CO_2	trace	trace	trace	94.091	0.324	trace
H_2SO_4						
H_3O^+	trace	trace	trace		<0.001	trace
OH^-	53.953	2.321	51.631		0.018	2.321
HCO_3^-	0.001	<0.001	0.001		67.439	<0.001
CO_3^{2-}	0.081	0.003	0.077		1.238	0.003
K^+	48.4	2.082	46.318		46.318	2.082
Na^+	4.845	0.208	4.636		4.636	0.208
Ca^{2+}	38.751	1.667	37.084		1.622	1.667
$CaOH^+$	7.229	0.311	6.918		<0.001	0.311
Mg^{2+}	0.001	<0.001	0.001		0.003	<0.001
$MgOH^+$	0.003	<0.001	0.003		trace	<0.001
Cl^-	0.275	0.012	0.263		0.263	0.012
HSO_4^-					trace	
SO_4^{2-}	15.687	0.675	15.012		15.012	0.675
Gypsum(aq)						
$CaCO_3$(aq)						
Gibbsite	204.448	204.448				204.448
$Mg(OH)_2$	0.425	0.425				0.425
$Ca(OH)_2$						
Ettringite	2156.609	2156.609				2156.609
Gypsum						
$CaCO_3$(S)	15.134	15.134			100.69	15.134

Continue...

Table A3. *Aspen results for the production of High Quality Industrial water*

Stream	25	26	27	28	29	30
State	liquid	solid	liquid	slurry	slurry	slurry
Temperature °C	25		25	25	25.072172	25.072172
Pressure bar	0.86	0.86	1	0.86	0.86	0.86
Vapor Fraction	0		0	0	0	0
Solid Fraction		1		1	1	1
Mass Flow kg/hr	550.707	0	806628.92	822865.43	3337.392	819528.04
Volume Flow m^3/hr	0.302	0	805.816	820.533	3.328	817.221
pH	-2.603		7.586	7	7	7

Component mass flow, kg/hr

H_2O	0.002		803601.21	818348.3	3319.072	815029.22
CO_2			4.888	3.242	0.013	3.229
H_2SO_4	479.74					
H_3O^+	11.628		0.001	0.002	trace	0.002
OH^-			0.007	0.002	trace	0.002
HCO_3^-			21.415	27.891	0.113	27.778
CO_3^{2-}			0.085	0.033	<0.001	0.032
K^+			117.006	119.177	0.483	118.694
Na^+			21.288	21.623	0.088	21.535
Ca^{2+}			791.709	1230.763	4.992	1225.771
$CaOH^+$			0.004	0.001	trace	0.001
Mg^{2+}			0.227	0.232	0.001	0.231
$MgOH^+$			<0.001	trace	trace	trace
Cl^-			14.94	15.186	0.062	15.124
HSO_4^-	59.337		<0.001	<0.001	trace	<0.001
SO_4^{2-}	<0.001		2049.603	3098.981	12.569	3086.412
Gypsum(aq)						
$CaCO_3$(aq)			6.533			
Gibbsite				486.626	462.295	24.331
$Mg(OH)_2$				0.425	0.404	0.021
$Ca(OH)_2$						
Ettringite		194.824		117.855	111.962	5.893
Gypsum						
$CaCO_3$(S)				15.043	14.291	0.752

Continue...

Table A3. *Aspen results for the production of High Quality Industrial water*

Stream	31	32	33	34	35	36
State	slurry	slurry	liquid	slurry	slurry	slurry
Temperature °C	25	25	25	24.994594	24.994594	24.997633
Pressure bar	0.86	1	1	1	1	0.86
Vapor Fraction	0	0	0	0	0	0
Solid Fraction	1	1		1	1	1
Mass Flow kg/hr	114725.36	932825.51	814696.02	114725.36	3707.899	1059.466
Volume Flow m^3/hr	114.611	931.886	813.875	114.61	3.704	1.058
pH	7.573	7.586	7.586	7.573	7.573	7.599

Component mass flow, kg/hr

H_2O	114294.65	929324.12	811638.03	114294.65	3693.979	1055.566
CO_2	0.736	5.653	4.937	0.736	0.024	0.006
H_2SO_4						
H_3O^+	<0.001	0.001	0.001	<0.001	trace	trace
OH^-	0.001	0.008	0.007	0.001	<0.001	0.007
HCO_3^-	3.134	24.765	21.629	3.134	0.101	0.027
CO_3^{2-}	0.012	0.099	0.086	0.012	<0.001	<0.001
K^+	16.618	135.312	118.176	16.618	0.537	0.154
Na^+	3.083	24.618	21.501	3.083	0.1	0.028
Ca^{2+}	112.687	915.572	799.627	112.687	3.642	1.02
$CaOH^+$	0.001	0.005	0.004	0.001	<0.001	0.003
Mg^{2+}	0.031	0.262	0.229	0.031	0.001	<0.001
$MgOH^+$	trace	<0.001	<0.001	trace	trace	trace
Cl^-	2.154	17.278	15.09	2.154	0.07	0.019
HSO_4^-	trace	<0.001	<0.001	trace	trace	trace
SO_4^{2-}	291.602	2370.262	2070.101	291.602	9.425	2.629
Gypsum(aq)						
$CaCO_3$(aq)	0.648	7.555	6.599	0.648	0.021	0.006
Gibbsite	916.569	940.9		916.569	29.623	29.623
$Mg(OH)_2$	0.804	0.825		0.804	0.026	0.026
$Ca(OH)_2$	trace	trace		trace	trace	trace
Ettringite	206.313	212.205		206.313	6.668	6.668
Gypsum						
$CaCO_3$(S)						<0.001

Table A4(i). *Aspen results showing the conversion of sulphate to ettringite at stage 3*

Conversion of SO_4^{2-} %	**sulphate kg/hr stream 14**	**sulphate kg/hr stream 16**	**sulphate kg/hr stream 17**	**sulphate kg/hr stream 18**	**Sulphate kg/hr stream R3**
10	448	18.0	4.69	1.73	60
28	448	14.9	5.44	5.39	60
46	448	14.5	6.77	9.31	60
64	448	14.7	6.75	15.44	60
82	448	15.3	8.92	17.20	60
90	448	15.4	10.01	21.71	60
100	448	15.6	9.98	21.39	60

Continue...

Table A4 (i). *Aspen results showing the conversion of sulphate to ettringite at stage 3*

Conversion of SO_4^{2-} %	**calcium kg/hr stream 14**	**calcium kg/hr stream 15**	**calcium kg/hr stream 16**	**calcium kg/hr stream 17**	**calcium kg/hr stream 18**	**Calcium kg/hr stream 19**
10	193	0.09	7.10	1.97	0.66	209
28	193	0.14	5.91	2.26	2.08	174
46	193	0.20	5.74	2.76	3.58	140
64	193	0.25	5.85	2.77	5.99	105
82	193	0.31	6.08	3.59	6.64	69
90	193	0.34	6.12	4.01	8.37	53
100	193	0.37	6.21	4.00	8.27	32

Continue...

Table A4 (i). *Aspen results showing the conversion of sulphate to ettringite at stage 3*

Conversion of SO_4^{2-} %	**Gibbsite recycled kg/hr stream 16**	**Gibbsite kg/hr stream 19**	**Ettringite kg/hr stream 19**
10	822	796	216
28	664	592	601
46	624	505	996
64	621	454	1403
82	615	398	1814
90	613	372	2014
100	612	345	2236

Table A4 (ii). *Aspen results showing the conversion of sulphate to ettringite at stage 3, Reagent costs*

conversion of sulphate %	Lime kg/hr stage 1	Lime kg/hr stage 3	cost of lime R/m^3	CO_2 kg/hr stage 1	CO_2 kg/hr stage 4	cost of CO_2 R/m^3	H_2SO_4 kg/hr stage 5	cost of H_2SO_4 R/m^3	total cost R/m^3
10	108	101	0.22	15.4	85.5	0.13	57	0.06	0.41
28	108	163	0.28	15.4	83.0	0.13	135	0.14	0.56
46	108	226	0.35	15.4	80.5	0.13	215	0.23	0.71
64	108	291	0.42	15.4	78.0	0.12	297	0.32	0.86
82	108	356	0.48	15.4	76.9	0.12	381	0.41	1.01
90	108	387	0.52	15.4	83.3	0.13	424	0.45	1.10
100	108	420	0.55	15.4	98.8	0.15	464	0.50	1.20

Table A5 (i). *Aspen results showing the decomposition of ettringite at stage 5*

Decomposition of ettringite stage 5 %	gibbsite recycled stream 16 kg/hr	gibbsite residue stream 19 kg/hr	gibbsite produced kg/hr	Ettringite stage 3 kg/hr	Ettringite stage 5 kg/hr	Ettringite produced kg/hr	Calcium removed %	sulphate removed %	gibbsite removed %
10	93	0	93	7319	6632	687	13.93	26.44	100
15	110	0	110	5877	5054	823	20.70	33.56	100
19	122	0	122	5260	4055	1205	26.46	39.42	100
24	161	0	161	5330	4035	1295	38.60	51.72	100
29	190	0	190	5200	3743	1457	48.27	61.59	100
34	224	0	224	5268	3527	1741	59.30	72.78	100
38	255	0	255	5273	3278	1995	71.67	85.24	100
43	427	160	267	4902	2815	2087	74.48	88.22	62.59
48	475	214	261	4319	2277	2043	74.14	88.07	54.94
53	544	290	254	3825	1835	1989	73.83	87.92	46.67

Continue...

Table A5 (i). *Aspen results showing the decomposition of ettringite at stage 5*

Decomposition of ettringite stage 5 %	gibbsite recycled stream 16 kg/hr	gibbsite residue stream 19 kg/hr	gibbsite produced kg/hr	Ettringite stage 3 kg/hr	Ettringite stage 5 kg/hr	Ettringite produced kg/hr	Calcium removed %	sulphate removed %	gibbsite removed %
57	547	295	252	3495	1511	1984	73.60	87.85	46.04
62	687	437	250	3206	1234	1972	73.49	87.80	36.42
67	692	444	248	2950	995	1955	73.30	87.74	35.79
72	704	459	245	2721	788	1934	73.13	87.66	34.79
76	701	459	243	2531	611	1920	72.97	87.60	34.58
81	679	439	240	2359	456	1902	72.82	87.54	35.40
86	714	474	240	2219	322	1897	72.74	87.51	33.57
91	713	476	237	2080	202	1879	72.59	87.44	33.27
95	654	419	235	1961	101	1860	72.44	87.38	35.92
95	704	468	236	1967	96	1872	72.51	87.41	33.56
100	746	511	235	1867	0	1867	72.46	87.39	31.55

Table A5 (ii). *Aspen results showing the decomposition of ettringite at stage 5, Reagent costs*

Decomposition of ettringite stage 5 %	Lime stage 1 kg/hr	Lime stage 3 kg/hr	cost of lime R/m3	CO_2 stage 1 kg/hr	CO_2 stage 4 kg/hr	cost of CO_2 R/m3	H_2SO_4 stage 5 kg/hr	cost of H_2SO_4 R/m3	total costs R/m3
10	108	217	0.34	15.4	73.4	0.118	13.3	0.014	0.472
15	108	236	0.36	15.4	76.3	0.122	20.5	0.022	0.503
19	108	247	0.37	15.4	76.7	0.123	26.8	0.029	0.521
24	108	298	0.42	15.4	76.2	0.122	55.3	0.059	0.605
29	108	337	0.46	15.4	75.5	0.121	76.9	0.082	0.667
34	108	380	0.51	15.4	74.3	0.120	101.6	0.108	0.737
38	108	416	0.55	15.4	74.2	0.119	124.8	0.133	0.799
43	108	434	0.57	15.4	78.1	0.125	133.4	0.142	0.833
48	108	424	0.56	15.4	78.4	0.125	128.3	0.137	0.817
50	108	412	0.54	15.4	78.1	0.125	122.2	0.130	0.798
53	108	409	0.54	15.4	78.6	0.125	121.1	0.129	0.794

Continue…

Table A5 (ii). *Aspen results showing the decomposition of ettringite at stage 5, Reagent costs*

Decomposition of ettringite stage 5 %	Lime stage 1 kg/hr	Lime stage 3 kg/hr	cost of lime R/m3	CO_2 stage 1 kg/hr	CO_2 stage 4 kg/hr	cost of CO_2 R/m3	H_2SO_4 stage 5 kg/hr	cost of H_2SO_4 R/m3	total costs R/m3
57	108	406	0.54	15.4	78.7	0.125	119.8	0.128	0.790
62	108	402	0.53	15.4	79.0	0.126	117.8	0.126	0.784
67	108	398	0.53	15.4	79.0	0.126	115.4	0.123	0.777
72	108	394	0.52	15.4	79.1	0.126	113.5	0.121	0.771
76	108	390	0.52	15.4	79.3	0.126	111.7	0.119	0.766
81	108	389	0.52	15.4	79.4	0.126	110.9	0.118	0.764
86	108	385	0.51	15.4	79.4	0.126	112.1	0.120	0.760
91	108	381	0.51	15.4	79.4	0.126	106.8	0.114	0.751
95	108	384	0.51	15.4	79.5	0.127	108.1	0.115	0.755
100	108	382	0.51	15.4	79.5	0.127	106.9	0.114	0.752

Table A6 (i). *Aspen results showing varying amounts of NaCl in the feed water*

NaCl stream 1 ppm	calcium stream 1 ppm	sulphate stream 1 ppm	$Mg(OH)_2$ stream 8 kg/hr	Gypsum stream 8 kg/hr	calcium stream 14 kg/hr	sulphate stream 14 kg/hr
0	568	1697	21	42	194	452
57	574	1713	21	33	197	457
114	581	1729	21	25	199	461
171	587	1744	21	16	201	466
229	594	1759	21	8	203	471
286	600	1774	21	0.12	205	475
343	600	1775	21	0	207	480
400	600	1775	21	0	209	485

Continue...

Table A6 (i). *Aspen results showing varying amounts of NaCl in the feed water*

NaCl stream 1 ppm	calcium removed %	sulphate removed %	ettringite stream 19 kg/hr	ettringite recycled stream 16 kg/hr	gibbsite stream 19 kg/hr	gibbsite recycled stream 16 kg/hr
0	72	97	1919	101	227	457
57	72	97	1940	102	230	462
114	72	98	1953	102	230	464
171	72	97	1991	104	235	473
229	73	97	2001	104	235	475
286	73	97	2033	106	237	480
343	73	96	2060	108	240	486
400	73	97	2062	108	240	486

Table A6 (ii). *Aspen results showing varying amounts of NaCl in the feed water, Reagent costs*

NaCl in feed water ppm	Lime kg/hr stage 1	Lime kg/hr stage 3	cost of lime R/m^3	CO_2 kg/hr stage 1	CO_2 kg/hr stage 4	cost of CO_2 R/m^3	H_2SO_4 kg/hr stage 5	cost of H_2SO_4 R/m^3	total cost R/m^3
0	108	370	0.50	15	80	0.13	432	0.46	1.09
57	108	374	0.50	15	80	0.13	436	0.46	1.10
114	109	374	0.50	15	80	0.13	437	0.47	1.10
171	109	383	0.51	15	81	0.13	447	0.48	1.12
229	109	383	0.51	15	81	0.13	448	0.48	1.12
286	109	391	0.52	15	81	0.13	458	0.49	1.14
343	109	396	0.53	15	82	0.13	466	0.50	1.15
400	109	396	0.53	15	82	0.13	467	0.50	1.15

Table A7. *Aspen results showing varying calcium to sulphate ratios at stage 3*

$[Ca^{2+}]/[SO_4^{2-}]$	**calcium stream 14 kg/hr**	**calcium stream 15 kg/hr**	**calcium stream 16 kg/hr**	**calcium stream 17 kg/hr**	**calcium stream 18 kg/hr**	**calcium stream 19**	**calcium removed %**
1.65	193	0.10	5.90	1.99	1.12	176.08	12.7
1.27	193	0.12	5.78	2.12	1.24	161.30	20.1
1.03	193	0.14	5.79	2.25	1.81	146.52	27.7
0.87	193	0.17	6.61	2.55	2.86	131.84	35.6
0.75	193	0.19	6.59	2.69	3.45	117.05	43.1
0.66	193	0.22	6.62	2.53	3.98	102.26	50.4
0.59	193	0.24	6.64	2.95	4.84	87.46	57.8
0.54	193	0.26	6.68	3.15	4.85	72.66	65.0
0.49	193	0.28	6.72	3.19	4.90	57.86	72.2
0.45	193	0.31	6.81	3.57	6.60	43.07	79.5
0.43	193	0.33	6.81	3.32	6.33	31.54	84.9

Continue…

Table A7. *Aspen results showing varying calcium to sulphate ratios at stage 3*

$[Ca^{2+}]/[SO_4^{2-}]$	sulphate stream 14 kg/hr	sulphate stream 16 kg/hr	sulphate stream 17 kg/hr	sulphate stream 18 kg/hr	sulphate stream 19 kg/hr	sulphate removed %
1.65	100	14.98	4.73	2.92	61	50.27
1.27	136	14.65	5.09	3.24	61	61.52
1.03	171	14.61	5.44	4.72	61	68.78
0.87	207	16.53	6.18	7.36	62	74.01
0.75	242	16.52	6.54	8.88	62	77.51
0.66	278	16.58	6.13	10.27	62	80.13
0.59	313	16.65	7.22	12.48	62	82.27
0.54	349	16.76	7.76	12.51	62	83.92
0.49	384	16.87	7.85	12.65	62	85.29
0.45	420	17.11	8.84	17.06	62	86.50
0.43	448	17.15	8.22	16.39	62	87.25

Continue...

Table A7. *Aspen results showing varying calcium to sulphate ratios at stage 3*

$[Ca^{2+}]/[SO_4^{2-}]$	ettringite produced stage 3 kg/hr	gibbsite recycled stream 16 kg/hr	gibbsite stream 19 kg/hr	gibbsite produced stage 5 kg/hr
1.65	794	674	641	33
1.27	1256	650	598	53
1.03	1735	634	569	65
0.87	2256	626	527	100
0.75	2736	620	505	115
0.66	3206	619	484	135
0.59	3704	617	461	156
0.54	4170	616	441	175
0.49	4632	614	419	195
0.45	5157	613	396	217
0.43	5498	611	380	231

Table A8(i). *Aspen results of the sensitivity analysis of $CaSO_4$ in the feed water*

$CaSO_4$ ppm feed water	Ca^{2+} ppm stream 1	SO_4^{2-} ppm stream 1	$Mg(OH)_2$ kg/hr stream 8	Gypsum kg/hr stream 8	Gypsum kg/hr stream 36	$CaSO_4$ kg/hr stream 36	$CaCO_3$ kg/hr stream 36
0	0	225	21.5	0	0.9	83	0.005
370	64	487	21.5	0	0.6	236	0.000
741	172	748	21.5	0	0	500	0.000
1111	281	1009	21.5	0	0	714	0.000
1481	390	1271	21.5	0	0	887	0.000
1852	499	1532	21.5	0	0	952	0.042
2222	568	1698	21.5	52	120	952	0.042
2593	568	1697	21.5	192	145	952	0.042
2963	567	1697	21.5	333	170	952	0.042
3333	567	1697	21.5	473	195	952	0.042

Continue…

Table A8(i). *Aspen results of the sensitivity analysis of $CaSO_4$ in the feed water*

$CaSO_4$ ppm feed water	Ca^{2+} kg/hr stream 14	Ca^{2+} kg/hr stream 15	Ca^{2+} kg/hr stream 16	Ca^{2+} kg/hr stream 17	Ca^{2+} kg/hr stream 18	Ca^{2+} kg/hr stream 19
0	34	0.07	6.14	0.44	0.52	35
370	66	0.12	5.76	0.98	1.63	38
741	99	0.17	5.80	1.76	3.13	43
1111	132	0.22	5.90	2.44	4.50	48
1481	164	0.28	6.05	2.90	5.56	53
1852	194	0.33	6.15	2.95	7.06	57
2222	194	0.33	6.15	3.05	7.32	57
2593	194	0.33	6.15	3.05	7.51	57
2963	194	0.33	6.15	3.05	7.69	57
3333	193	0.33	6.15	3.05	7.87	57

Continue…

Table A8(i). *Aspen results of the sensitivity analysis of $CaSO_4$ in the feed water*

$CaSO_4$ ppm feed water	SO_4^{2-} kg/hr stream 14	SO_4^{2-} kg/hr stream 16	SO_4^{2-} kg/hr stream 17	SO_4^{2-} kg/hr stream 18	SO_4^{2-} kg/hr stream 19
0	68	15.60	0.99	1.36	60
370	146	14.58	2.37	4.24	60
741	224	14.57	4.31	8.08	60
1111	303	14.83	6.03	11.61	60
1481	381	15.17	7.17	14.28	60
1852	453	15.46	7.28	18.19	60
2222	452	15.46	7.49	18.85	60
2593	451	15.46	7.48	19.34	60
2963	450	15.46	7.48	19.81	60
3333	450	15.46	7.48	20.28	60

Continue…

Table A8(i). *Aspen results of the sensitivity analysis of $CaSO_4$ in the feed water*

$CaSO_4$ ppm feed water	**Ettringite kg/hr stream 19**	**Ettringite kg/hr stream 16**	**Gibbsite kg/hr stream 19**	**Gibbsite kg/hr stream 16**
0	112	8	695	708
370	474	26	589	646
741	851	45	527	628
1111	1225	63	469	616
1481	1594	81	423	613
1852	1933	98	380	611
2222	1933	98	380	611
2593	1933	98	380	611
2963	1932	98	380	611
3333	1932	98	380	611

Table A8(ii). *Aspen results of the sensitivity analysis of $CaSO_4$ in the feed water, Reagent costs*

$CaSO_4$ ppm feed water	CO_2 kg/hr stage 1	CO_2 kg/hr stage 4	cost of CO_2 R/m^3	Lime kg/hr stage 1	Lime kg/hr stage 3	cost of lime R/m^3	H_2SO_4 kg/hr stage 5	cost of H_2SO_4 R/m^3	total cost R/m^3
0	15.6	81.4	0.13	97	76	0.18	35	0.04	0.35
370	15.5	79.5	0.13	100	134	0.24	108	0.12	0.49
741	15.4	80.2	0.13	102	196	0.31	185	0.20	0.64
1111	15.4	80.2	0.13	105	258	0.38	262	0.28	0.78
1481	15.4	80.0	0.13	107	319	0.44	336	0.36	0.93
1852	15.4	80.0	0.13	108	375	0.50	406	0.43	1.06
2222	15.4	79.9	0.13	108	374	0.50	406	0.43	1.06
2593	15.4	79.9	0.13	108	374	0.50	406	0.43	1.06
2963	15.4	79.9	0.13	108	374	0.50	406	0.43	1.06
3333	15.4	79.8	0.13	108	374	0.50	406	0.43	1.06

Figure A9(i). *Aspen results of sensitivity analysis of feed water flow rate*

mass flow feed water kg/hr	flow rate of feed water m^3/hr	Ettringite kg/hr	gypsum stream 36 kg/hr	$Mg(OH)_2$ stream 8 kg/hr	Ettringite stream 19 kg/hr
40000	40	1197	12	3	493
257778	258	3544	87	18	1458
299954	300	4654	84	21	1915
475556	476	6265	161	34	2578
693333	693	9236	234	50	3801
911111	911	11977	308	65	4929
1128889	1129	14929	503	81	6144
1346667	1347	17157	605	96	7061
1564444	1564	20466	626	112	8422
1782222	1782	23549	642	128	9691
2000000	2000	26685	678	143	10981

Figure A9(ii). *Aspen results of sensitivity analysis of feed water flow rate, Reagent costs*

flow rate of feed water	lime	lime	costs of lime	CO_2	CO_2	costs of CO_2	H_2SO_4	cost of H_2SO_4	total cost
	stage 1	stage 3		stage 1	stage 4		stream 25		
m^3/hr	kg/hr	kg/hr	R/m^3	kg/hr	kg/hr	R/m^3	kg/hr	R/m^3	R/m^3
40	14	139	1.20	2	7	0.09	0	0.00	1.29
258	93	362	0.55	13	67	0.12	99	0.12	0.80
300	108	475	0.61	15	78	0.12	157	0.17	0.90
476	171	639	0.53	24	125	0.13	233	0.16	0.82
693	250	942	0.54	36	184	0.13	380	0.18	0.84
911	329	1221	0.53	47	240	0.13	517	0.18	0.84
1129	407	1525	0.54	58	301	0.13	664	0.19	0.85
1347	486	1747	0.52	69	351	0.12	778	0.18	0.83
1564	564	2087	0.53	80	413	0.13	940	0.19	0.85
1782	643	2399	0.53	91	474	0.13	1093	0.20	0.86
2000	721	2728	0.54	102	536	0.13	1241	0.20	0.87

Figure A10(i). *Aspen results of sensitivity analysis of lime input to stage 1*

lime stage 1 kg/hr	pH stage 1 stream 3	$Mg(OH)_2$ stream 8 kg/hr	Gypsum stream 8 kg/hr	pH stage 2 stream 11	$CaSO_4$ stream 36 kg/hr	$CaCO_3$ stream 36 kg/hr
0	9.50	0	41.6	9.50	1658	0.08
78	11.50	21.5	41.6	11.51	1336	0.02
156	11.89	21.5	41.6	11.90	1271	0.01
233	12.09	21.5	41.6	12.10	1057	0.02
311	12.22	21.5	41.6	12.23	1083	0.02
389	12.32	21.5	41.6	12.33	1083	0.00
415	12.34	21.5	41.6	12.36	1054	0.00
467	12.36	21.5	41.6	12.37	1212	0.00
544	12.36	21.5	41.6	12.37	1212	0.00
622	12.36	21.5	41.6	12.37	1212	0.00
700	12.36	21.5	41.6	12.37	1212	0.00

Continue…

Figure A10(i). *Aspen results of sensitivity analysis of lime input to stage 1*

pH	calcium	Ca^{2+} removed	sulphate	SO$_4^{2-}$ removed	ettringite	ettringite recycled	gibbsite residue	gibbsite recycled
stream 3	stream 14 kg/hr	%	stream 14 kg/hr	%	stream 19 kg/hr	stream 16 kg/hr	stream 19 kg/hr	stream 16 kg/hr
9.50	170	69.1	508	96.3	2242	117	258	526
11.50	186	70.9	462	96.4	1977	103	233	470
11.89	208	73.7	439	96.5	1863	98	223	445
12.09	230	76.0	420	97.0	1760	92	214	424
12.22	252	78.1	406	96.8	1694	89	208	410
12.32	275	79.8	394	94.3	1688	89	209	410
12.34	282	80.3	391	96.7	1621	85	200	394
12.36	287	80.3	388	96.5	1620	83	206	399
12.36	287	80.3	388	96.5	1620	83	206	399
12.36	287	80.4	388	96.3	1620	83	206	399
12.36	286	80.4	387	96.4	1620	83	206	399

Figure A10(ii). *Aspen results of sensitivity analysis of lime input to stage 1, Reagent costs*

pH stream 3 m^3/hr	lime stage 1 kg/hr	lime stage 3 kg/hr	costs of lime R/m^3	CO_2 stage 1 kg/hr	CO_2 stage 4 kg/hr	costs of CO_2 R/m^3	H_2SO_4 stream 25 kg/hr	cost of H_2SO_4 R/m^3	total cost R/m^3
11.50	76.90	411.24	0.51	15.37	80.29	0.13	443.80	0.47	1.11
11.89	154.68	314.65	0.49	15.37	80.27	0.13	419.14	0.45	1.06
12.09	232.46	218.52	0.47	15.37	79.90	0.13	396.71	0.42	1.02
12.22	310.23	130.79	0.46	15.37	80.11	0.13	381.86	0.41	0.99
12.32	388.01	42.70	0.45	15.37	80.01	0.13	369.27	0.39	0.97
12.34	413.63	13.87	0.45	15.37	79.89	0.13	367.22	0.39	0.96
12.36	465.79	0.00	0.49	15.37	82.95	0.13	362.23	0.39	1.00
12.36	543.57	0.00	0.57	15.37	83.01	0.13	362.28	0.39	1.08
12.36	621.34	0.00	0.65	15.37	82.51	0.13	362.11	0.39	1.17
12.36	699.12	0.00	0.73	15.37	82.56	0.13	362.16	0.39	1.25

Figure A11(i). *Aspen results of sensitivity analysis of lime input to stage 3*

lime stream 15 kg/hr	pH stream 19	Ca^{2+} removed %	SO_4^{2-} removed %	calcium stream 19 ppm	ettringite stream 19 kg/hr	ettringite recycled stream 16 kg/hr	gibbsite residue stream 19 kg/hr	gibbsite recycled stream 16 kg/hr
300	11.60	88	96	79	1929	101	230	461
400	12.03	66	96	226	1927	101	229	459
452	12.14	56	96	296	1927	101	229	459
500	12.23	46	97	359	1928	101	228	458
600	12.35	28	97	481	1928	101	229	458
700	12.44	12	96	593	1929	101	229	460

Figure A11(ii). *Aspen results of sensitivity analysis of lime input to stage 3, Reagent costs*

pH stream 3 m^3/hr	lime stage 1 kg/hr	lime stage 3 kg/hr	costs of lime R/m^3	CO_2 stage 1 kg/hr	CO_2 stage 4 kg/hr	costs of CO_2 R/m^3	H_2SO_4 stream 25 kg/hr	cost of H_2SO_4 R/m^3	total cost R/m^3
11.60	108	299	0.42	15.4	38.5	0.07	427	0.46	0.95
12.03	108	399	0.53	15.4	95.8	0.15	434	0.46	1.14
12.14	108	451	0.58	15.4	125.5	0.19	436	0.46	1.24
12.23	108	499	0.63	15.4	153.4	0.22	437	0.47	1.32
12.35	108	599	0.74	15.4	210.8	0.30	440	0.47	1.51
12.44	108	699	0.84	15.4	265.9	0.38	448	0.48	1.70

APPENDIX B.

SOLUBILITY DATA

Mass balance equations with solubility products (log K_{sp}, $I = 0.0$, $T = 25°C$)

[Mohammed *et al.*, 1985]

Chemical reactions	**log K_{sp}**
$Ca(OH)_2(s) \rightleftharpoons Ca^{2+} + 2OH^-$	5.19
$Ca^{2+} + OH^- \rightleftharpoons CaOH^+$	1.3
$Ca^{2+} + 2OH^- \rightleftharpoons Ca(OH)_2^0$	-5.19
$CaSO_4 \cdot 2H_2O(s) \rightleftharpoons Ca^{2+} + SO_4^{2-} + 2H_2O$	-4.64
$Ca^{2+} + SO_4^{2-} \rightleftharpoons CaSO_4^0(aq)$	-2.31
$Ca_6Al_2O_3(SO_4)_3 \cdot 32H_2O \rightleftharpoons 6Ca^{2+} + 2Al(OH)_4^- + 3SO_4^{2-} + 4\,OH^- + 26H_2O$	-43.13
$Ca^{2+} + CO_3^{2-} \rightleftharpoons CaCO_3^0(aq)$	3.15
$Ca^{2+} + HCO_3^- \rightleftharpoons CaHCO_3^+$	1.0
$H^+ + OH^- \rightleftharpoons H_2O$	14.0
$H_2O + CO_2(g) \rightleftharpoons H_2CO_3$	-1.464
$H_2CO_3 \rightleftharpoons HCO_3^- + H^+$	-6.352
$HCO_3^- \rightleftharpoons CO_3^- + H^+$	-10.33
$HSO_4^- \rightleftharpoons SO_4^{2-} + H^+$	-1.99
$Al(OH)_3(s) \rightleftharpoons Al^{3+} + 3OH^-$	33.5
$Al^{3+} + OH^- \rightleftharpoons AlOH^{2+}$	9.01
$Al^{3+} + 2OH^- \rightleftharpoons Al(OH)_2^+$	18.7
$Al^{3+} + 3OH^- \rightleftharpoons Al(OH)_3^0(aq)$	27.0
$Al^{3+} + 4OH^- \rightleftharpoons Al(OH)_4^-$	33.0
$Al(OH)_3(s) \rightleftharpoons Al^{3+} + 3OH^-$	33.5
$Al^{3+} + OH^- \rightleftharpoons AlOH^{2+}$	9.01
$Al^{3+} + 2OH^- \rightleftharpoons Al(OH)_2^+$	18.7
$Al^{3+} + 3OH^- \rightleftharpoons Al(OH)_3^0(aq)$	27.0

Mass Action Equations	**log K_{sp}**
$Al^{3+} + 4OH^- \rightleftharpoons Al(OH)_4^-$	33.0
$Fe(OH)_2(s) \rightleftharpoons Fe^{2+} + 2OH^-$	-15.1
$Fe^{2+} + OH^- \rightleftharpoons FeOH^+$	4.5
$Fe^{2+} + 2OH^- \rightleftharpoons Fe(OH)_2$	7.4
$Fe^{2+} + 3OH^- \rightleftharpoons Fe(OH)_3^-$	10.0
$Fe^{2+} + 4OH^- \rightleftharpoons Fe(OH)_4^{2-}$	9.6
$Mg(OH)_2(s) \rightleftharpoons Mg^{2+} + 2OH^-$	-11.15
$Mg^{2+} + OH^- \rightleftharpoons MgOH^+$	2.58
$Mg^{2+} + 4OH^- \rightleftharpoons Fe(OH)_4^{4+}$	16.3

APPENDIX C.

COMPUTATIONAL ORDER OF THE FLOWSHEET

Convergence

For Aspen to solve the unknown stream variables in the recycling loops, it uses a solution technique, which is based on tear stream guesses. In the recycle loop, a guess is taken of the variables of one of the streams (tear stream) in the loop and information is passed from unit to unit until new values of the variables in the tear stream are computed. These new values are used to repeat the calculations until the convergence tolerances are satisfied. This is the principle behind the method of successive substitutions for convergence. Upon satisfying the convergence criteria, control is transferred to the unit following the recycle loop in the calculation order. Aspen Plus names the recycle convergence units $OLVER01, $OLVER02,..., in sequence. This method of tearing streams is not only implemented in stream recycle loops but it is also used to solve design specification recycle loops. An example of how Aspen implements the tearing of streams and convergence of these streams in a design spec recycle loop is when setting the pH at stream R1. The recycle convergence unit for R1-PH design specification is called $OLVER03 by Aspen. This unit and its stream are dotted as though imaginary as shown in Figure C1.

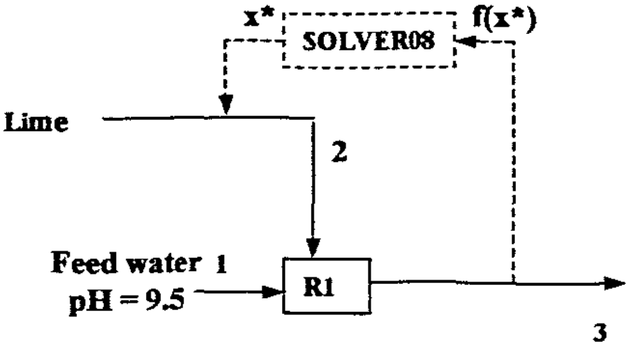

Figure C1
Diagrammatic representation of convergence to set the pH at stream 3

The R1-PH specification states that at stream R1, the pH should be set to 11.7. Aspen chooses a stream to tear, namely the stream leaving $OLVER03. It lets x be the value of a particular variable (element) of the output of the convergence unit $OLVER03. It now computes the reactions at reactor R1 using the guessed value x*. It produces a value f(x*) now entering convergence unit $OLVER03. If y = f(x*)-x*, then the objective of convergence is to drive y towards zero.

All the specifications have a convergence unit ($OLVER) assigned to it as well as all the recycle loops as shown by Table C1. To speed up convergence, the programmer can choose which streams he wants to tear, however for this simulation, Aspen chose all the tear streams.

Aspen uses a number of convergence methods to converge recycle loops. Two methods are specified in this particular program, namely the Wegstein and Secant methods respectively.

TABLE C1. *Design Specifications of the ASPEN model.*

Name	SOLVER no.	Design Spec. of set point	Vary variable to achieve set point
FEED	1	Flow rate of feed water =300 m^3/hr	Mass flow of feed (stream 1)
FEED PH	2	pH (stream 1) = 9.5	Mass flow of CO_2 (stream AA)
R1-PH	3	pH (stream R1)= 11.7	Mass flow of lime (stream 2)
2-SEED	4	% Solids entering reactor R2 = 5%	Flow fraction of stream 12
R3-PH	5	pH (stream R3) = 11.95	Mass flow of lime (stream 15)
3-PPTN	6	$[SO_4^{2-}]$ at stream R3 = 200ppm	Conversion of SO_4^{2-} in the ettringite formation reaction (stage 3)
4-PH	7	pH (stream R4) = 8.5	Mass flow of CO_2 (stream 22)
R5-PH	8	pH (stream R5A1) = 9	Mass flow of H_2SO_4 (stream 25)
5-SEED	9	% Solids entering reactor R5B = 5%	Flow fraction of stream 34
l-FEED	10	Ratio of SO_4^{2-} entering reactor R3 to solids entering reactor R5A = 1.59 (for every kg of SO_4^{2-} fed to stage 3, ~ 1 kg of $Al(OH)_3$ is fed to stage 5)	Mass flow of stream 26
F1	11	Metal hydroxides (stream 8) = 25% solids	Flow fraction of stream 8
F2	12	Gypsum (stream 36) = 60% solids	Flow fraction of stream 36
S1A	13	% Solids in stream 5 = 1.5%	Flow fraction of stream 5
[illegible]	14	% Solids in stream 7 = 5%	Flow fraction of stream 7
S2	15	% Solids in stream 11 = 30%	Flow fraction of stream S2
S3	16	% Solids in stream 20 = 15%	Flow fraction of stream 20
S5A	17	% Solids in stream 29 = 15%	Flow fraction of stream 29
S5B	18	% Solids in stream 35 = 30%	Flow fraction of stream 35
T5	19	$[Ca^{2+}]$ at stream 28 =1.5 kg/m^3	Flow fraction of stream 27

Computational order of the flowsheet

Table C1 in conjunction with Figure C2 best describes the order in which Aspen calculates the values of this model. All the design specifications are converged by means of the secant method, while the recycle loops in this simulation are converged via the wegstein method. The first task that Aspen performs is to set the feed water flow rate as shown by $OLVER1. Next it sets the pH of stream 1 as shown by $OLVER2. When $OLVER2 has converged, it returns to $OLVER1 to check whether the convergence of $OLVER2 has affected the convergence of $OLVER1. If $OLVERS 1 and 2 now both converge, Aspen proceeds to $OLVER3. Here the pH of stream R1 is set, and is done together with reactor R1. A value for the pH at $OLVER3 is predicted, which influences the amount of lime (stream 2) added. This lime will affect the reactions at reactor R1 and since the feed water, now having a pH of 9.5 is brought into contact with limewater reactor R1. The convergence of $OLVER3 is followed by $OLVER13. The flow fraction at separator S1A is altered until stream 5 contains 1.5% solids. The convergence of $OLVER13 is followed by the convergence of $OLVER14 and then $OLVER11. Here the flow fractions of separators S1B and F1 are altered until stream 7 contains 5% solids and stream 8 contains 25% solids respectively.

$OLVER20 is the convergence of the first recycle loop for this simulation. This loop is made up of streams 11, 12 and 10. Aspen tears stream 11 after which it starts with $OLVER4. Here the ratio of the solids in stream 12 to the liquids entering reactor R2 is set in place until convergence takes place. Stream 12 is pumped to reactor R2 where gypsum is formed at stream R2. This is followed by $OLVER15, which states that stream 11, should have 30% solids. After convergence, $OLVER15 proceeds back to the start of $OLVER20 (i.e. stream 11). This circular procedure continues until $OLVER20 converges.

$OLVER21 is the next recycle loop for this simulation. Now two streams are torn, namely stream 28 and 35. Stream 28 is torn to converge the recycle loop from stage 5 to stage 3, while the tearing of stream 35 is done to converge the loop at stage 5B. Two streams are selected as tear streams simultaneously because the smaller loop (stage 5B) is inside the bigger loop. The next design specification to follow $OLVER21 is $OLVER17. Here the flow fraction of stream 29 at separator S5A is varied until stream 29 contains 15% solids and convergence takes place. After the slurry of stream 29 is pumped, $OLVER9 is implemented. Convergence takes place as soon as 5% solids enters reactor R5B. Streams 30 and 31 react at reactor R5B to produce stream R5B. The components of stream R5B now reactor at reactor R5B1. Solution is pumped to separator S5B where $OLVER18 is implemented. Convergence takes place so that stream S5B contains 30% solids. This completes the recycle loop of stage 5B. The solution from stream 35 flows to the gypsum separator F2 where $OLVER12 starts. Here the flow fraction of stream 36 is varied until the gypsum outlet stream contains 60% solids. When this is achieved, splitter T5 splits the solution from stream 33.

$OLVER19 *is started whereby the flow fraction of stream* 27 *is changed so that stream* R5A has a calcium concentration of 1.5 kg/m^3. The program next selects a value for the mass flow of lime (stream 15), in order to implement $OLVER5 to stabilise the pH of stream 19 at 11.95. It then proceeds with $OLVER6, which varies the conversion of sulphate in the ettringite formation reaction (stage 3), to establish the concentration of sulphate of stream 19 at 0.2 kg/m^3. After $OLVER6 has converged, it returns to $OLVER 5 to verify whether the conditions for $OLVER 5 still hold. Once these conditions are met simultaneously, $OLVERS 5 and 6 both converge. The program now performs the various reactions at reactor R3A, followed by separation at splitter S3A and pumping at B2. $OLVER16 is now put into action by varying the flow fraction of stream 20 at separator S3, so that stream 20 contains 15% solids until convergence takes place. $OLVER10 which ensures that the ratio of mole flow of sulphate entering reactor R3 to the mole flow of ettringite and $Al(OH)_3$ into reactor R5A remains constant. The convergence of $OLVER10 is preceded by $OLVER8, which ensures the pH at stream 28 to be 9, by altering the flow of sulphuric acid into stage 5. Once $OLVER8 is completed, the program returns to $OVER19 to check whether its conditions are still met. If $OLVER19's conditions are not met, then the loop starting with $OLVER19 starts from the beginning using the values that it obtained at the end of $OLVER19 until convergence takes place. The end of R5A returns to $OLVER21, and a check is made to see if the results at the end of $OLVER21 are the same as those the beginning. When they are the same, convergence has taken place. Once the largest loop in this program has converged, the pH at stage 4 is altered to 8.5 at $OLVER7. The convergence of $OLVER7 is followed by reactions at reactor R4A to produce product water at stream 23.

Computational order of the flowsheet:

```
$OLVER1
     |$OLVER2
     | (RETURN $OLVER2)
 (RETURN $OLVER1)
$OLVER3 R1
 (RETURN $OLVER3)
$OLVER13 S1A
 (RETURN $OLVER13)
$OLVER14 S1B
 (RETURN $OLVER14)
$OLVER11 F1
 (RETURN $OLVER11)
$OLVER20
     |$OLVER4
     | (RETURN $OLVER4)
     | R2
     |$OLVER15 S2
     | (RETURN $OLVER15)
 (RETURN $OLVER20)

$OLVER21
     |$OLVER17 S5A
     | (RETURN $OLVER17)
     |
     |$OLVER9
     | (RETURN $OLVER9)
     | R5B
     |$OLVER18 S5B
     | (RETURN $OLVER18)
     |$OLVER12 F2
     | (RETURN $OLVER12)
     |$OLVER19
     |     |$OLVER5
     |     |     |$OLVER6 R3
     |     |     | (RETURN $OLVER6)
     |     | (RETURN $OLVER5)
     |     | $OLVER16 S3
     |     | (RETURN $OLVER16)
     |     |
     |     |$OLVER10
     |     | (RETURN $OLVER10)
     |     |$OLVER8 R5A
     |     | (RETURN $OLVER8)
     | (RETURN $OLVER19)

 (RETURN $OLVER21)
$OLVER7 R4
 (RETURN $OLVER7)
R4A
```

Figure C2. *Computational order of the flowsheet*

APPENDIX D.

CONVERGENCE METHODS

Wegstein Method

This method is illustrated in Figure D1 (Seider *et al.*). When the method of successive substitutions is specified, and a guess is made, the new guess is simply made equal to f(x^*). A sequence of iterations may exhibit the behaviour as shown in Figure D1a. The locus of iterates intercepts the 45° line after a number of interactions, thereby giving the converged value of x. Convergence will take a long time if the slope of the locus of iterates {f(x),x} is close to unity (processes with high recycle ratios). The Wegstein method is an accelerator method and speeds up the convergence process where the *method of successive substitutions requires a large number of iterations. As shown in* Figure D1b, the previous two iterates of f(x^*) and x^* are extrapolated linearly to obtain the next value of x at the point of intersection with the 45° line. The equation for this straight-line extrapolation is:

$$x = \left(\frac{s}{s-1}\right)x^* - \left(\frac{1}{s-1}\right)f(x^*)$$

where s is the slope of the extrapolated line. The first two points of the wegstein method are obtained by the method of successive substitutions.

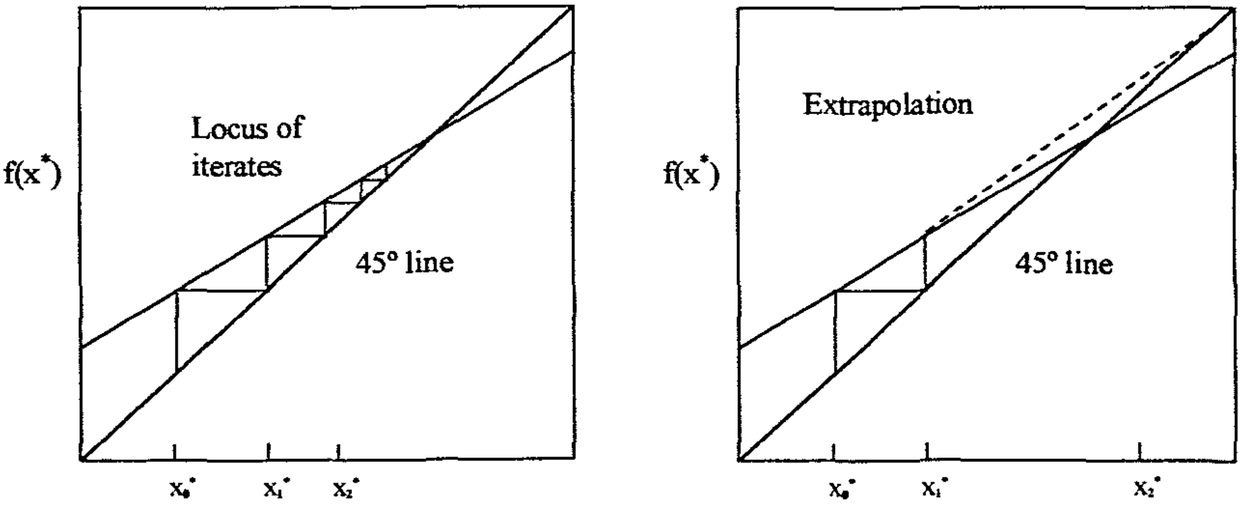

(a) (b)

Figure D1.
Illustration of the Wegstein convergence method

Secant method

It is important to note that the secant of a curve is the straight line passing through two points on the curve. This convergence method as illustrated by Figure D2 is similar to the Newton method. The non-linear function $f(x)$, and the solution for $g(x) = 0$ is found. The solution $g(x) = 0$ is the taken as the next approximation to the solution $x = \alpha$ of $f(x) = 0$. This procedure is applied repetitively until convergence is achieved. In order to initiate this method, two initial points x_0 and x_1 are required. The slope of the secant passing through these two points is:

$$g'(x) = \frac{f(x_i) - f(x_{i-1})}{x_i - x_{i-1}}$$

The equation of the secant line is then given by:

$$g'(x) = \frac{f(\alpha) - f(x_i)}{x_{i+1} - x_i}$$

Therefore

$$x_{i+1} = x_i + \frac{f(\alpha) - f(x_i)}{g'(x_i)}$$

The convergence criteria is satisfied when:

$$\left| \frac{x_{i+1} - x_i}{x_{i+1}} \right| \le \text{tolerance}$$

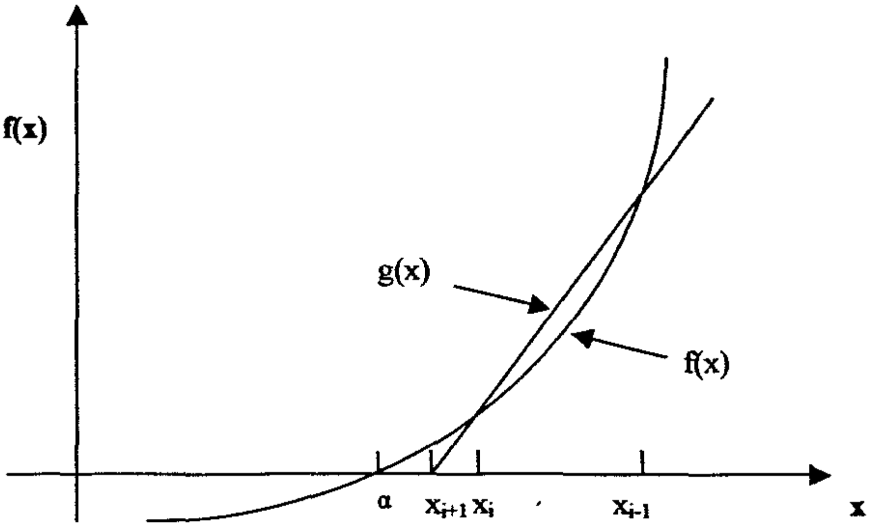

Figure D2.
Illustration of the Secant convergence method

APPENDIX E

Article for Publication

Submitted to:

The European Journal of Mineral Processing and Environmental Protection
(2001)

DEVELOPMENT OF AN ASPEN MODEL FOR THE TREATMENT OF ACID MINE DRAINAGE

RE Damons and FW Petersen

Department of Chemical Engineering
Cape Technikon, PO Box 652
Cape Town, 8000, South Africa
Fax: 27 21 460-3282
Email: fwp@ctech.ac.za

ABSTRACT

Although numerous methods exist to treat mine water that is rich in $CaSO_4$ they all have inherent disadvantages. A means of treating acid mine drainage is by forming a precipitate known as ettringite. Ettringite is a low solubility calcium hydrosulphoaluminate that is stable between pH values of 11.4 and 12.4. Ettringite is made up of calcium, sulphate, aluminium and a large amount of water. Decomposition of ettringite takes place by dropping the pH to about 7. A 5 stage process is proposed to treat acid mine drainage of which the formation of ettringite forms the cornerstone of this process. The process incorporates the formation of more than one precipitate as well as the recycling of aluminium hydroxide when ettringite is decomposed. The results obtained in this paper is as a result of modeling this process.

Keywords: acid mine drainage; ettringite; model

INTRODUCTION

Mining in South Africa is a necessity, and is influential to its economy. The greenhouse effect and global warming has largely been responsible for less frequent rainfall and therefore a shortage of water. This problem has been compounded by millions of litres of water being polluted through the mining and other industries each year. Finding a cost effective solution to the pollution problem, with specific reference to acid mine drainage (AMD), is of utmost importance. The formation of AMD is as a result of a series of complex geo-chemical and microbial reactions that occur when water comes in contact with pyrite (iron disulphide minerals) in coal mining operations. This water is usually high in acidity and dissolved metals.

Calcium sulphate is one of the most widely distributed pollutants of both natural and wastewaters. Even though a number of methods exist to purify solutions from sulphates, such as precipitation with lime, precipitation with barium salts, co-precipitation with calcium carbonate, reverse osmosis and ion exchange, each of these has an inherent disadvantage. The addition of lime, although facilitating the removal of heavy metals, is unable to reduce the sulphate content to an acceptable level. Ion exchange technology could reduce calcium and sulphate levels considerably, but the associated costs are significantly high. A fairly low cost method of purifying AMD is based on the precipitation of SO_4^{2-} in the form of a low-solubility calcium hydrosulphoaluminate, by treating water with milk of lime and an aluminium-containing agent. This family of phases that show potential to immobilize sulphate belongs to the ettringite species, and has been investigated by numerous authors (Bambauer, 1991; Gougar *et al.*, 1996; Moore & Taylor, 1968). Ettringite in its natural form has been known for more than 100 years and was first discovered at the Ettringer Bellerberg in Eifel, West Germany. It is commonly found in weathered cement, cement based solidification by-products and alkaline fly ashes (McCarthy *et al.*, 1992; Myneni *et al.*, 1997). Ettringite, as we know it today, represents a whole group of acicular calcium aluminate hydrates, which have the general composition:

$$3CaO.Al_2O_3.3CaX_2.nH_2O$$

or

$$3CaO.Al_2O_3.3CaY.nH_2O$$

with $X = OH^-, NO_3^-, \ldots$ and $Y = SO_4^{2-}, CO_3^{2-}, \ldots$

The crystal structure of minerals of the ettringite group consists of columns, which run parallel to the c-axis (Moore & Taylor, 1970). These columns, which have the composition $[Ca_6Al_2(OH)_{12}.24H_2O]^{6+}$, *contain* $Al(OH)_6$ *units* attached to hydrated Ca^{2+} arranged in a hexagonal array. The channels in between the columns are made up of SO_4^{2-} and water molecules. Crystallization of ettringite normally takes place as prismatic needles (c-axis) of high aspect ratio and hexagonal cross section. Visible changes in morphology occur when ettringite crystals grow in the presence of organic additives, some of which are known to act as set-retarders in Portland cement (Pöllmann *et al.* 1989).

Ettringite can withstand modest deviations in composition without a change in structure. This compositional change can occur on a crystal chemical level in the form of ionic substitution. Al^{3+} in ettringite can be substituted by Ti^{3+}, Cr^{3+}, Mn^{3+} and Fe^{3+} to form similar compounds of the type $Ca_6[M(OH)_6](SO_4)_3.26H_2O$ (Bensted and Varma,1972). According to McCarthy *et al.*, (1992), SO_4^{2-} can be replaced by CrO_4^{2-}, MnO_4^-, Cl^-, OH^-, CO_3^{2-} and NO_3^-. Similarly, Sr^{2+}, Ba^{2+}, Ni^{2+} and Zn^{2+} may replace Ca^{2+}. There exists a series of related compounds, known as a mineral group or family, and they include the following minerals:

Charlesite	$Ca_6(Si,Al)_2(SO_4)_2(B[OH]_4)(OH)_{12}.26H_2O$
Sturmanite	$Ca_6Fe_2(SO_4)_2(B[OH]_4)(OH)_{12}.26H_2O$
Thaumasite	$Ca_6Si_2(SO_4)_2(CO_3)_2(OH)_{12}.24H_2O$
Jouravskite	$Ca_6Mn_2(SO_4)_2(CO_3)_2(OH)_{12}.24H_2O$
Bentorite	$Ca_6(Cr,Al)_2(SO_4)_2(OH)_{12}.26H_2O$

Ettringite is a stable mineral between pH values of 11.4 and 12.4 and dissolves congruently with a log K_{sp} of -43.13 (according to Reardon.,1990). Temperature, dissolved CO_2, and H_2O activity can strongly influence ettringite stability. According to Damidot and Glasser (1992), monosulphoaluminate is more stable than ettringite at high temperatures. Nishikawa *et al.* (1992), stated that at high CO_2 and low H_2O activity level, ettringite decomposed to aragonite with vaterite as an intermediate phase.

In solution at pH values used for ettringite synthesis, aluminium exists largely as the amphoteric $Al(OH)_4^-$ species. The solubility curves for aluminium hydroxide species show that below a pH of 10.3, aluminium exists largely as insoluble amorphous aluminium hydroxide ($Al(OH)_3$(am)). The aqueous formation of ettringite should therefore not be possible below a pH of 10.3, since it is assumed that the aluminium must be present as the amphoteric species for ettringite to form. In addition to this, once the synthesis of ettringite takes place, its stability is pH dependent. Ettringite is an alkaline solid, which dissolves at a much lower pH. The stability of the mostly ettringite product is further enhanced if it contains additional alkaline components such as calcium hydroxide (portlandite), since the portlandite has additional acid-neutralizing potential. The optimum pH for ettringite decomposition takes place at a value of 6.5 (Petersen,1998). Ettringite could also be thermally decomposed into calcium aluminate monosulphate and calcium sulphate hemi hydrate at high temperatures, which exceed 110°C (Hall *et al.*, 1996).

THE CHEMICAL PRECIPITATION PROCESS

Process Description

This precipitation process to remediate AMD involves the addition of lime to waste water to precipitate the metal hydroxides, and the subsequent formation of ettringite to remove the calcium and sulphates. The process consists of 5 main stages as described below and illustrated by Figure 1.

Stage 1: Precipitation of heavy metals

Here the polluted mine water, at an approximate pH value of 6, is brought into contact with lime in order to raise the pH to greater than 11.5. These heavy metals are precipitated as hydroxides and although most metal hydroxide species will precipitate at relatively low pH values, a higher pH is required to precipitate magnesium. These hydroxides are sent away for land filling.

Stage 2: Gypsum saturation

The solution from stage 1 is contacted with gypsum crystals in stage 2. One of the characteristics of dissolved calcium sulphate, is that when a suitable surface such as gypsum is not present to crystallize on it, it can be short lived or metastable at concentrations that exceed it equilibrium solubility. For this reason the solution from stage 1 which is rich in calcium sulphate is brought in contact with gypsum, which results in the precipitation of the 'supersaturated' gypsum. This precipitated gypsum is thickened and filtered, and leaves the process as waste or as a by-product, depending on the specific situation. Part of the precipitated gypsum is returned to the mixing tank of stage 2 to provide the seed crystals for the rapid crystallization of the supersaturated portion of the dissolved calcium sulphate.

Stage 3: Ettringite precipitation

Stage 3 is the heart of the Ettringite process and involves the addition of aluminium hydroxide to the saturated gypsum solution from stage 2. This results in the formation of the insoluble salt known as ettringite, thereby removing both calcium and sulphate from the solution. The stoichiometry for ettringite precipitation is given by the following reaction:

$$6Ca^{2+} + 2Al(OH)_4^- + 3SO_4^{2-} + 4OH^- + 26H_2O \rightarrow Ca[Al(OH)_6]2(SO_4)_3 \cdot 26H_2O \text{.......[1]}$$

The ideal conditions for ettringite formation range between pH values 11.4 and 12.4. In order to keep the pH between these limits, lime is added resulting in the maximization of ettringite precipitation. The end product of stage 3 is filtered and the solid ettringite proceeds to stage 5 while the liquid goes to stage 4.

Stage 4: Carbonation

The solution from stage 3, which is now free from all heavy metals, calcium and sulphates is treated with carbon dioxide to reduce the pH to a suitable level. Pure calcium carbonate is precipitated, and can be separated from the resulting product water by filtration. The pH can however also be controlled so that calcium bicarbonate is formed instead of calcium carbonate, but this however depends on certain case specific factors.

Stage 5: Regeneration of Aluminium Hydroxide

Ettringite slurry is transported to stage 5 so that it may decompose in order to regenerate the amorphous aluminium hydroxide for recycle. The decomposition of ettringite is achieved by bringing it into contact with sulphuric acid, which in turn lowers the pH of the slurry and thereby renders it unstable. The decomposition reaction stoichiometry is the reverse of that for ettringite formation. The end of this stage is characterised by thickening and filtration, which separates into an aluminium hydroxide and gypsum. The gypsum is recycled to the beginning of stage 5 while the aluminium hydroxide is recycled as feed for stage 3.

ASPEN MODELLING

Simulating the ettringite process on an Aspen Plus simulation package serves as a useful tool to predict the behaviour of the process. It is a cost effective means of examining how the process is affected by using certain quantities of chemicals, various grades of polluted water, varying flow rates, and altering the split fractions at separators. Simulators are often used at the laboratory and pilot plant stages of plant design, and it is no different for this process. This simulation acts as a guideline as to how this process will react under actual conditions. Aspen Plus makes it possible to determine the effects of non-ideal conditions on ettringite formation and serves as a guide for the trends that are obtained when analyzing various sensitivities.

The Aspen simulation flow sheet is illustrated in Figure 2. The feed water (stream A) enters at a flow rate of 300 m^3/h and has the following composition.

$MgSO_4$(ppm)	$FeSO_4$(ppm)	H_2SO_4(ppm)	$CaSO_4$(ppm)
148	100	10	2200

Carbon dioxide gas (stream AA) is inserted at stage 1 so as to increase the pH of the feed water so that less lime is required to raise the pH to the heavy metal precipitation level. A 40% lime concentration was made-up at streams B and D, and enters at a flow rate of 1036 kg/hr, in order to adjust the pH at stages 1 and 3 respectively. 90 % Sulphuric acid is added at stream 25 at a flow rate of 558.01 kg/hr in order to decompose the ettringite from stage 3. The chemical reactions that take place at the various reactors (i.e. R1, R2, R3, R4, R5A, R5B) are tabulated in Table 1. To further enhance the model, certain design specifications were inserted into the system. These are tabulated in Table 2. Design specifications indicate to the program which variable needs to be changed in order to achieve a certain set point for another variable e.g. in order to keep the pH in stream 1 at 9.5, the composition of CO_2 at stream AA needs to be varied. This means that even though the composition and acidity of the feed water may change, the pH of stream 1 will remain constant.

Convergence

For Aspen to solve the unknown stream variables in the recycling loops, it uses a solution technique, which is based on tear stream guesses. In the recycle loop, a guess is taken of the variables of one of the streams (tear stream) in the loop and information is passed from unit to unit until new values of the variables in the tear stream are computed. These new values are used to repeat the calculations until the convergence tolerances are satisfied. This is the principle behind the method of successive substitutions for convergence. Upon satisfying the convergence criteria, control is transferred to the unit following the recycle loop in the calculation order. This method of tearing streams is not only implemented in stream recycle loops, but it is also used to solve design specification recycle loops.

RESULTS AND DISCUSSION

Potable water (Ca^{2+} < 150 ppm; SO_4^{2-} < 200 ppm) was recovered by treating AMD using the Aspen modeling approach. Table 3 shows the removal of 97% calcium and 87.6% sulphate over the entire system. The removal of the heavy metals was 100%, while virtually no sodium ions were removed from the system.

Stage 3 produced 3997 kg/hr of ettringite while 373 kg/hr of gibbsite was recycled. A sensitivity analysis was performed on the model.

Calcium sulphate in the feed water

By varying the $CaSO_4$ in the feed water means that varying quantities of Ca^{2+} and SO_4^{2-} ions will be available at stage 3 to react to form ettringite. An increase in the concentration of $CaSO_4$ in the feed water will lead to a linear increase in Ca^{2+} and SO_4^{2-} in solution at stage 1. The K_{sp} of $CaSO_4$ is 2.01×10^{4}, making it soluble in water. However, for high degrees of oversaturation, the $CaSO_4$ solution will experience rapid precipitation through spontaneous nucleation and crystal growth. $CaSO_4$ is saturated in water at 1852 ppm. At this level and at fairly low degrees of oversaturation ("metastable" region), *no noticeable precipitation will occur for* long periods of time (Benefield *et al. 1982*). $CaSO_4$ crystallizes as insoluble gypsum upon reaching a concentration of 2105 ppm, since it is outside the "metastable" region. The Ca^{2+} and SO_4^{2-} concentrations increase until crystallizes takes place, after which it remains constant. When the Ca^{2+} and SO_4^{2-} concentration remains constant, precipitated gypsum is formed which is removed with the metal hydroxides at stream 8. The dissolved $CaSO_4$ is contacted with gypsum crystals from stage 2. This is to enable the precipitation of $CaSO_4$. Virtually no $CaSO_4$ is precipitated while the $CaSO_4$ concentration is below 1930 ppm. This is in contrast to *gypsum first precipitating when the $CaSO_4$ was at 2105 ppm. This is because of the* presence of gypsum crystals in stage 2 catalyses the precipitation of gypsum when dissolved $CaSO_4$ is saturated and "metastable". After the $CaSO_4$ is at a saturated level, their exists a linear increase in the gypsum precipitated at stage 2.

A result of the precipitation of gypsum is that an increase in $CaSO_4$ in the feed water will lead to a linear increase in the Ca^{2+} and SO_4^{2-} concentration being fed to the ettringite formation stage (stage 3), until the $CaSO_4$ is at its saturation point. This is depicted in Figure 3(a), which shows that 1496 ppm SO_4^{2-} and 622 ppm Ca^{2+} leaves stage 2 for stage 3 once saturation of $CaSO_4$ takes place. This means that whenever AMD containing supersaturated quantities of $CaSO_4$ is fed into this process to be treated, by the time the dissolved $CaSO_4$ reaches the ettringite formation stage, it will be at its saturation level. This inevitably means that a constant amount of ettringite will be formed when supersaturated quantities of $CaSO_4$ is fed to stage 1. When undersaturated quantities of $CaSO_4$ are fed to stage 1, this leads to a linear increase in the amount of ettringite formed.

The program is written in such a way that the amount of ettringite formed is dependent on the amount of sulphate given off and this sulphate converted increases, as more sulphate is made available. The amount of sulphate converted to ettringite also affects the amount of calcium and gibbsite being removed at stage 3 by the formation of ettringite. Figure 3(b) shows that an increase in $CaSO_4$ into the feed water results in an increase in the amount of sulphate being converted to ettringite until it remains constant (~ 87%), while the calcium and aluminium hydroxide increase until saturation of $CaSO_4$ takes place. Thereafter 72% and 39% are removed from the system respectively. As more ettringite is formed, so less calcium and gibbsite is left as residue exiting stage 3. However, by decomposing more ettringite, more gibbsite will be formed, but the trend shows a decreases in the recycle of gibbsite (see Figure 3(c)). This is because the amount of gibbsite entering stage 5 is more than that being formed. As with the formation of ettringite, once supersaturated $CaSO_4$ is fed to stage 1, the gibbsite recycled will remain constant at 611 kg/hr.

Mono-valent cations in feed water

The presence of Na^+ and K^+ in the feed water has the effect that alters the solubility of the sulphate in the water. The preliminary results contained 15 ppm Na^+ showed the solubility of sulphate at a pH of 9.5 at stream 1 to be 1.697 g/l. As more sodium was added to the feed water, so the solubility of sulphate increased as can be seen by Figure 4. Therefore, in the presence of mono-valent cations the concentration of sulphate leaving stage 2 is substantially higher resulting in larger quantities of ettringite being formed. These cations however do not affect the formation and decomposition of ettringite nor the recycling of gibbsite.

$[Ca^{2+}]/[SO_4^{2-}]$ ratio at stage 3

At stage 3, the formation of ettringite is dependent on the conversion of sulphate in the ettringite formation reaction. This means that the mole flow of calcium taking part in this reaction is dependent on the sulphate taking part in the reaction. An increase in the $[Ca^{2+}]/[SO_4^{2-}]$ ratio entering stage 3 (ettringite formation stage) therefore results in less ettringite being formed (Figure 5). The increase in ratio is due to an increase in calcium or otherwise a decrease in the amount of sulphate at this stage. Ettringite formation first uses the mole flow of sulphate at its disposal, and then calculates how much calcium, gibbsite and water is required for this reaction. Therefore, if less sulphate reacts, then less calcium, gibbsite and water will react, and therefore less ettringite will be formed. This explains why more sulphate is always removed than calcium. All the sulphate is not removed because the ettringite formation reaction converts 90% of the mole flow of sulphate into ettringite and this model also ensures that stream R3 contains 0.2 kg/m^3 of sulphate. An increase in the $[Ca^{2+}]/[SO_4^{2-}]$ ratio results in a decrease in the amount of gibbsite produced when 95% of the ettringite is decomposed. Less gibbsite produced at this stage, means more gibbsite is recycled back to stage 3 because of the large quantity of gibbsite entering stage 5.

Decomposition of ettringite

The decomposition of ettringite takes place due to the stoichiometric reaction (2) at stage 5:

$$\text{ettringite (s)} \rightarrow 3Ca(OH)_2 + \text{gibbsite (s)} + 3CaSO_4 + 25\ H_2O \qquad \ldots\ldots \quad [2]$$

As more ettringite decomposes, so more gibbsite will be formed and ultimately more gibbsite will be recycled as shown by Figure 6(a). In order to meet all the conditions of the recycle loop, a large amount of ettringite needs to be made available to be decomposed when very little decomposition of ettringite takes place. This also means that when very little ettringite is decomposed, a large amount of ettringite will be recycled (Figure 6(a)). It would therefore not make economic sense if decomposition is low. When the decomposition of ettringite is between 10% and 43%, all the gibbsite that is formed and recycled is once again used to form ettringite at stage 3. This results in a 100% removal of gibbsite when ettringite is formed. As more ettringite is decomposed between these decomposition ranges, so more sulphate and calcium is also recycled and ultimately reacts to form ettringite (Figure 6(b)).

When more than 43% of ettringite is decomposed, enough gibbsite is formed and recycled in order to meet the demand set for ettringite formation. From this point onwards, the amount of sulphate entering stage 3 remains constant and therefore a constant removal of sulphate to form ettringite takes place. The increasing amount of gibbsite recycled as more ettringite is decomposed means that less of this gibbsite will react to form ettringite when the amount of sulphate reacting at stage 3 remains constant (Figure 6(b)). This results in a fairly constant formation of ettringite.

Reagent Costs

The uses of reagents are of paramount importance to the treatment of wastewater in this process. The success and economic viability of the process is largely dependent on the costs incurred while running this plant. Results from the preliminary model showed that the total reagent costs amounted to R0.81 per m^3 of feed water used. These costs are calculated using slaked lime ($Ca(OH)_2$) at R313/ton, carbon dioxide at R400/ton and H_2SO_4 at R320/ton. These estimates were obtained from MINTEK, South Africa and it is interesting to notice that the amount of lime used has the greatest effect on the total reagent costs. Reagent costs will vary depending on the quality of water produced, namely agricultural water ($Ca^{2+} < 300$ ppm, $SO_4^{2-} < 500$ ppm), potable ($Ca^{2+} < 150$ ppm, $SO_4^{2-} < 200$ ppm), and high quality industrial water ($Ca^{2+} < 50$ ppm, $SO_4^{2-} < 50$ ppm).

As the quality of the water increases, so the reagent costs increase as shown by Figure 7(a). When the $CaSO_4$ in the feed water was increased (see Figure 7(b)), reagent costs increased while the calcium sulphate was unsaturated. As more ettringite is formed, so also more H_3O^+ is formed, which leads to a drop in pH. Since the pH needs to be at a certain level (i.e. 11.95), more lime needs to be added to meet this condition. The increase in the reagent costs is also due to the increasing quantities of sulphuric acid needed to break down the increasing amount of ettringite at stage 5. When ettringite decomposes, OH^- ions are given off, which increases the pH. The pH however needs to remain at 7. This requires the addition of sulphuric acid to drop the pH. Once $CaSO_4$ reaches saturation point, the reagent cost stay constant at R1.06 per m^3 of feed water used. When the flow rate of the feed water is varied the reagent costs remain fairly constant at R 0.81/m^3. (Current exchange rate: 1US \$ = R 9.23)

CONCLUSIONS

This process, which was modeled on an Aspen simulation package, is able to treat water that contains small as well as large quantities of $CaSO_4$. The modeling was done in such a way as to produce water of a potable quality ($Ca^{2+} < 150$ ppm; $SO_4^{2-} < 200$ ppm). Metal hydroxides, especially magnesium hydroxide, precipitate at high pH ranges at stage 1, and virtually all the metals are removed here. When the feed water contains a high degree supersaturated $CaSO_4$, it precipitates as an insoluble gypsum that is also removed at stage 1. Calcium and sulphate is removed from the water at stage 2 where $CaSO_4$ is contacted with gypsum. The formation of $CaSO_4$ at this stage is so that when supersaturated $CaSO_4$

is fed into the process, the Ca^{2+} and SO_4^{2-} leaving stage 2 will remain the same (i.e. $Ca^{2+} = 622$ ppm and $SO_4^{2-} = 1496$ ppm).

A constant supply of sulphate to stage 3 will lead to a constant formation of ettringite. An increase in the presence of mono-valent cations like Na^+ and K^+ in the feed water increases the solubility of SO_4^{2-}, which ultimately results in more ettringite being produced. None of the mono valent cations are however removed during the treatment water in this process. Decomposition takes place at about a pH a 7 and it is assumed that 95% of the ettringite is decomposed to gibbsite. An increase in the $[Ca^{2+}]$ to $[SO_4^{2-}]$ into stage 3 will result in less ettringite being formed as less sulphate is being made available to be converted to ettringite. Reagent costs are largely dependent on the amount of ettringite formed and decomposed. An increase in the amount of ettringite formed results in more lime being used and an increase in the amount of ettringite decomposed results in more H_2SO_4 being used.

References

Bambauer, H.U., The Application of mineralogy to environmental management – an overview. *Proc. Int. Conf. Min.*, 1991., Paper 3, 1, pp 31.

Benefield, L.D., Judkins, J.F. and Weand, B.L., Process Chemistry for water and wastewater treatment, Prentice Hall, Inc., 1982.

Bensted, J. and Varma, S.P., Ettringite and its derivatives II: Chromate substitution. *Silicates Ind.*, 1972, **37**, pp. 315 - 318.

Damidot, D. and Glasser, F.P., Thermodynamic investigation of the CaO-Al2O3-CaSO4-H2O system at 50°C and 85°C. *Cement and Concrete Research*, 1992, **22**, pp. 1179.

Gougar, M.L.D., Scheetz, B.E. and Roy, D.M., Ettringite and C-S-H Portland cement phases for waste ion immobilization: a review., *Waste management*, 1996, **16**, no. 4, pp 295.

Hall, C., Barnes, P., Billimore, A.D., Jupe, A.C. and Turrilas, X., Thermal Decomposition of ettringite $Ca_6[Al(OH)_6]_2(SO_4)_3 \cdot 26H_2O$, *Journal Chem. Soc., Faraday Trans.*, 1996, **92**, no. 12, pp 2125 – 2129.

McCarthy, G.J., Hassett, D.J. and Bender, J.A., Synthesis, crystal chemistry and stability of ettringite, a material with potential applications in hazardous waste immobilization. *Advanced Cementitious Systems: Mechanisms and Properties, Materials. Research Society Symposium Proceedings*, 1992, pp. 129 –149.

Moore, A.E. and Taylor, H.F.W., Crystal structure of ettringite. *Nature*. 1968, **218**, pp. 1048 – 1049.

Moore, A.E. and Taylor, H.F.W., *Crystal structure of ettringite. Acta Cryt*, 1970, **B26**, pp. 386 – 393.

Myneni, S.C.B., Traina, S.J., Logan, T.J. and Waychunas, G.A., Oxyanion behaviour in alkaline environments: sorption and desorption of arsenate in ettringite., *Environ. Sci. Technol.*, 1997, **31**, p 1761.

Nishikawa, T., Suzuki, K. and Ito, S., Decomposition of synthesized ettringite by carbonation, *Cement and Concrete Research*, 1992, **22**, pp. 6 – 14.

Petersen, F.W., The fundamentals of the ettringite process., *Mintek Technical Memorandum.*, 1998, **18707**

Pōllmann, H.; Kuzel, H.-J.; Erlangen & Wenda, R.; Neusäss; Compounds with ettringite structure; *Neues Jahrbúch Miner. Abh.,* 1989, **160**, (2), p133 –158.

Reardon, E.J., An ion interaction model for the determination of chemical equilibrium in cement/water systems. *Cement and Concrete Research*, 1990, **20**, pp. 175 – 192.

TABLE 1. **Chemical reactions at different stages of the process**

Stage 1

1. $FeSO_4 \rightarrow Fe^{2+} + SO_4^{2-}$
2. $Al_2(SO4)_3 \rightarrow 2Al^{3+} + 3SO_4^{2-}$
3. $Fe_2(SO4)_3 \rightarrow 2Fe^{3+} + 3SO_4^{2-}$
4. $MgSO_4 \rightarrow Mg^{2+} + SO_4^{2-}$
5. $Al^{3+} + 12H_2O \rightarrow Al_2(OH)_6\ (s) + 6H_3O^+$
6. $Fe^{3+} + 6H_2O \rightarrow Fe(OH)_3\ (s) + 3H_3O^+$
7. $Fe^{2+} + 4H_2O \rightarrow Fe(OH)_3\ (s) + 2H_3O^+$
8. $CaSO_4 \rightarrow Ca^{2+} + SO_4^{2-}$
9. $Ni^{2+} + Ca(OH)_2 \rightarrow Ni(OH)_2\ (s) + Ca^{2+}$
10. $Zn^{2+} + Ca(OH)_2 \rightarrow Zn(OH)_2\ (s) + Ca^{2+}$
11. $Ca^{2+} + 2F^- \rightarrow CaF_2\ (s)$

Stage 2

$Ca^{2+} + SO_4^{2-} + 2H_2O \rightarrow \text{gypsum}$

Stage 3

1. $CaOH^+ \rightarrow Ca^{2+} + OH^-$
2. $Ca(OH)_2\ (s) \rightarrow Ca^{2+} + 2OH^-$
3. $\text{gypsum (s)} \rightarrow Ca^{2+} + SO_4^{2-} + 2H_2O$
4. $6Ca^{2+} + 3SO_4^{2-} + Al_2(OH)_6\ (s) + 37H_2O \rightarrow \text{ettringite (s)} + 6\ H_3O^+$
5. $H_3O^+ + OH^- \rightarrow 2H_2O$

Stage 4

$Ca^{2+} + CO_2 + 2OH^- \rightarrow CaCO_3 + H_2O$

Stage 5

Reactor 5A

1. $\text{ettringite (s)} \rightarrow 3Ca(OH)_2 + Al_2(OH)_6\ (s) + 3CaSO_4 + 25\ H_2O$
2. $CaSO_4 \rightarrow Ca^{2+} + SO_4^{2-}$
3. $Ca(OH)_2 \rightarrow Ca^{2+} + 2OH^-$
4. $H_2SO_4 + H_2O \rightarrow HSO_4^- + H_3O^+$
5. $HSO_4^- + H_2O \rightarrow SO_4^{2-} + H_3O^+$
6. $H_3O^+ + OH^- \rightarrow 2\ H_2O$

Reactor 5B

$Ca^{2+} + SO_4^{2-} + 2H_2O \rightarrow \text{gypsum}$

TABLE 2. Design Specifications of the ASPEN model.

Design Spec. of set point	Vary variable to achieve set point
flow rate of feed water =300 m^3/hr	mass flow of feed (stream A)
pH (stream 1) = 9.5	mass flow of CO_2 (stream AA)
pH (stream R1)= 11.7	mass flow of lime (stream B)
% solids entering reactor R2 = 5%	flow fraction of stream 12
pH (stream R3) = 11.95	mass flow of lime (stream D)
[SO_4^{2-}] at stream R3 = 200ppm	conversion of SO_4^{2-} in the ettringite formation reaction (stage 3)
pH (stream R4) = 8.5	mass flow of CO_2 (stream 22)
pH (stream R5A1) = 9	mass flow of H_2SO_4 (stream 25)
% solids entering reactor R5B = 5%	flow fraction of stream 34
ratio of SO_4^{2-} entering reactor R3 to solids entering reactor R5A = 1.59 (for every kg of SO_4^{2-} fed to stage 3, ~ 1 kg of $Al(OH)_3$ is fed to stage 5)	mass flow of stream 26
Metal hydroxides(stream 8) = 25% solids	flow fraction of stream 8
Gypsum(stream 36) = 60% solids	flow fraction of stream 36
% solids in stream 5 = 1.5%	flow fraction of stream 5
% solids in stream 7 = 5%	flow fraction of stream 7
% solids in stream S2 = 30%	flow fraction of stream S2
% solids in stream 20 = 15%	flow fraction of stream 20
% solids in stream 29 = 15%	flow fraction of stream 29
% solids in stream S5B = 30%	flow fraction of stream S5B
[Ca^{2+}] at stream R5A =1.5kg/m^3	flow fraction of stream 27

TABLE 3: Percentage removal of species from solution as predicted by Aspen model.

components	Ca^{2+}	SO_4^{2-}	K^+	Na^+	Mg^{2+}
Feed water (ppm)	578	1614	154.7	14.89	29.7
Product water (ppm)	17.2	199.8	1.44	14.83	0.01
% removal	97	87.6	99	0	100

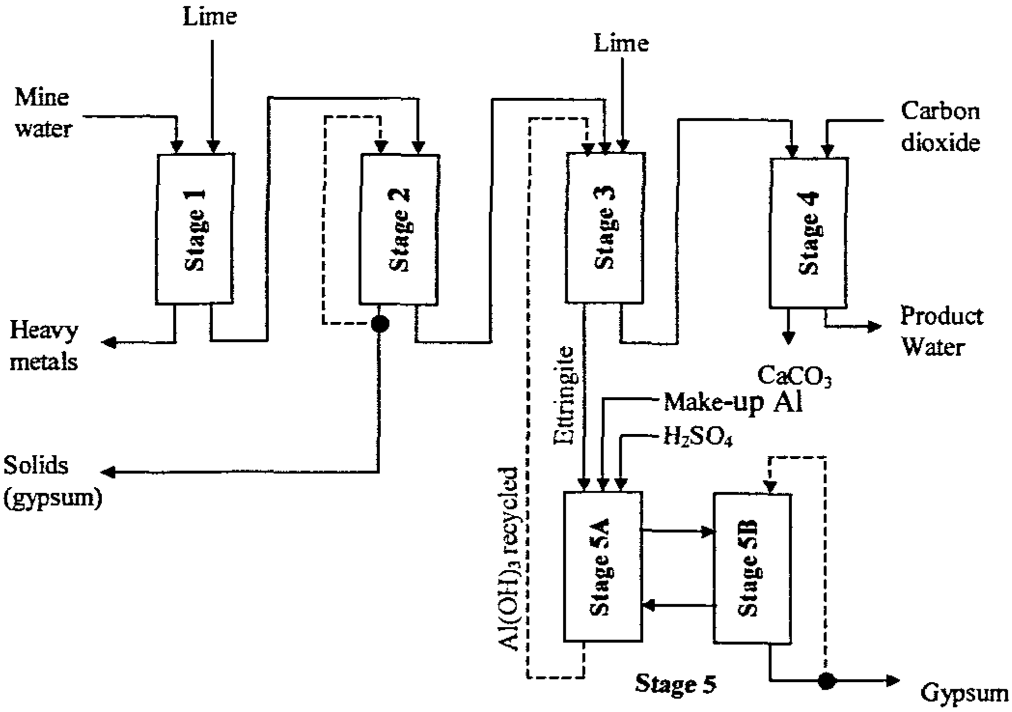

Figure 1: Ettringite process to treat AMD

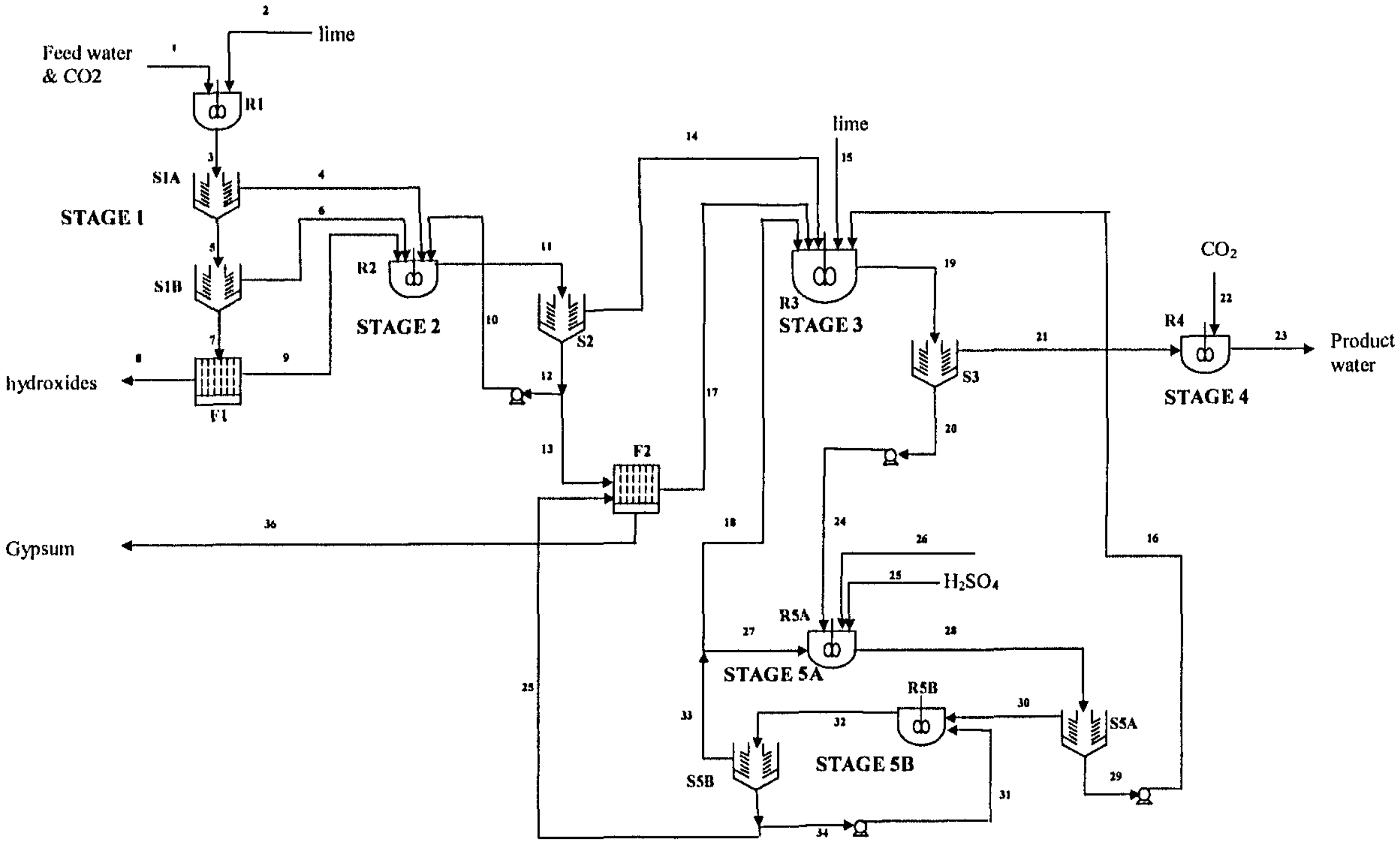

Figure 2: Aspen simulation flowsheet

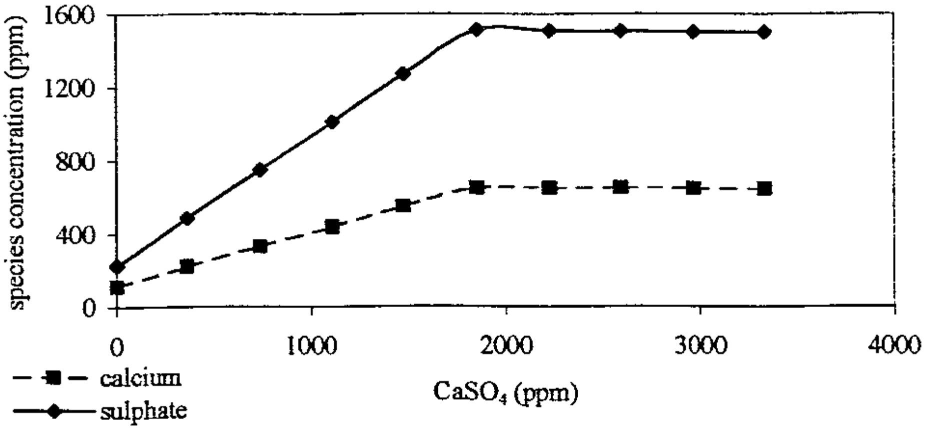

Figure 3(a): Aspen results of varying CaSO$_4$ in the feed water vs. species fed to stage 3

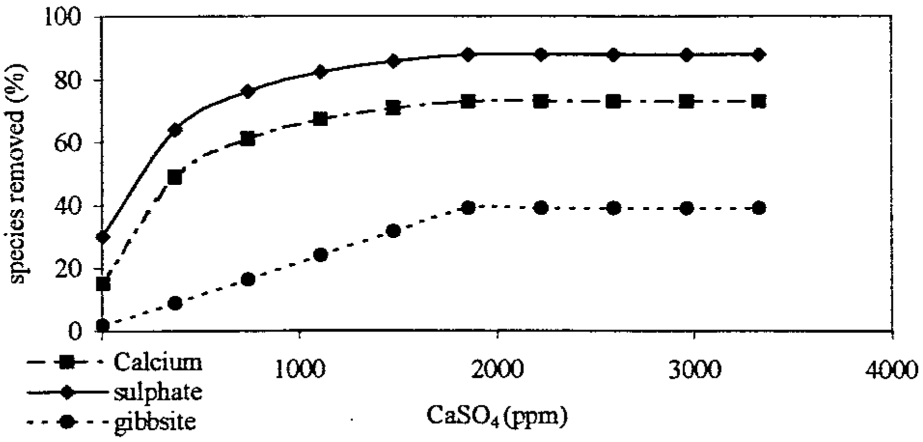

Figure 3(b): Aspen results of varying $CaSO_4$ in the feed water vs. percentage species removed at stage 3

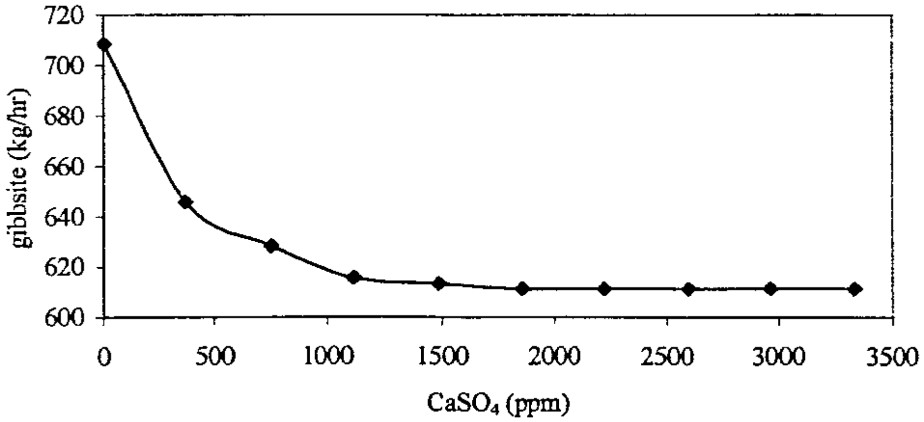

Figure 3(c): Aspen results of varying $CaSO_4$ in the feed water vs. gibbsite recycled

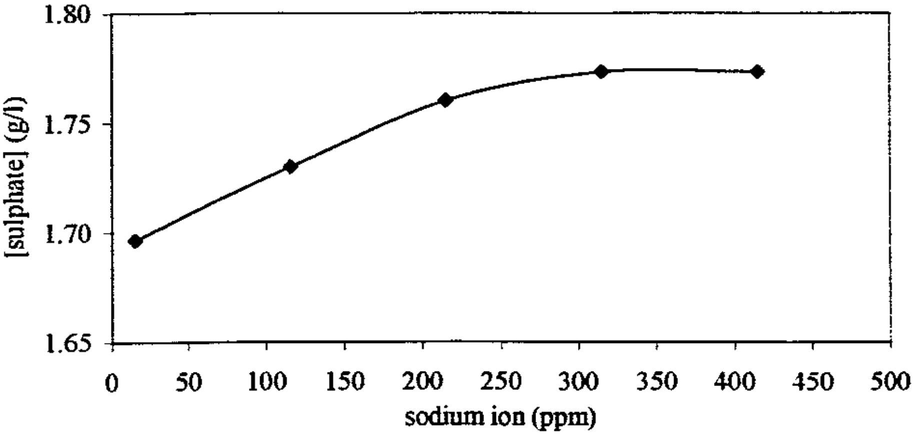

Figure 4: Aspen results showing Na^+ in feed water vs. the solubility of sulphate

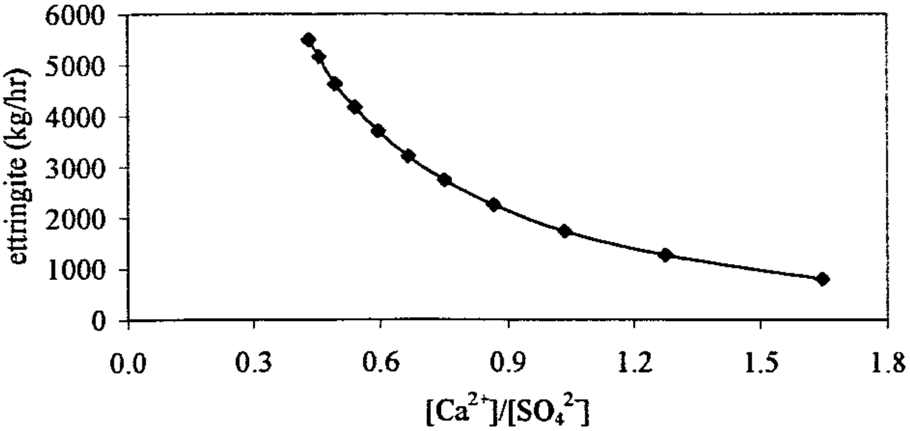

Figure 5: Aspen results showing the effect the calcium to sulphate ratio on ettringite produced

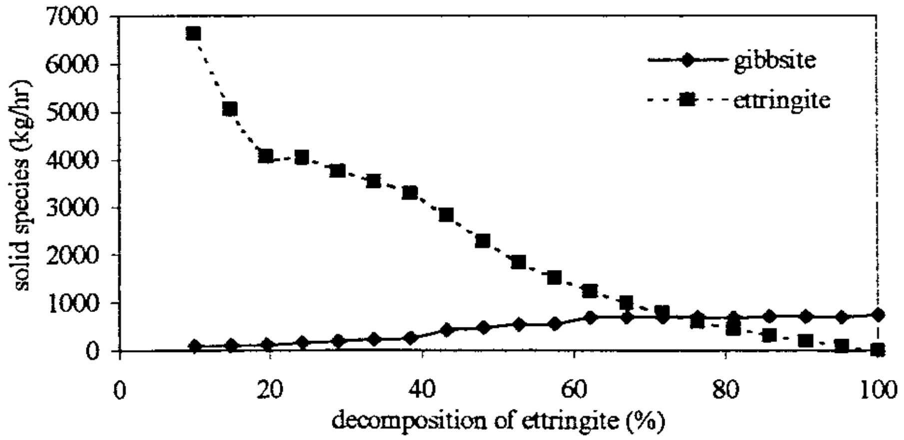

Figure 6(a): Varying the decomposition of ettringite vs. solid species recycled

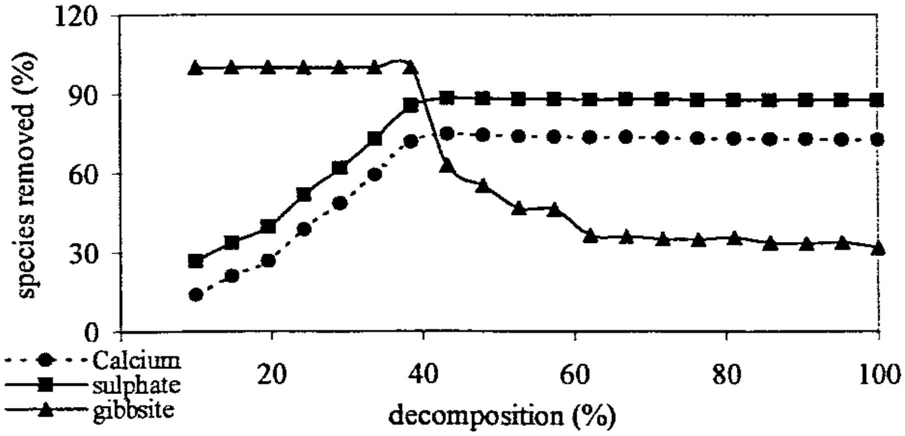

Figure 6(b): Varying the decomposition of ettringite vs. percentage species removed at stage 3

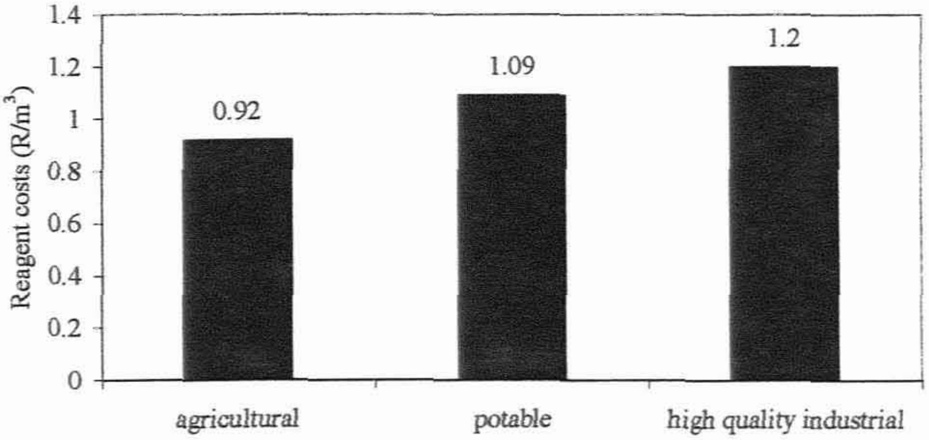

Figure 7(a): Aspen results of varying quality of water vs. total reagent costs

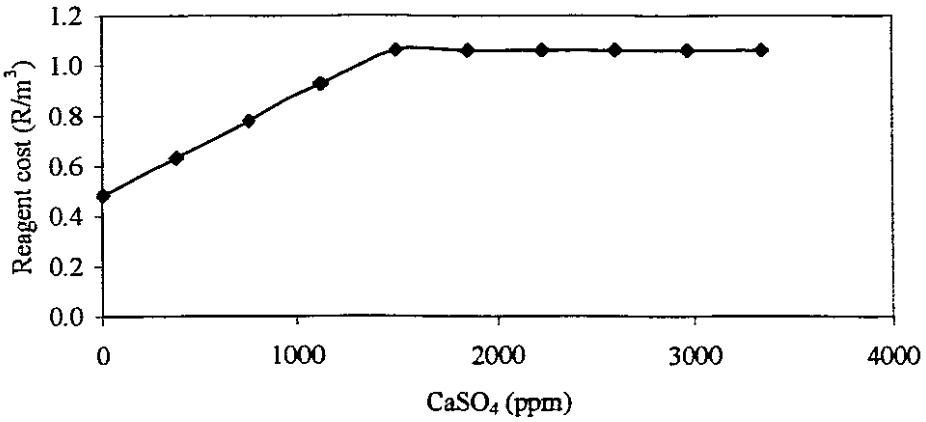

Figure 7(b): Aspen results of varying the CaSO$_4$ in the feed water vs. the total reagent costs.